Distance Dependence of Entanglement Generation via a Bosonic Environment

Inaugural-Dissertation

zur

Erlangung des Doktorgrades

der Mathematisch-Naturwissenschaftlichen Fakultät

der Universität zu Köln

vorgelegt von

Thomas Zell

aus Köln

Hundt Druck GmbH, Köln

2011

Berichterstatter PD Dr. Rochus Klesse

Prof. Dr. Claus Kiefer

Tag der mündlichen Prüfung 24.05.2011

Abstract

The search for methods to create and maintain entanglement has led to the idea of *environmentally induced entanglement*. Roughly speaking, the usually detrimental effect of coupling a non-interacting bipartite system to an environment is turned into an advantage by using the environment to mediate an indirect interaction, which can result in entanglement of the two parts of the system under certain conditions. Of course, care has to be taken to properly evaluate the conflicting influences of the environment. Only if the indirect interaction overcompensates for the decoherence, entanglement creation can be expected.

It has been suggested that entanglement creation can be achieved in bosonic heat baths even over finite spatial separations with only a moderate polynomial decay of entanglement with distance. In this work, we look more closely at the distance dependence, for the first time employing an oscillator model that is both exactly solvable and includes dissipation. We numerically prove that entanglement creation is, in fact, extremely distance-sensitive and it is not possible to entangle objects which are further apart than approximately their own size.

Additionally, we suggest an approach how to mitigate the distance dependence. It comes at the cost of geometrically modifying the bath modes by imposing physical boundary conditions resulting in a gap in the spectrum. This is implemented by placing the system inside of an infinitely long superconducting cavity. An experimental implementation of this could be feasible.

Zusammenfassung

Die Suche nach Möglichkeiten Verschränkung zu erzeugen und zu erhalten brachte die Idee der *umgebungsinduzierten Verschränkung* hervor. Grob gesagt wird die normalerweise hinderliche Auswirkung der Kopplung eines zweigeteilten Systems an eine Umgebung in einen Vorteil verwandelt, indem über die Umgebung eine indirekte Wechselwirkung vermittelt wird, die unter bestimmten Voraussetzungen zu einer Verschränkung der beiden Systemteile führen kann. Natürlich müssen die gegensätzlichen Einflüsse der Umgebung sorgfältig betrachtet werden. Nur wenn die indirekte Wechselwirkung stärker ist als die Dekohärenz kann man eine Entstehung von Verschränkung erwarten.

Bei der Untersuchung über das Abstandsverhalten von Verschränkungserzeugung wurde bisher ein polynomieller Abfall der Verschränkung mit dem Abstand gefunden, der endliche Abstände zwischen den zu verschränkenden Teilsystemen zulassen würde. In dieser Arbeit wird die Abstandsabhängig genauer untersucht. Dabei wird erstmals ein exakt lösbares Oszillatormodell verwendet, welches auch Dissipation berücksichtigt. Numerisch kann gezeigt werden, dass im Gegensatz zu vorherigen Ergebnissen die Verschränkungserzeugung sehr stark vom Abstand abhängt und dass es nicht möglich ist, Objekte über eine weitere Entfernung zu verschränken als einen Abstand, der in etwa ihrer eigenen Ausdehnung entspricht.

Zusätzlich wird ein neuer Ansatz vorgeschlagen, in dem die Abstandsabhängigkeit geringer ausfällt. Dieser beinhaltet den zusätzlichen Aufwand, dass die Badmoden durch physikalische Randbedingungen geometrisch eingeschränkt werden, so dass eine Lücke im Spektrum entsteht. Das wird bewerkstelligt durch die Platzierung des Systems in einer unendlich langen supraleitenden Kavität. Eine experimentelle Implementierung könnte durchführbar sein.

Contents

1. Introduction

The problem treated in this thesis is located at the intersection of open quantum systems and quantum information theory. Compared to the time span the theory of quantum mechanics has been known, these fields of research have only been established relatively recently, but have already yielded many fascinating results. Open quantum systems are used to consistently model dissipation and decoherence [JZK+03]. Quantum information theory has improved our knowledge about quantum correlations and has brought forward quantum information processing (QIP), which includes such ideas as the quantum computer and the already commercially viable quantum cryptography [NC00].

Entanglement is a quantity measuring quantum correlations and plays an important role in QIP as a resource. Therefore, creating and preserving entanglement is a crucial task. Unfortunately, the study of open quantum systems teaches us that preserving entanglement is extremely difficult, because even tiny interactions with the environment can destroy entanglement very efficiently.

Surprisingly, Braun [Bra02] provided theoretical arguments suggesting that two non-interacting quantum systems coupled to a common thermal bath can also become entangled, because the environment mediates an indirect interaction. He later substantiated his claims by showing that a finite spatial separation between the two systems does not destroy the effect [Bra05]. Such a scheme would be very helpful, since it would not require full unitary control over the system and a coupling to the environment would actually be beneficial.

Despite looking counterintuitive, Braun's results are widely accepted and followed in the scientific community [BFP03, STP06, CL07, HB08, PR08, Isa08, XSS08, FNGM09, MNBF09, CP09, ASH09, LSF10, RBK11]. Since Braun uses a rather simple model, we decided to investigate the problem more closely employing a model which is more realistic and includes dissipation as well as a spatial separation, yet which can be solved exactly. Our findings do not support the results of Braun, but suggest a strong distance dependence instead. We claim that the effect does not persist over distances larger than the spatial extent of the objects to be entangled.

As a model, we consider two harmonic oscillators representing the quantum mechanical systems to be entangled, which are bilinearly coupled to bosonic modes at different spatial positions but not to each other. With bosonic modes many different types of baths can be modelled, including photons, phonons and many effective baths, however, with the exception of spin baths. Because we use an oscillator model, exact solutions are possible, at least with some numerical effort.

The harmonic oscillators can, of course, be thought of as particles trapped in a potential that is approximated as quadratic at low energies, but at very low energies they can also be viewed as two-state systems, since the oscillators will be dynamically truncated to their two lowest levels.

We first give an introduction on the topic of entanglement in chapter two and then proceed to introduce entanglement measures. In the following, we give an overview over Gaussian states of quantum mechanical systems and how their entanglement can be determined.

In the third chapter, we define a model of two harmonic oscillators coupled to a bosonic modes, which is solved formally using a quantum Langevin equation approach.

The fourth chapter contains a presentation of numerical results for the entanglement that can be generated by a free bosonic bath. Both long-term asymptotic states are examined as well as the full time development. The chapter concludes with a discussion of the overall maximum of the entanglement and its dependence on the parameters involved, most importantly the spatial separation of the two oscillators.

While the free bath is a quite general case, more special situations can also be considered. As an example, in the fifth chapter we calculate the behavior of the system inside of a cavity, which has the form of a tube with a quadratic cross-section. This imposes boundary conditions on the bath modes, resulting in a drastic modification of the coupling spectral density. The entanglement generation capabilities are then compared to the case of a free bath.

In the conclusion in chapter six we summarize our results and compare them to other works concerned with the topic of entanglement creation in bosonic environments.

2. Concepts

> Although it [entanglement] is usually fragile to the environment, it is robust against conceptual and mathematical tools.
>
> *([HHHH09])*

2.1. Entanglement

2.1.1. Fundamental Aspects

The theory of quantum mechanics was very successful from its beginning, yet it included some unusual properties, which were met with scepticism. Most famously, the thought experiment given by Einstein, Podolsky, and Rosen [EPR35] in 1935 leads to the conclusion that the quantum mechanical wave function cannot describe physical reality completely if one assumes the principle of local realism. The authors were unwilling to accept a quantum mechanical feature which Schrödinger called *entanglement* later in the same year [Sch35]: If two particles have interacted in the past so that they have to be described by a joint wave function, a measurement on one of them influences the measurement outcomes of the other particle, even after the particles have been separated spatially. To put it in a different way: Full knowledge of the whole system does not necessarily give you full knowledge of its parts. Some attempts were made to fix this seeming deficiency with *local hidden variable* models, but none were successful.

It took 30 years, until Bell showed that, in fact, all local hidden variable theories are incompatible with the predictions of quantum mechanics [Bel64] and derived an inequality which can be used to verify experimentally that quantum mechanics violates locality. It took some more time until it was attempted to actually perform such an experiment [FC72]. The most well known one is by Alain Aspect [AGR82] using entangled photons. While theoretically, there still remain some loopholes for local hidden variables mainly due to

detector inefficiencies, all experiments have confirmed quantum mechanics, and the loopholes are expected to be closed soon.

It is important to stress that the type of non-locality inherent to quantum mechanics is not at odds with special relativity. The correlations due to entanglement are not strong enough to allow information transfer, i.e. they are *non-signaling*. Therefore, quantum mechanics adheres to the restriction of special relativity that no information can be transmitted faster than the speed of light. In fact, it is possible to construct even more non-local correlations than quantum mechanics allows, which are non-signaling. The most non-local correlations possible are implemented by the Popescu-Rohrlich non-local box [PR94].

Entanglement also plays a central role in the mechanism of *decoherence*, which is crucial for our understanding of the quantum to classical transition. Zeh [Zeh70] and Zurek [Zur81] have started the modern discussion about this issue. The observation, that quantum states are very fragile and quickly start to behave classically, can be explained by taking into account interactions with environmental degrees of freedom. Quantum states become entangled with the (much larger) environment and lose their internal entanglement in that process. More precisely, entanglement within the system is destroyed by entanglement with environmental degrees of freedom.

At the level of qubits the principle of *monogamy* of entanglement forbids a qubit that is maximally entangled with another qubit to be correlated at all with a third qubit [KW04]. In the same way, two qubits, each of which is maximally entangled with the environment, cannot themselves be entangled. Since the environment has a much larger dimension, already a small amount of entanglement with individual environmental degrees of freedom has a very pronounced effect.

Of course, decoherence does not solve the measurement problem. It only describes a *seeming* wave function collapse. Still, it remains an open question whether the wave function really collapses at some point eventually or not. In the first case, a yet to be discovered mechanism has to provide non-unitary dynamics for the collapse. In the second case, no collapse occurs ever, leading to a many-worlds interpretation of quantum mechanics.

2.1.2. Formal Definition of Entanglement

Entanglement exists only relative to a given partition of a quantum system. It does not make sense to ask about entanglement contained in a system as

a whole. While it is possible to consider more than two subsystems, I will restrict myself to the case of a bipartite quantum system with Hilbert space $H = H_A \otimes H_B$. The definition of entanglement is negative: A pure state

$$|\psi\rangle \in H_A \otimes H_B$$

of the composite system is *entangled* if it is not separable. The state is *separable* if it can be written as a product state

$$|\psi\rangle = |\psi_A\rangle \otimes |\psi_B\rangle \tag{2.1}$$

with $|\psi_A\rangle \in H_A$ and $|\psi_B\rangle \in H_B$ being state vectors of the subsystems.

A mixed state ρ is separable if it can be written as a convex combination of product states [Wer89]

$$\rho = \sum_i p_i \rho_i^A \otimes \rho_i^B \tag{2.2}$$

with $p_i \geq 0$ and $\sum_i p = 1$.

Unfortunately, the above definition is unhelpful if the task is to decide whether a mixed given state is entangled or not. In fact, classifying an unknown mixed state turns out to be a computationally hard problem in the general case [Gur03]. Criteria which give partial answers are introduced in section 2.1.5.

2.1.3. Relations to other Concepts

In non-rigorous treatments the terms *entanglement*, *non-locality*, and *non-classicality* are often used synonymously. Here, I want to point out that they are not equivalent (but also not disjunct). Quantum correlations can be looked at from slightly different angles.

The non-existence of a local hidden variable description of a state is called non-locality and is demonstrated by the violation of bell inequalities. Surprisingly, some mixed entangled states actually do admit a local hidden variable description [Wer89]. In this case, however, it is possible to transform the state into one that violates Bell inequalities by local operations [Pop95]. It is also remarkable that maximally non-local states are almost[1] always not maximally entangled [MS07].

It is confusing that the term non-locality is sometimes also used in an information theoretic sense, which has little to do with hidden local variables. A

[1] except for the two qubit case

state is *informationally non-local* if not all of the information contained in the state can be distilled by local operations [HHH+05]. A similar notion is to associate non-locality with *local indistinguishability* [BDF+99].

All information about a classical state can be extracted by local measurements and without perturbing it. This is not possible for most separable mixed states. Ollivier and Zurek have introduced *quantum discord* [OZ01], which vanishes for all classical states. In quantum computing an exponential speedup can sometimes be achieved with very little entanglement and a non-zero quantum discord [DV07].

2.1.4. Entanglement as a Resource

The concept of entanglement has gained increasing attention over the past decade because of its importance as an operational resource in quantum information processing and quantum computing.

Ekert [Eke91] introduced a *quantum cryptography* protocol based on entanglement. The two distant parties share entangled states. As the first step, they ensure that the states are indeed entangled and then they distill a key from them. The security of the key is guaranteed, because a maximally entangled state cannot be correlated (even classically) to a third system. In practice, it is possible to guarantee security even if the entanglement is not perfect.

By Holevo's bound, the maximum amount of classical information that can be encoded in a qubit is one classical bit. However, with the help of pre-shared entanglement this can be extended to two bits by a protocol called *quantum dense coding* [BW92].

Pre-shared entanglement can also be used to *teleport* an unknown quantum state to a remote location using only classical communication [BBC+93]. The original state is destroyed in order not to violate the quantum no-cloning theorem.

By *entanglement swapping* [YS92] particles that never directly interact can be entangled. This can be used to build a quantum repeater for entanglement distribution over long distances. Such a device is necessary to overcome the distance limit set by fiber loss.

In classical information theory the *communication complexity* of functions is investigated by determining the minimal amount of bits of communication necessary between distant parties in order to jointly compute the value of the function from the input values, which are distributed among the parties.

Surprisingly, pre-shared entangled states can reduce the number of necessary classical bits in certain cases [CB97].

Entangled cluster states are the basis of the *one-way quantum computer*, which is universal [RB01]. Any quantum computation can be performed by single spin measurements on a cluster state. During the process the entanglement is gradually reduced or "used up". However, maximally entangled states are not optimal because they tend to turn into a much less entangled state after measuring one qubit [BR01].

Entanglement is often claimed to be the reason for the *speed-up* in quantum computing. While this is certainly true for pure states [Vid03], it is not clear for mixed states. In fact, examples can be given which exhibit an exponential speed-up over all known classical algorithms but use only states with little or no entanglement [DV07]. Jozsa and Linden [JL03] suggest that it is more appropriate to attribute the power of quantum computing to the fact that an exponential amount of parameters is strictly necessary to describe the involved states mathematically.

2.1.5. Entanglement Criteria

The definition of entanglement cannot be used to answer the question whether a given state is entangled or not, but sufficient criteria can be developed. Again, I will only consider the bipartite case.

For pure states, the answer can easily be given by constructing the *Schmidt decomposition*, which can be done explicitly by performing a singular value decomposition. Given two Hilbert spaces H_A and H_B with dimensions n and m, respectively, and a state $|\psi\rangle \in H_A \otimes H_B$ one can always find orthonormal vectors $\{|\psi_1^A\rangle, |\psi_2^A\rangle, \ldots, |\psi_n^A\} \subset H_A$ and $\{|\psi_1^B\rangle, |\psi_2^B\rangle, \ldots, |\psi_m^B\} \subset H_B$ so that

$$|\psi\rangle = \sum_{i=1}^{m} \alpha_i |\psi_i^A\rangle \otimes |\psi_i^B\rangle\,, \quad \alpha_i \geq 0\,, \quad \sum_i \alpha_i^2 = 1\,.$$

The number of α_i which are non-zero is called the *Schmidt rank* r. It can now be seen from the definition of separability (2.1) that $|\psi\rangle$ is entangled if and only if $r > 1$.

All separable pure states have the property that they will stay pure if one of the parts is traced out. Therefore, entanglement can be checked by calculating the *purity* of the reduced state, which is strictly smaller than unity for all

entangled states:

$$\mathrm{Tr}(\mathrm{Tr}_B\,|\psi\rangle\langle\psi|)^2 < 1 \quad \Leftrightarrow \quad |\psi\rangle \text{ is entangled.}$$

For mixed states the situation is more complicated. As already mentioned, the general problem of deciding whether a mixed state is separable is NP-hard. Fortunately, useful criteria exist which can be calculated quickly and are able to detect entanglement in many important cases. Here I present only the widely used Peres-Horodecki or positive partial transpose (PPT) criterion [Per96, HHH96].

Again, we have a bipartite Hilbert space $H = H_A \otimes H_B$ and two bases spanning the factor spaces $\{|\psi_1^A\rangle, |\psi_2^A\rangle, \ldots, |\psi_N^A\rangle\} \subset H_A$ and $\{|\psi_1^B\rangle, |\psi_2^B\rangle, \ldots, |\psi_M^B\rangle\} \subset H_B$, which can be chosen arbitrarily. The matrix elements of the density matrix are given by

$$\rho_{m\mu n\nu} = \langle \psi_m^A \otimes \psi_\mu^B | \rho | \psi_n^A \otimes \psi_\nu^B \rangle \,.$$

Then the *partial transpose* of ρ with respect to B is defined by transposing the indices μ and ν only

$$\rho^{T_B}_{m\mu n\nu} = \rho_{m\nu n\mu} \,.$$

A different way of expressing the same operation is to write ρ as an $N \times N$ matrix of $M \times M$ matrices A_{nm}

$$\rho = \begin{pmatrix} A_{11} & \cdots & A_{1N} \\ \vdots & \ddots & \vdots \\ A_{N1} & \cdots & A_{NN} \end{pmatrix} .$$

Partially transposing ρ with respect to B amounts to transposing all matrices A_{nm}

$$\rho^{T_B} = \begin{pmatrix} A_{11}^T & \cdots & A_{1N}^T \\ \vdots & \ddots & \vdots \\ A_{N1}^T & \cdots & A_{NN}^T \end{pmatrix} .$$

It is easy to see that separable states will stay valid density matrices under partial transposition by looking at the definition of Werner (2.2).

In the same way, ρ can be partially transposed with respect to A, but conclusions about entanglement are independent of which subsystem is transposed.

The *Peres-Horodecki* (or *PPT*) criterion states that if ρ^{T_B} is not a positive matrix, ρ is entangled. This criterion for entanglement is sufficient, but not necessary.

However, if the dimension of ρ is less than six, it is both necessary and sufficient. All entangled states that are not detected by the criterion are denoted as *bound entangled* states, because it has been shown that no entanglement can be distilled from them by local operations [HHH98].

2.1.6. Entanglement Measures

Since entanglement is regarded as a resource, it is desirable not only to detect its presence, but also to quantify it. The decision problem is easy for pure states and difficult for mixed states. Obviously, this property generalizes to the quantification problem.

For pure states the von Neumann entropy $S(\rho) = -\operatorname{Tr}(\rho \log_2 \rho)$ of the reduced density matrix of either subsystem is the unique[2][3] [PR97] measure of entanglement called *entropy of entanglement* [BBPS96]

$$E(\psi) \coloneqq S(\operatorname{Tr}_A |\psi\rangle\langle\psi|) = S(\operatorname{Tr}_B |\psi\rangle\langle\psi|) \,.$$

Many mixed state measures reduce to the entropy of entanglement on pure states.

For mixed states it is not possible to define a unique measure. Different measures impose different orderings of the states, which can be interpreted as the existence of different "types" of entanglement [HHHH09]. Good entanglement measures should be monotonous under local operations and classical communication (LOCC) as has first been demanded by Bennett *et al.* [BDSW96], because entanglement by definition cannot be increased by LOCC. The operationally defined measures *entanglement cost* E_C and *distillable entanglement* E_D fulfill this axiom. E_C and E_D are complementary in the sense that E_C is the number of Bell pairs that are needed to create a given state by LOCC, and E_D is the number of Bell pairs that can be distilled out of a given state by LOCC[2]. It is always $E_D \leq E_C$ and on pure states $E_D = E_C$.

The number of mixed state measures is quite large, most of them are either defined by their distance $\mathcal{D}$ to the set of separable states S

$$E(\rho) = \inf_{\sigma \in S} \mathcal{D}(\rho, \sigma)$$

[2] In the limit of infinitely many copies of the state.

[3] It becomes unique by only imposing that it does not increase under local operations.

or by the convex roof extension [Uhl98] of a pure state measure

$$E(\rho) = \inf_{p_i,\psi_i} \sum_i p_i E(\psi_i)\,, \quad \rho = \sum_i p_i |\psi_i\rangle\langle\psi_i|\,, \quad p_i \leq 1\,, \quad \sum_i p_i = 1\,.$$

In the first case, a suitable distance measure $\mathcal{D}$ has to be chosen.

Entanglement measures are hard to evaluate. The only exception is *negativity* which was introduced by Życzkowski *et al.* [ZHSL98] and Vidal and Werner [VW02]. It is based on the PPT criterion and indicates "how much" a partially transposed state ρ^{T_B} violates positivity. The absolute value of all negative eigenvalues of ρ^{T_B} are summed up. This can be conveniently written as

$$\mathcal{N}(\rho) = \frac{\|\rho^{T_B}\|_1 - 1}{2}\,,$$

with $\|\rho\|_1 = \mathrm{Tr}\,\sqrt{\rho\rho^\dagger}$ being the trace norm. $\mathcal{N}$ is a LOCC monotone. A slight variation called *logarithmic negativity*, which is essentially the logarithm of the quantity defined above, is even more useful

$$E_{\mathcal{N}}(\rho) = \log_2 \|\rho^{T_B}\|_1 \equiv \log_2(2\mathcal{N}(\rho) + 1)/2\,. \tag{2.3}$$

It is additionally additive and an upper bound of the distillable entanglement E_D.

Logarithmic negativity does not reduce to the entropy of entanglement on pure states. Nevertheless, due to the advantage of being easily calculable, it is the measure of choice in this work.

2.2. Continuous Variable Systems

2.2.1. Motivation

The previous sections are applicable to finite dimensional systems. Without doubt, the two-state ("qubit") system is the most popular physical system in quantum information theory. However, many ideas of how to implement various steps of quantum information processing make use of infinite dimensional systems, most importantly coherent states of light. Even if the use of continuous variables is not the natural description of a system, it sometimes turns out that infinite dimensional systems are easier to treat than two-dimensional ones. The dissipative oscillator is exactly solvable, whereas the dissipative two-state

(spin-boson) model is not. At low temperatures the oscillator model effectively reduces to a two-state system. Therefore, one can expect conclusions drawn from solving an oscillator model in this limit to be valid for the two-state case as well [SH04].

2.2.2. Gaussian States and the Covariance Matrix

An n-mode continuous variable system is described by $2n$ canonical operators $\hat{q}_1, \ldots, \hat{q}_n$ and $\hat{p}_1, \ldots, \hat{p}_n$. They can be combined into a vector $\hat{\xi}$

$$\hat{\xi} = (\hat{q}_1, \ldots, \hat{q}_n, \hat{p}_1, \ldots, \hat{p}_n)^T .$$

We also define a corresponding c-number vector

$$\xi = (q_1, \ldots, q_n, p_1, \ldots, p_n)^T \equiv (q, p)^T .$$

A state of the system can be specified by the density matrix

$$\rho(q, q') = \langle q|\rho|q'\rangle ,$$

which determines the expectation values of all observables. The *Wigner function* W is obtained by applying the *Wigner transformation* to the density matrix [Wig32]

$$W(\xi) = \frac{1}{(2\pi\hbar)^n} \int dx_1 \ldots dx_n \, \rho(q - x/2, q + x/2) e^{ip^T x/\hbar} , \tag{2.4}$$

which is a quasi-probability distribution over phase space. It equally determines the expectation values of observables, but unlike a real probability distribution it can assume negative values. Fourier transforming the Wigner function leads to the *characteristic function*

$$\chi(\xi) = \int d^{2n}\eta \, W(\eta) e^{i\xi^T \eta} = \mathrm{Tr}(\rho W_\xi) ,$$

where $W_\xi = e^{i\xi^T \hat{\xi}}$ is the *phase space displacement* (or *Weyl*) *operator* [Wey27].

A state is a *Gaussian state* if its characteristic function is a Gaussian function

$$\chi(\xi) = e^{-\frac{1}{4}\xi^T C \xi + d^T \xi} .$$

$C_{\mu\nu} = \langle\{\hat{\xi}_\mu, \hat{\xi}_\nu\}\rangle \equiv \mathrm{Tr}[(\hat{\xi}_\mu\hat{\xi}_\nu + \hat{\xi}_\nu\hat{\xi}_\mu)\rho]$ is the *covariance matrix* collecting the second moments. As any covariance matrix, C is positive-semidefinite $C \geq 0$. We will see in the next section that C has to fulfill more stringent relations to be a valid quantum mechanical covariance matrix, however.

By phase space translations of individual modes, the displacement vector d can always be set to zero. This does not affect entanglement. Therefore, we will assume $d = 0$ in the following. Since the covariance matrix is real, symmetric, and defines a Gaussian state completely, only $n(n+1)/2$ real numbers are required to describe it. By restricting oneself to Gaussian states, still many states are covered that can be created easily in experiments. This includes vacua, as well as coherent, thermal, and squeezed states.

The *purity* μ of a Gaussian state is given by the determinant of the covariance matrix C

$$\mu = \mathrm{Tr}\,\rho^2 = \int d^{2n}\xi\, W(\xi)^2 = \frac{1}{\sqrt{\det C}}\,,$$

where $\mu = 1$ corresponds to a pure state. Therefore, C describes a pure state if and only if $\det C = 1$.

2.2.3. Uncertainty Relations

Correlations in quantum mechanics are restricted by uncertainty relations. The familiar inequality $\Delta x \Delta p \geq \hbar/2$ is not strong enough to characterize the covariance matrix C. We are going to derive the full *generalized uncertainty relations* in this section (see [SMD94]).

Let us define the *symplectic form*

$$\sigma = \begin{pmatrix} 0 & \mathbb{1}_n \\ -\mathbb{1}_n & 0 \end{pmatrix}\,, \quad \sigma^{-1} = \sigma^T = -\sigma\,,$$

which can be used to write the canonical commutation relations as ($\hbar = 1$)

$$[\hat{\xi}_\mu, \hat{\xi}_\nu] = i\sigma_{\mu\nu}\,.$$

The operator matrix $\hat{\xi}\hat{\xi}^T$ has the entries

$$(\hat{\xi}\hat{\xi}^T)_{\mu\nu} = \hat{\xi}_\mu\hat{\xi}_\nu = \frac{1}{2}\{\hat{\xi}_\mu, \hat{\xi}_\nu\} + \frac{i}{2}\sigma_{\mu\nu}$$

with the expectation values

$$\mathrm{Tr}(\rho(\hat{\xi}\hat{\xi}^T)_{\mu\nu}) = \frac{1}{2}C_{\mu\nu} + \frac{i}{2}\sigma_{\mu\nu}\,.$$

Furthermore, we consider the vector $c = (c_1, \ldots, c_{2n})$ and use it to define the operator

$$\hat{Y} = c^T\hat{\xi} = c_1\hat{q}_1 + \ldots + c_{2n}\hat{p}_n\,.$$

Then $\hat{Y}^\dagger\hat{Y}$ is obviously a positive operator and $\mathrm{Tr}(\rho\hat{Y}^\dagger\hat{Y}) \geq 0$ is a positive number for all $c \in \mathbb{C}^{2n}$. This can be rewritten as

$$\mathrm{Tr}(\rho\hat{Y}^\dagger\hat{Y}) = c^\dagger\,\mathrm{Tr}(\rho\hat{\xi}\hat{\xi}^T)c \geq 0 \qquad \forall c \in \mathbb{C}^{2n}\,.$$

The last statement is equivalent to $\mathrm{Tr}(\rho\hat{\xi}\hat{\xi}^T)$ being a positive matrix, or in other words

$$C + i\sigma \geq 0\,, \tag{2.5}$$

which are the generalized uncertainty relations the covariance matrix C has to fulfill to be physical.

2.2.4. Separability

The PPT criterion from section 2.1.5 can now be applied to the continuous variable case in a very simple way [Simoo]. From the definition of the Wigner transformation (2.4) it follows immediately that transposing the density matrix is equivalent to time reversing the Wigner function

$$\begin{aligned}\rho &\to \rho^T\\ W(q,p) &\to W(q,-p)\,.\end{aligned}$$

Partial transposition is then equivalent to partial time reversal, i.e. only the impulses belonging to one subsystem are multiplied by -1. For example, in the two-mode bipartite case this gives

$$W(q_1,q_2,p_1,p_2) \to W(q_1,q_2,p_1,-p_2)\,.$$

The covariance matrix C transforms accordingly by reversing the sign of all entries containing exactly one p of the subsystem. In the two-mode case this amounts to conjugating C with the matrix

$$P = \mathrm{diag}(1,1,1,-1)\,, \qquad C^{T_B} = PCP\,.$$

Instead of checking whether the partially transposed density matrix ρ^{T_B} is still a valid density matrix, we require the partially time reversed covariance matrix C^{T_B} to fulfill the uncertainty relations $C^{T_B} + i\sigma \geq 0$ as a necessary criterion for separability. Conversely, a violation of the uncertainty relations is sufficient for entanglement. Similarly to the finite dimensional case, for two modes the criterion is both necessary and sufficient [Simoo].

2.2.5. Symplectic Eigenvalues

By Williamson's theorem [Wil36], there exists a real symplectic matrix $S \in \mathrm{Sp}(2n, \mathbb{R})$ which diagonalizes C by a *symplectic transformation*

$$S^T C S = D = \mathrm{diag}(\lambda_1, \ldots, \lambda_n, \lambda_1, \ldots, \lambda_n)\,,$$

where $\lambda_1, \ldots, \lambda_n$ are the *symplectic eigenvalues* of C. The transformation is called *normal-mode decomposition*. Conjugating the symplectic form σ by a symplectic matrix S leaves it invariant by definition, so $C + i\sigma$ transforms as

$$S^T(C + i\sigma)S = D + i\sigma = \begin{pmatrix} \lambda_1 & & & i & & \\ & \ddots & & & \ddots & \\ & & \lambda_n & & & i \\ -i & & & \lambda_1 & & \\ & \ddots & & & \ddots & \\ & & -i & & & \lambda_n \end{pmatrix}.$$

The positivity of $C + i\sigma$ is preserved, because the transformation is non-singular (it is a matrix congruence). Reading off the eigenvalues of $D + i\sigma$, we obtain the spectrum $\lambda_i \pm 1$. This allows the uncertainty relations (2.5) be reformulated as [SMD94]

$$\lambda_i \geq 1\,.$$

Conveniently, simple expressions can be given to calculate the symplectic eigenvalues of an arbitrary covariance matrix C, without having to find the diagonalizing symplectic transformation S first [VW02]. We will discuss two possibilities here. The symplectic eigenvalues are the absolute values of the eigenvalues of

$$i\sigma C\,,$$

or the positive square roots of the eigenvalues of

$$-\sigma C \sigma C \,.$$

Both statements can be proven by looking at the matrix

$$\sigma D = \begin{pmatrix} & & & \lambda_1 & & \\ & & & & \ddots & \\ & & & & & \lambda_n \\ -\lambda_1 & & & & & \\ & \ddots & & & & \\ & & -\lambda_n & & & \end{pmatrix} .$$

It has the eigenvalues $\pm i\lambda_i$. Since a similarity transformation does not change the eigenvalues, we see by writing

$$\sigma D = \sigma S^T C S = S^{-1}(\sigma C) S$$

that σC has the same eigenvalues, this proves the first statement. The second one can be shown by applying the same consideration to the matrix $-(\sigma D)^2$, which has the eigenvalues λ_i^2

$$\sigma D \sigma D = \sigma S^T C S \sigma S^T C S = S^{-1} \sigma C S S^{-1} \sigma C S = S^{-1}(\sigma C \sigma C) S \,.$$

2.2.6. Logarithmic Negativity

The main advantage of using logarithmic negativity as an entanglement measure is its easy computability. Fortunately, this property generalizes to the infinite dimensional case. A simple formula for the logarithmic negativity $E_{\mathcal{N}}$ of a continuous variable system can be given in terms of the symplectic eigenvalues of its partially time reversed covariance matrix C^{T_B}.

Following the derivation in [VW02], we note that the computation of the trace norm (2.3) is simplified by applying the normal-mode decomposition to C^{T_B}. In the Hilbert space description, the state is turned into a product state. Hence, the contribution to the trace norm can be calculated separately for each oscillator, resulting in a sum over all modes $i = 1, \ldots, n$. Each summand depends only on the single symplectic eigenvalue $\tilde{\lambda}_i$ corresponding to the mode i

$$E_{\mathcal{N}} = \sum_{i=1}^{n} \log_2 \|\rho_i\|_1 \,,$$

where ρ_i is the density matrix of a single oscillator Gaussian state with the 2×2 covariance matrix $\mathrm{diag}(\tilde{\lambda}_i, \tilde{\lambda}_i)$. Now, the only remaining task is to calculate $\log_2 \|\rho_i\|_1$. For this we introduce a general Gaussian state

$$\rho_i = (1 - z_i) \sum_{m=0}^{\infty} z_i^m |m\rangle\langle m| \,,$$

where $|m\rangle$ is the usual number basis and $-1 < z_i < 1$. Negative z_i correspond to unphysical states, which occur after partially transposing an entangled state. Calculating the trace norm is straightforward

$$\begin{aligned} \|\rho_i\|_1 &= \mathrm{Tr}\sqrt{\rho_i \rho_i^\dagger} \\ &= \mathrm{Tr}\Big((1 - z_i) \sum_{m}^{\infty} |z_i|^m |m\rangle\langle m|\Big) \\ &= (1 - z_i) \sum_{m}^{\infty} |z_i|^m \\ &= \frac{1 - z_i}{1 - |z_i|} \,. \end{aligned}$$

Since the covariance matrix is diagonal, the symplectic eigenvalue is equal to the expectation values of $2\hat{q}^2$ and $2\hat{p}^2$

$$\begin{aligned} \tilde{\lambda}_i &= 2\langle \hat{q}^2 \rangle = 2\langle \hat{p}^2 \rangle \\ &= 2\,\mathrm{Tr}\Big(\rho_i \frac{1}{2}(\hat{q}^2 + \hat{p}^2)\Big) \\ &= 2(1 - z_i) \sum_{m}^{\infty} z_i^m \Big(m + \frac{1}{2}\Big) \\ &= \frac{2}{1 - z_i} + 1 \,. \end{aligned}$$

Solving for z_i gives

$$z_i = \frac{\tilde{\lambda}_i - 1}{\tilde{\lambda}_i + 1}$$

and plugging this result into the expression for the trace norm completes the calculation

$$\|\rho_i\|_1 = \begin{cases} 1 & \text{if } \tilde{\lambda}_i > 1 \,, \\ 1/\tilde{\lambda}_i & \text{if } \tilde{\lambda}_i < 1 \,. \end{cases}$$

Finally, we are able to write down the formula for the logarithmic negativity

$$E_{\mathcal{N}} = -\sum_{i=1}^{n} \log_2(\min(1, \tilde{\lambda}_i)) ,$$

where $\tilde{\lambda}_1, \ldots, \tilde{\lambda}_n$ are the symplectic eigenvalues of C^{T_B}.

2.3. Dissipation and Quantum Mechanics

For a long time it remained unclear how to properly model *dissipation* in a quantum mechanical system. In most real physical systems it obviously plays a significant role, but the Schrödinger equation is unable to describe it due to its unitarity. Any ad hoc modifications of the Schrödinger dynamics, which were constructed to yield known dissipative behavior in the classical limit, have been shown to be inconsistent. In the quantum regime they clearly lead to incorrect results [Weio8].

The only viable approach is the *system-plus-reservoir* concept. The quantum system is modeled as the system of interest combined with a large, often infinite number of reservoir modes. The dynamics of the whole system are always unitary, guaranteeing valid quantum behavior. At some point, the degrees of freedom of the reservoir are simply disregarded. In this way, energy can be "lost" by transferring it from the system to the reservoir. Of course, a finite number of reservoir modes leads to a finite recurrence time, so for truly irreversible dynamics an infinite number of modes is necessary. However, a finite number of modes still gives correct results for sufficiently short times.

At this point it should be clear that dissipation is modeled in a similar way as decoherence (section 2.1.1). In fact, these notions are often used synonymously. Strictly speaking, however, they have a slightly different meaning. While dissipation denotes the irreversible loss of energy to the environment, decoherence signifies the loss of quantum coherence between different parts of the system, which is possible without any dissipation.

Two possible choices to determine the time evolution are either to work in the density matrix formalism or in the Heisenberg picture. In the first case one arrives at a *quantum master equation*, which describes the dynamics of the reduced density matrix. In the second case the dynamics of the system operators are given by a *quantum Langevin equation* [Sen60, Mor65, FKM65].

Formally, both approaches are equivalent, but in practice most approximations are easier to apply to the master equation. The most popular approximation is the *Lindblad master equation* [Lin76, GKS76]. Because it is local in time, it can be easily solved. It is a completely positive map, which means that it manifestly has valid reduced density matrices as solutions for all initial conditions. It is widely used and quite successful in NMR and quantum optics. Since it is based on second order perturbation theory, the rotating-wave approximation, and the Born-Markov approximation, it is only valid in the weak coupling limit and only if the dynamical time scale of the environment is much shorter than the time scale of the system.

A third powerful approach to open quantum systems is the the *Feynman-Vernon influence functional* method [FV63]. It has given rise to numerous analytical and numerical results, which go beyond the capabilities of the usual Lindblad master equation [Wei08].

One more method that should be mentioned is the *Nakajima-Zwanzig projection operator* technique [Nak58, Zwa60], which was later developed into the *time convolution-less projection operator* method by Shibata *et al.* [STH77] (see also [BP02]).

The main focus of this work will be on the quantum Langevin equation method applied to a two-oscillator extension of the *Caldeira-Leggett model*. The Caldeira-Leggett model was originally introduced by Ullersma [Ull66] and later generalized by Zwanzig [Zwa73] as well as by Caldeira and Leggett [CL83a] (who employed the influence functional method). The Langevin method is limited to bilinear interactions, but in that case it allows for finding exact solutions with relatively little effort.

3. Modelling Dissipation with Quantum Langevin Equations

3.1. Introduction

Modeling dissipation with oscillators has a long history. Some of the origins have been introduced in the previous chapter. Instead of directly writing down a Hamiltonian with infinitely many oscillators, we will start with a model used by Dekker [Dek85], Yurke [Yur86], and Unruh and Zurek [UZ89]. The position of an oscillator is coupled to the velocity of a quantum field. This results in a manifestly positive Hamiltonian (no "runaway" solutions). In this way, we can provide a clean and straightforward derivation of the quantum Langevin equation. Another advantage of this approach is that the quantum field inherently respects causality, so we do not need to worry about this.

Comparing with the Caldeira-Leggett model with a bilinear amplitude coupling, it turns out that both models are equivalent and can be transformed into each other by a Legendre transformation. However, a so called "counter-term" has to be added to the Hamiltonian of the Caldeira-Leggett model by hand, which appears naturally starting from the model by Dekker.

We will see that the Quantum Langevin Equation turns into an integro-differential equation over the real numbers for the special case of Gaussian states. The solution of this will be presented in later chapters.

3.2. Lagrangian

We extend the Lagrangian from [UZ89] to include two identical oscillators Q_1 and Q_2 at the positions $\mathbf{d}/2$ and $-\mathbf{d}/2$, respectively, coupled to a three-

dimensional free scalar field ϕ,

$$L = \frac{1}{2}\sum_{i=1,2} M(\dot{Q}_i^2 - \Omega_0^2 Q_i^2) + \frac{1}{2}\int d^3\mathbf{x}(\dot{\phi}^2 - (\nabla\phi)^2) \\ - \int d^3\mathbf{x}\,\dot{\phi}(\mathbf{x})\left[f\left(\left|\mathbf{x} - \frac{\mathbf{d}}{2}\right|\right)Q_1 + f\left(\left|\mathbf{x} + \frac{\mathbf{d}}{2}\right|\right)Q_2\right],$$

where $f(x)$, sharply peaked around $x = 0$, determines the coupling of the oscillators to the field. The results in this section have been developed in collaboration with Friedemann Queisser [Que11].

Later, we will also consider the case of a one-dimensional field. Whenever the one-dimensional expressions differ significantly from the three-dimensional ones, this will be pointed out. Not all differences can be encapsulated in the spectral density of the coupling as it can be done for systems with no spatial extension.

The total energy is clearly always positive, because the velocity coupling cancels out when writing down the energy

$$E = \frac{1}{2}\int d^3\mathbf{x}(\dot{\phi}^2 + (\nabla\phi)^2) + \frac{1}{2}\sum_{i=1,2} M(\dot{Q}_i^2 + \Omega_0^2 Q_i^2) \geq 0\,.$$

Equivalently, one can say that the field does not renormalize the mass of the system oscillators.

Decomposing the field into eigenmodes, where $\mathbf{k}$ is a wave vector $\mathbf{k} \in \frac{2\pi}{L}\mathbb{Z}^3$, we obtain

$$\phi(\mathbf{x}) = \frac{1}{\sqrt{V}}\sum_{\mathbf{k}} \phi_{\mathbf{k}} e^{i\mathbf{k}\mathbf{x}}\,,$$

and $V = L^3$ is the quantization volume. Then, the field part of the Lagrangian turns into

$$L_{\text{bath}} = \frac{1}{2}\sum_{\mathbf{k}}(\dot{\phi}_{\mathbf{k}}\dot{\phi}_{-\mathbf{k}} - k^2\phi_{\mathbf{k}}\phi_{-\mathbf{k}})$$

and the interaction part into

$$L_{\text{int}} = -\sum_{\mathbf{k}} g_k(\dot{\phi}_{\mathbf{k}} e^{i\mathbf{k}\mathbf{d}/2}Q_1 + e^{-i\mathbf{k}\mathbf{d}/2}Q_2)\,,$$

where the g_k are the Fourier coefficients of the coupling function $f(x)$. In one dimension the summation is over one dimensional modes with one dimensional

wave vectors $\mathbf{k} \in \frac{2\pi}{L}\mathbb{Z}$ and the quantization volume is $V = L$. To simplify notation we use the bold face symbol $\mathbf{k}$ even if the wave vector is just a single number.

To facilitate the interpretation as a harmonic oscillator model, masses can be reintroduced by $c = 1$, $\omega_k = k$, $\phi_\mathbf{k} \to \sqrt{m_k}\phi_\mathbf{k}$, and $g_k \to g_k/\sqrt{m_k}$. The full Lagrangian then reads

$$L = \sum_{i=1,2} \frac{1}{2}(M\dot{Q}_i^2 - M\Omega_0^2 Q_i^2) + \sum_\mathbf{k} \frac{1}{2}(m_k \dot{\phi}_\mathbf{k}\dot{\phi}_{-\mathbf{k}} - m_k\omega_k^2\phi_\mathbf{k}\phi_{-\mathbf{k}}) - g_k\dot{\phi}_\mathbf{k}(Q_1 e^{i\mathbf{k}\mathbf{d}/2} + Q_2 e^{-i\mathbf{k}\mathbf{d}/2})\,.$$

3.3. Hamiltonian

We now switch to the Hamiltonian formalism by considering the generalized momenta

$$\pi_\mathbf{k} = \frac{\partial L}{\partial \dot{\phi}_\mathbf{k}} = m_k\dot{\phi}_{-\mathbf{k}} - g_k(Q_1 e^{i\mathbf{k}\mathbf{d}/2} + Q_2 e^{-i\mathbf{k}\mathbf{d}/2})$$
$$P_i = \frac{\partial L}{\partial \dot{Q}_i} = M\dot{Q}_i\,.$$

While the transformations of the system and the bath part are standard, in the interaction part an additional term is generated, which is generally referred to as the *counter-term* [DCo6]

$$H = \sum_{i=1,2}\Big(\frac{P_i^2}{2M} + \frac{1}{2}M\Omega_0^2 Q_i^2\Big) + \sum_\mathbf{k}\Big[\frac{\pi_\mathbf{k}\pi_{-\mathbf{k}}}{2m_k} + \frac{1}{2}m_k\omega_k^2\phi_\mathbf{k}\phi_{-\mathbf{k}} + \frac{g_k}{m_k}\pi_\mathbf{k}(Q_1 e^{-i\mathbf{k}\mathbf{d}/2} + Q_2 e^{i\mathbf{k}\mathbf{d}/2}) + \underbrace{\frac{g_k^2}{2m_k}(Q_1^2 + Q_2^2 + 2Q_1Q_2\cos(\mathbf{k}\mathbf{d}))}_{\text{counter-term}}\Big]\,.$$

Finally, the canonical transformation $\pi_\mathbf{k} \to \omega_k\tilde{\phi}_\mathbf{k}$, $\phi_\mathbf{k} \to \tilde{\pi}_\mathbf{k}/\omega_k$ with the rescaling $g_k \to g_k/\omega_k$ (for a cleaner notation the tilde will be immediately dropped again) leads to the Hamiltonian with bilinear amplitude coupling which is

familiar from the Caldeira-Leggett model

$$H = \sum_{i=1,2}\Big(\frac{P_i^2}{2M} + \frac{1}{2}M\Omega_0^2 Q_i^2\Big) + \sum_{\mathbf{k}}\Big[\frac{\pi_{\mathbf{k}}\pi_{-\mathbf{k}}}{2m_k} + \frac{1}{2}m_k\omega_k^2\phi_{\mathbf{k}}\phi_{-\mathbf{k}} + \frac{g_k}{m_k}\phi_{\mathbf{k}}(Q_1 e^{-i\mathbf{k}\mathbf{d}/2} + Q_2 e^{i\mathbf{k}\mathbf{d}/2}) + \frac{g_k^2}{2m_k\omega_k^2}(Q_1^2 + Q_2^2 + 2Q_1Q_2\cos(\mathbf{k}\mathbf{d}))\Big].$$

As already mentioned, the counter-term occurs naturally in the derivation and cannot simply be dropped without introducing unwanted side effects. We will see that it cancels out later and leads to causality preserving Quantum Langevin Equations (QLEs).

3.4. Quantum Langevin Equations

Building on this Hamiltonian, the first steps towards the full time evolution of the Heisenberg operators $Q_i(t)$ can be pursued by elementary means [FK87]. We write down the Heisenberg equations of motion

$$\begin{aligned}\dot{Q}_{1/2}(t) &= \frac{1}{M}P_{1/2}(t)\\ \dot{P}_{1/2}(t) &= -M\Omega_0^2 Q_{1/2}(t)\\ &\quad - \sum_{\mathbf{k}}\Big[\frac{g_k^2}{m_k\omega_k^2}(Q_{1/2}(t) + Q_{2/1}(t)\cos(\mathbf{k}\mathbf{d})) + g_k\phi_{\mathbf{k}}(t)e^{\mp i\mathbf{k}\mathbf{d}/2}\Big] \quad (3.1)\end{aligned}$$

and

$$\begin{aligned}\dot{\phi}_{\mathbf{k}} &= \frac{1}{m_k}\pi_{-\mathbf{k}}\\ \dot{\pi}_{-\mathbf{k}}(t) &= -\omega_k\phi_{\mathbf{k}}(t) - \frac{g_k}{m_k}\Big(Q_1(t)e^{i\mathbf{k}\mathbf{d}/2} + Q_2(t)e^{-i\mathbf{k}\mathbf{d}/2}\Big).\end{aligned}$$

The equations for the bath degrees of freedom $\phi_{\mathbf{k}}$ can be solved using standard Laplace transform techniques, which leads to the expression

$$\begin{aligned}\phi_{\mathbf{k}}(t) = \sqrt{\frac{1}{2m_k\omega_k}}(b_{\mathbf{k}}e^{-i\omega_k t} + b_{-\mathbf{k}}^\dagger e^{i\omega_k t})\\ - \frac{g_k}{m_k\omega_k}\int_0^t dt'\sin(\omega_k(t-t'))\Big(Q_1(t')e^{i\mathbf{k}\mathbf{d}/2} + Q_2(t')e^{-i\mathbf{k}\mathbf{d}/2}\Big)\end{aligned}$$

where $b_{\mathbf{k}}$, $b_{\mathbf{k}}^{\dagger}$ are the standard creation and annihilation operators defined by

$$\phi_{\mathbf{k}}(0) = \sqrt{\frac{\hbar}{2m_k\omega_k}}(b_{\mathbf{k}} + b_{-\mathbf{k}}^{\dagger})$$
$$\pi_{\mathbf{k}}(0) = -i\sqrt{\frac{\hbar m_k\omega_k}{2}}(b_{\mathbf{k}} - b_{-\mathbf{k}}^{\dagger})\,.$$

The solution can be substituted into (3.1). Bringing all system operators to the left side and all bath operators to the right side, we have

$$\ddot{Q}_{1/2}(t) + \Omega_0^2 Q_{1/2}(t) + \sum_{\mathbf{k}} \frac{g_k^2}{Mm_k\omega_k^2}\Big[\Big(Q_{1/2}(t) + Q_{2/1}(t)\cos(\mathbf{kd})\Big) - \omega_k \int_0^t dt' \sin(\omega_k(t-t'))\Big(Q_{1/2}(t') + Q_{2/1}(t')e^{\mp i\mathbf{kd}}\Big)\Big] = B_{1/2}(t)\,,$$

with the abbreviations

$$B_{1/2}(t) = -\sum_{\mathbf{k}} \sqrt{\frac{g_k^2\hbar}{2M^2m_k\omega_k}}\, e^{\mp i\mathbf{kd}/2}(b_{\mathbf{k}}e^{-i\omega_k t} + b_{-\mathbf{k}}^{\dagger}e^{i\omega_k t})\,,$$

where the index 1 corresponds to the negative sign in the exponent and the index 2 to the positive sign. Now, we can rewrite the integral using the identity

$$\frac{d}{dt}\int_0^t dt' \cos(\omega_k(t-t'))Q_{1/2}(t') = -\omega_k \int_0^t dt' \sin(\omega_k(t-t'))Q_{1/2}(t') + Q_{1/2}(t)\,.$$

Note that due to the identity

$$\sum_{\mathbf{k}} \cos(\mathbf{kd}) f(k) = \frac{1}{2}\sum_{\mathbf{k}}(e^{i\mathbf{kd}} + e^{-i\mathbf{kd}})f(k) = \sum_{\mathbf{k}} e^{\pm i\mathbf{kd}} f(k)\,,$$

the additional term produced here exactly cancels the counter term

$$\ddot{Q}_{1/2}(t) + \Omega_0^2 Q_{1/2}(t) + \sum_{\mathbf{k}} \frac{g_k^2}{Mm_k\omega_k^2} \cdot \frac{d}{dt}\int_0^t dt' \cos(\omega_k(t-t'))\Big(Q_{1/2}(t') + Q_{2/1}(t')e^{\mp i\mathbf{kd}}\Big) = B_{1/2}(t)\,.$$

The remaining step to arrive at the QLEs is to take the continuum limit of bath modes characterized by the *coupling spectral density* [CL83b]

$$J(\omega) = \sum_{\mathbf{k}} \frac{g_k^2}{2Mm_k\omega_k}\delta(\omega - \omega_k)\,. \tag{3.2}$$

In theoretical works the spectral density is usually used to *define* the coupling constants g_k, because most physical situations can be mapped onto a spectral density of the form $J(\omega) \propto \omega^s$, where $s < 1$ is called a *sub-ohmic* environment, $s = 1$ is an *ohmic* environment, and $s > 1$ *super-ohmic*. In this way, it is possible to cover all relevant cases without having to specify the underlying model in detail. Of course, in reality it is the other way around: The coupling constants g_k are fixed and the spectral density $J(\omega)$ follows from them.

For a three-dimensional bath, the angles can be integrated out

$$\int_{\mathbb{R}^3} \mathrm{d}\mathbf{k}\, e^{\pm i\mathbf{kd}} f(k) = 4\pi \int_0^\infty \mathrm{d}k\, \frac{\sin(kd)}{kd} k^2 f(k)\,.$$

A one-dimensional bath leads to

$$\int_{-\infty}^{\infty} dk\, e^{\pm ikr} f(k) = 2\int_0^\infty dk \cos(kd) f(k)\,.$$

With the coupling spectral density, we also introduce the position r dependent *damping kernel* $\Gamma_r(t)$ [Mor65] (see also [BP02]) by

$$\begin{aligned}\Gamma_r(t) &= \sum_{\mathbf{k}} \frac{g_k^2}{Mm_k\omega_k^2}\cos(w_k t)e^{-i\mathbf{kr}} \\ &= \begin{cases} 2\displaystyle\int_0^\infty d\omega\, \frac{J(\omega)}{\omega}\cos(\omega t)\cos(\omega r) & \text{for a 1D bath} \\ 2\displaystyle\int_0^\infty d\omega\, \frac{J(\omega)}{\omega}\cos(\omega t)\frac{\sin(\omega r)}{\omega r} & \text{for a 3D bath.}\end{cases}\end{aligned} \tag{3.3}$$

Close inspection of the damping kernel $\Gamma_r(t)$ reveals that it is always strongly peaked around $t = r$ independently of the exact form of $J(\omega)$ (see figure 3.1 and 3.2). This ensures that the oscillators feel the influence of each other only after a time r/c ($c = 1$) has passed. Finally, we have

$$\begin{aligned}&\ddot{Q}_{1/2}(t) + \Omega_0^2 Q_{1/2}(t) \\ &\qquad + \frac{d}{dt}\int_0^t dt' \Big(\Gamma_0(t-t')Q_{1/2}(t') + \Gamma_d(t-t')Q_{2/1}(t')\Big) = B_{1/2}(t)\,,\end{aligned}$$

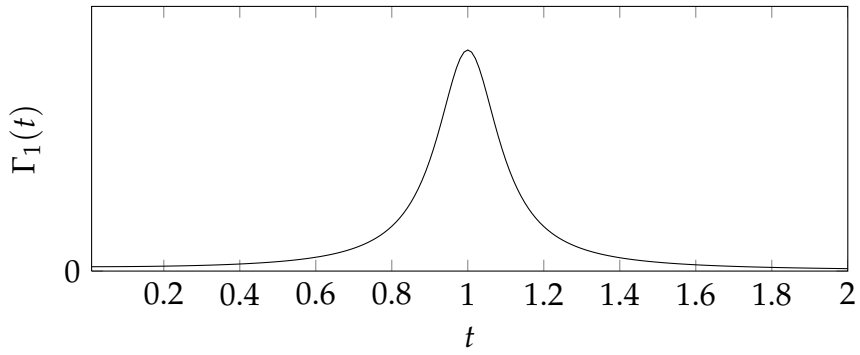

Figure 3.1.: Damping kernel for a free one-dimensional bath with a spectral density of the form $J(\omega) \propto \omega\, e^{-\omega/(10\Omega_0)}$ and $r = 1$.

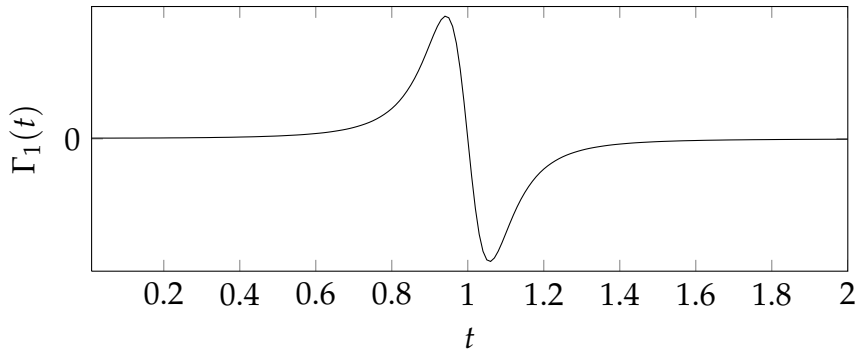

Figure 3.2.: Damping kernel for a free three-dimensional bath with a spectral density of the form $J(\omega) \propto \omega^3\, e^{-\omega/(10\Omega_0)}$ and $r = 1$.

which can be written in the more compact form

$$\dot{\mathbf{y}}(t) + \mathcal{Z}\mathbf{y}(t) + \frac{d}{dt}\int_0^t dt'\, \Gamma(t-t')\mathbf{y}(t') = \mathbf{B}(t)\,, \tag{3.4}$$

where $\mathbf{y} = (Q_1, Q_2, \dot{Q}_1, \dot{Q}_2)$, $\mathbf{B} = (0, 0, B_1, B_2)$, and

$$\mathcal{Z} = \begin{pmatrix} 0 & 0 & -1 & 0 \\ 0 & 0 & 0 & -1 \\ \Omega_0^2 & 0 & 0 & 0 \\ 0 & \Omega_0^2 & 0 & 0 \end{pmatrix}, \; \Gamma(t) = \begin{pmatrix} 0 & 0 & 0 & 0 \\ 0 & 0 & 0 & 0 \\ \Gamma_0(t) & \Gamma_d(t) & 0 & 0 \\ \Gamma_d(t) & \Gamma_0(t) & 0 & 0 \end{pmatrix}.$$

There is a clear classical interpretation of the dynamics at hand: The two oscillators are coupled via a retarded, bath-mediated interaction and are subject

to friction as well as a stochastic driving force. As promised before, due to the retardation by the peaked $\Gamma_d(t)$, this equation does not violate causality.

The solution $\mathbf{y}(t)$ of (3.4) for initial $\mathbf{y}(0)$ and inhomogeneity $\mathbf{B}(t)$ is

$$\mathbf{y}(t) = \mathcal{G}(t)\mathbf{y}(0) + \int_0^t dt'\, \mathcal{G}(t-t')\mathbf{B}(t')\,,$$

where the Green's function $\mathcal{G}(t)$ solves the homogeneous part of (3.4). The matrix $\mathcal{G}(t)$ has real entries and its time evolution is given by the solution of the corresponding classical equations of motion.

The matter is simplified enormously by restricting oneself to Gaussian states of the system. This is still exact, because Gaussian states are preserved by the quadratic Hamiltonian [SSM88]. We then only need the time evolution of the covariance matrix, which is given by

$$C_{lm} = \langle \mathbf{y}_l \mathbf{y}_m + \mathbf{y}_m \mathbf{y}_l \rangle_{\rho_S} \equiv \mathrm{Tr}[(\mathbf{y}_l \mathbf{y}_m + \mathbf{y}_m \mathbf{y}_l)\rho_S]\,.$$

We assume that the system and bath are initially in a factorizing state $\rho_{SB} = \rho_S \otimes \rho_T$ with ρ_T being a thermal state of the bath with temperature T. The time evolution of the covariance matrix $C(t)$ can then be expressed as

$$\boxed{C(t) = \mathcal{G}(t)C(0)\mathcal{G}(t)^\intercal + \int_0^t dt' \int_0^t dt'' \mathcal{G}(t-t')\mathcal{K}(t'-t'')\mathcal{G}(t-t'')^\intercal}\,. \tag{3.5}$$

Here, $C(0)$ is the initial covariance matrix of the system, corresponding to ρ_s, and the matrix $\mathcal{K}(t) = 2\langle\{\mathbf{B}(t)\mathbf{B}(0)^\intercal\}\rangle_{\rho_T}$ contains the bosonic bath correlations. The only non-vanishing entries are $\mathcal{K}_{34}(t) = \mathcal{K}_{43}(t) = K_d(t)$ and $\mathcal{K}_{33}(t) = \mathcal{K}_{44}(t) = K_0(t)$ with

$$K_r(t) = \begin{cases} 2\int_0^\infty d\omega\, J(\omega) \coth\left(\frac{\omega}{2T}\right)\cos(\omega t)\cos(\omega r) & \text{for a 1D bath} \\ 2\int_0^\infty d\omega\, J(\omega) \coth\left(\frac{\omega}{2T}\right)\cos(\omega t)\frac{\sin(\omega r)}{\omega r} & \text{for a 3D bath,} \end{cases} \tag{3.6}$$

which are obtained via a standard calculation.

The important point is that we have turned the operator valued QLE into an integro-differential equation over the real numbers that only requires the solutions of the classical equations of motion. While there is still some work remaining, it is now possible to calculate the exact open dynamics of the

covariance matrix with some numerical effort. This is what we are going to do in the next chapters.

As a last remark it shall be noted that upon changing the coordinates Q_1 and Q_2 to center of mass $Q_c = Q_1 + Q_2$ and relative position $Q_r = Q_1 - Q_2$, it is easy to see that for $d = 0$ only the center of mass motion is damped, whereas the relative motion is not

$$\ddot{Q}_c(t) + \Omega_0^2 Q_c(t) + 2\frac{d}{dt}\int_0^t dt' \Gamma_0(t-t') Q_c(t') = B_1(t) + B_2(t)$$
$$\ddot{Q}_r(t) + \Omega_0^2 Q_r = B_1(t) - B_2(t)\,.$$

The degree of freedom of the relative motion therefore acts as a kind of *decoherence free subspace*. This has already been noticed by Hörhammer and Büttner [HB08] and deemed unrealistic. While they artificially added damping to the relative motion, our model always includes damping for $d > 0$.

4. Free Space Environment

4.1. Introduction

In this chapter we will discuss solutions of the model introduced in the previous chapter. The environment in this model is a free scalar field, which might also be thought of as a simplified description of electromagnetic vacuum modes interacting with the system oscillators via the dipole approximation.

First, we will present a class of coupling spectral densities which cover most common real physical cases. Then, we will calculate the asymptotic state of the system in equilibrium with the environment in order to determine the amount of entanglement that is contained in it. Finally, we will also present the full time evolution of the entanglement of the system, because the amount of entanglement during the evolution can be larger than in the equilibrium state.

4.2. Coupling Spectral Density

In general, the coupling spectral density of an environment is typically assumed to be of the form

$$J(\omega) = \frac{2}{\pi}\gamma\omega \left(\frac{\omega}{\Omega_c}\right)^{s-1} e^{-\omega/\Omega_c} . \tag{4.1}$$

In the case $s = 1$, the limit $\Omega_c \to \infty$ leads to Ohmic damping with the damping constant γ. The damping kernel $\Gamma_r(t)$ turns into a δ-peak and the QLE can be written as a *delay differential equation* (DDE) [BP02, Zel06]

$$\ddot{Q}_{1/2}(t) + \Omega_0^2 Q_{1/2}(t) + 2\gamma Q_{1/2}(t) + 2\gamma Q_{2/1}(t-d) = B_{1/2}(t) .$$

This, however, results in unphysical divergence of some of the observables, as for example the mean kinetic energy [BP02]. Therefore, we will not discuss it further and consider only finite Ω_c.

Since the spectral density is defined by a summation over frequencies (3.2), but a three-dimensional bath contains a summation over all wave vectors $\mathbf{k}$ and not just scalar wave numbers k, we need to think about how this can be mapped onto each other. A simple strategy is to demand that the total coupling strength remains the same

$$\sum_{k\geq 0} \tilde{g}_k^2 \stackrel{!}{=} \sum_{\mathbf{k}} g_k^2 ,$$

where the g_k and $\tilde{g}_k$ are the coupling constants defined in the previous chapter. Taking the continuum limit and integrating out the angles gives

$$\begin{aligned} &\Rightarrow \int_0^{\Omega_c} d\omega\, \omega^s = 4\pi c \int_0^{\Omega_c} d\omega\, \omega^{s+2} \\ &\Rightarrow c \propto \frac{1}{\Omega_c^2} . \end{aligned}$$

Thus, the only difference that matters between one and three dimensions is the increase in the power of ω by two

$$J^{3\mathrm{D}}(\omega) \propto J^{1\mathrm{D}}(\omega) \left(\frac{\omega}{\Omega_c}\right)^2 .$$

The proportionality constant only depends on s and can be absorbed into the coupling γ.

As soon as the systems has a spatial extension $d > 0$, not all of the differences between different dimensions can be captured by adjusting the spectral density. This leads to the two different expressions for the damping kernel (3.3) and the bath correlations (3.6).

For an ohmic one-dimensional environment we will also consider a Drude cut-off

$$J(\omega) = \frac{2}{\pi}\gamma\omega \frac{\Omega_c^2}{\Omega_c^2 + \omega^2} , \tag{4.2}$$

which will enable us to find an analytic expression for the ultra-short time evolution of the entanglement.

The cut-off frequency Ω_c is a property of the coupling mechanism rather than the bath. Typically, the coupling strength $|g_k|$ drops steeply when the wavelength $\lambda = 2\pi|k|^{-1}$ falls below the system size l. Therefore, a good order of magnitude estimate is $\lambda \sim l$, which is equivalent to $\Omega_c \sim 2\pi c/l$.

4.3. Long-term Asymptotic Entanglement

If it exists, the asymptotic state $t \to \infty$ can be calculated by taking the Fourier transform of the Langevin equation (3.4) [GZ04], from which we have dropped the quickly decaying term $\mathbf{y}(0)\Gamma(t)$. The QLE

$$\dot{\mathbf{y}}(t) + \mathcal{Z}\mathbf{y}(t) + \int_{-\infty}^{t} dt'\, \theta(t-t')\Gamma(t-t')\dot{\mathbf{y}}(t') = \mathbf{B}(t)$$

is transformed into the algebraic equation

$$-i\omega\mathbf{y}(\omega) + \mathcal{Z}\mathbf{y}(\omega) - i\omega\mathcal{R}(\omega)\mathbf{y}(\omega) = \mathbf{B}(\omega)$$

with the matrix $\mathcal{R}(\omega)$ defined by

$$\begin{aligned}\tilde{\Gamma}(\omega) &= \frac{1}{2}\int_{-\infty}^{\infty} dt\, e^{i\omega t}\Gamma(t) \\ \mathcal{R}(\omega) &= \int_{0}^{\infty} dt\, e^{i\omega t}\Gamma(t) = \tilde{\Gamma}(\omega) + \frac{i}{\pi}P\int_{-\infty}^{\infty} d\omega' \frac{\tilde{\Gamma}(\omega')}{\omega'-\omega}\,,\end{aligned}$$

where P denotes the principal value. The Fourier transformation of $\Gamma(t)$ cancels with the integration over ω, so that the matrix elements $\tilde{\Gamma}_r(\omega)$ of $\tilde{\Gamma}(\omega)$ (corresponding to the elements $\Gamma_r(t)$ of $\Gamma(t)$) are simply given by

$$\tilde{\Gamma}_r(\omega) = \frac{\pi}{M}\frac{J(|\omega|)}{|\omega|}\cos(\omega r)\,.$$

The equilibrium equal time correlation function of the system can then be expressed in terms of the matrix

$$\mathcal{F}(\omega) = (-i\omega + \mathcal{Z} - i\omega\mathcal{R}(\omega))^{-1}$$

for a one-dimensional bath as the integral

$$\langle\{\mathbf{y}_i(0), \mathbf{y}_j(0)\}\rangle = 4\sum_{k,l\in\{3,4\}}\int_0^\infty d\omega\, \mathcal{F}_{ik}(\omega)\mathcal{F}_{jl}(-\omega)J(\omega)\coth\left(\frac{\omega}{2T}\right)\cos(\omega d\delta_{kl})\,,$$

which can be evaluated numerically. For a three-dimensional bath $\cos(\omega d)$ is replaced by $\sin(\omega d)/(\omega d)$ as before. The above procedure only leads to valid results if a unique asymptotic state actually exists. This is the case for a generic bath in free space and $d > 0$.

Alternatively, it is possible to find the asymptotic state of the model with a Drude cut-off by applying a Laplace transformation $f(s) = \int_0^\infty dt\, e^{-ts} f(t)$ to the QLE

$$\dot{\mathbf{y}}(t) + \mathcal{Z}\mathbf{y}(t) + \int_0^t dt'\, \Gamma(t-t')\dot{\mathbf{y}}(t') = \mathbf{B}(t)\,.$$

which results in the algebraic equation

$$s\mathbf{y}(s) - \mathbf{y}(0) + \mathcal{Z}\mathbf{y}(s) + s\Gamma(s)\mathbf{y}(s) = \mathbf{B}(s)\,.$$

It should be noted that the Laplace transformation is better suited to solve differential equations with initial value conditions than the Fourier transformation, since the lower boundary of the integral is at $t = 0$. Solving the equation gives

$$\mathbf{y}(s) = (sI + \mathcal{Z} + s\Gamma(s))^{-1}(\mathbf{y}(0) + \mathbf{B}(s))\,,$$

from which it follows that the Laplace transformation of the Green's function $\tilde{\mathcal{G}}$ is given by

$$\tilde{\mathcal{G}}(s) = (sI + \mathcal{Z} + s\Gamma(s))^{-1}\,.$$

The asymptotic covariance matrix can be read off of equation (3.5). The first term, which depends on the initial conditions, necessarily has to decay if an asymptotic state exists, which leaves only

$$C(\infty) = \int_0^\infty dt' \int_0^\infty dt''\mathcal{G}(t-t')\mathcal{K}(t'-t'')\mathcal{G}(t-t'')^\dagger\,.$$

The bath correlator $\mathcal{K}(t)$ (3.6) contains an oscillating factor $\cos(\omega t)$, which can be expanded into exponential functions. One can readily see that the above expression is equivalent to

$$C_{ij}(\infty) = 2\sum_{k,l\in\{3,4\}} \int_o^\infty d\omega\, (\tilde{\mathcal{G}}_{ik}(i\omega)\tilde{\mathcal{G}}_{jk}(-i\omega) + \tilde{\mathcal{G}}_{ik}(-i\omega)\tilde{\mathcal{G}}_{jk}(i\omega)) \cdot J(\omega)\coth\left(\frac{\omega}{2T}\right)\cos(\omega d\delta_{kl})\,.$$

The advantage of this approach is that for a Drude cut-off $\tilde{\mathcal{G}}(s)$ can be calculated analytically and only one numerical integration remains. $\tilde{\mathcal{G}}(s)$ is a complicated and long expression, which is printed in appendix A. It is based on the damping kernel

$$\begin{aligned}\Gamma_r(t) &= \frac{8}{\pi}\gamma\int_0^\infty d\omega \frac{\Omega_c^2}{\Omega_c^2+\omega^2}\cos(\omega t)\cos(\omega r)\\ &= \gamma\Omega_c\left(e^{-|r+t|\Omega_c} + e^{-|r-t|\Omega_c}\right)\,,\end{aligned}$$

which has the Laplace transformation

$$\Gamma_r(s) = 2\gamma\Omega_c \frac{e^{-rs}\Omega_c - e^{-r\Omega_c}s}{\Omega_c^2 - s^2}\,.$$

4.3.1. One-Dimensional Bath

In this section we will present numerical results for the asymptotic state of two oscillators coupled to the modes of a free one-dimensional bath. We assume the oscillators to be identical ($m = 1$, $\Omega_0 = 1$). The remaining parameters are the cut-off frequency Ω_c, the coupling constant γ, distance d, and temperature T. Frequencies are measured in units of Ω_0, distances in units of c/Ω_0, and temperatures in units of $\hbar\Omega_0/k_B$.

For a one-dimensional bath we have calculated the asymptotic entanglement $E_{\mathcal{N}}$ for a Drude cut-off (4.2) and an exponential cut-off with $s = 1$ (4.1). In the following plots the results for the Drude cut-off are drawn in gray, for the exponential cut-off in black. Both cut-offs lead to a very similar behavior. In figure 4.1 we see that the asymptotic entanglement decreases strictly monotonically with distance and vanishes at some critical distance $d_{\max}$. The value of the entanglement $E_{\mathcal{N}}$ generally decreases with decreasing coupling γ, increasing cut-off Ω_c, or increasing temperature T.

The remaining plots show the dependence of $d_{\max}$ on the parameters of our model. Most importantly, we see in figure 4.2 that $d_{\max}$ is inversely proportional to the cut-off frequency Ω_c with a proportionality constant of the order of one.

In figure 4.3 we see the dependence on temperature. As expected $d_{\max}$ is reduced with increasing temperature. In fact, above a certain threshold there is no entanglement to be found, even at zero distance. Decreasing the coupling γ reduces the temperature threshold.

Apart from influencing the temperature threshold the maximal distance $d_{\max}$ only depends marginally on the coupling strength γ, as can be seen in figure 4.4. This can be explained by the fact that γ controls *both* the entanglement and the decoherence. The effects seem to approximately balance out.

This concludes our discussion of a one-dimension bath and we will now proceed to a three-dimensional one.

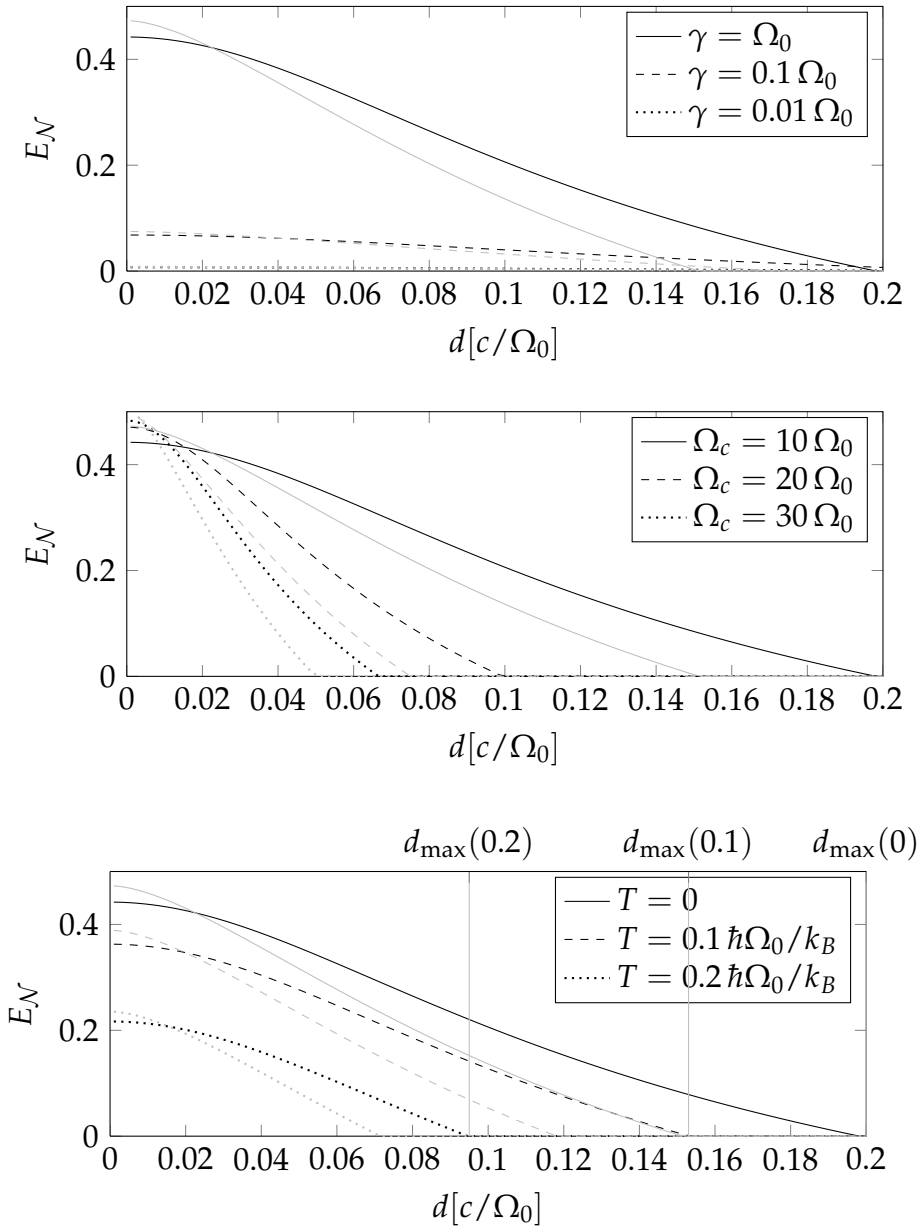

Figure 4.1.: Asymptotic entanglement as a function of distance d for a one dimensional bath. The first plot shows the dependence on the coupling strength γ, the second plot the dependence on the cut-off frequency Ω_c, and the third on the temperature T. The entanglement drops to zero at a maximal distance $d_{\max}$. The Drude cut-off is shown in gray and the exponential cut-off with $s = 1$ in black.

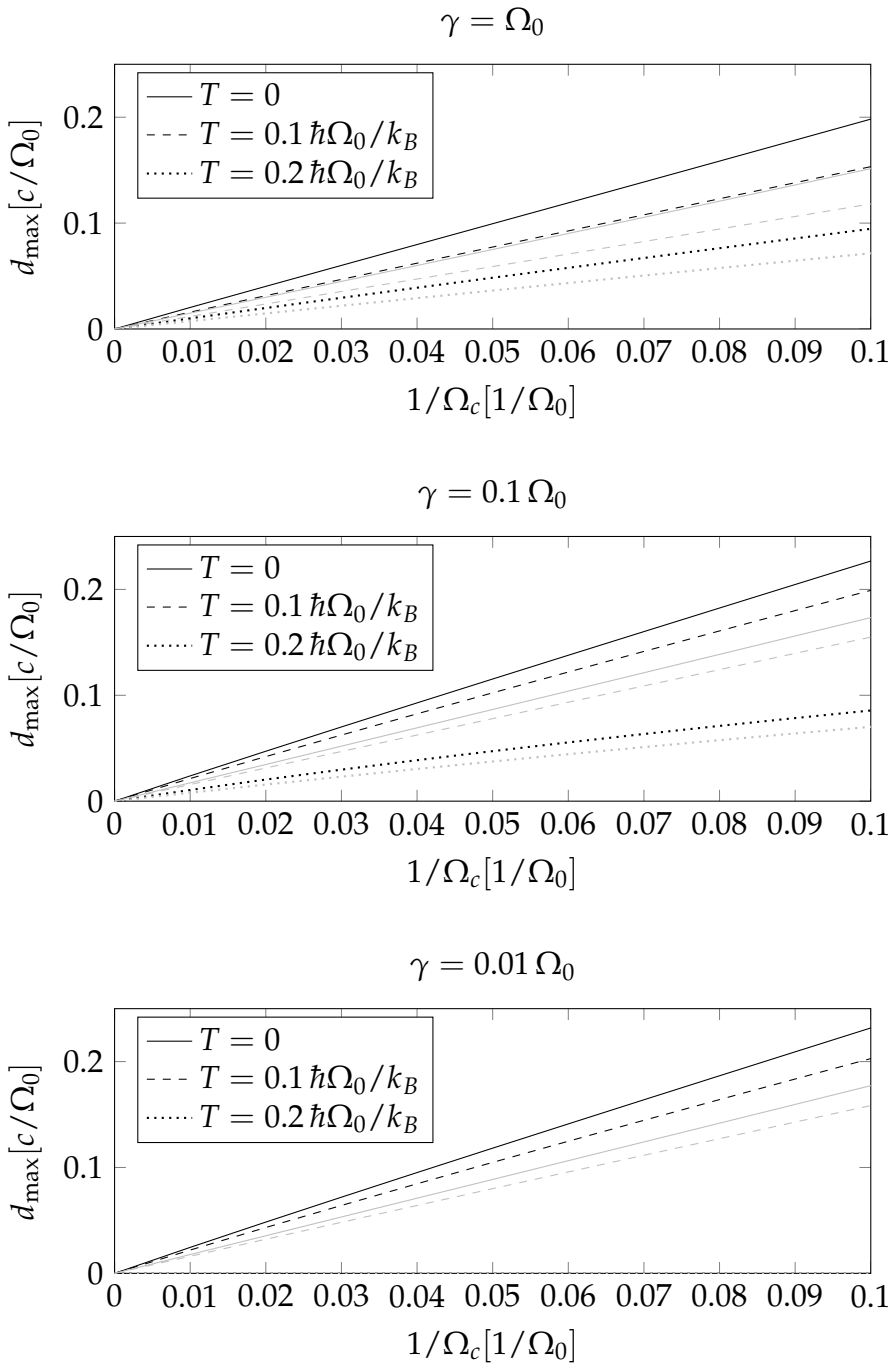

Figure 4.2.: Maximal distance $d_{\max}$ as a function of the inverse cut-off frequency $1/\Omega_c$. The Drude cut-off is shown in gray and the exponential cut-off with $s = 1$ in black.

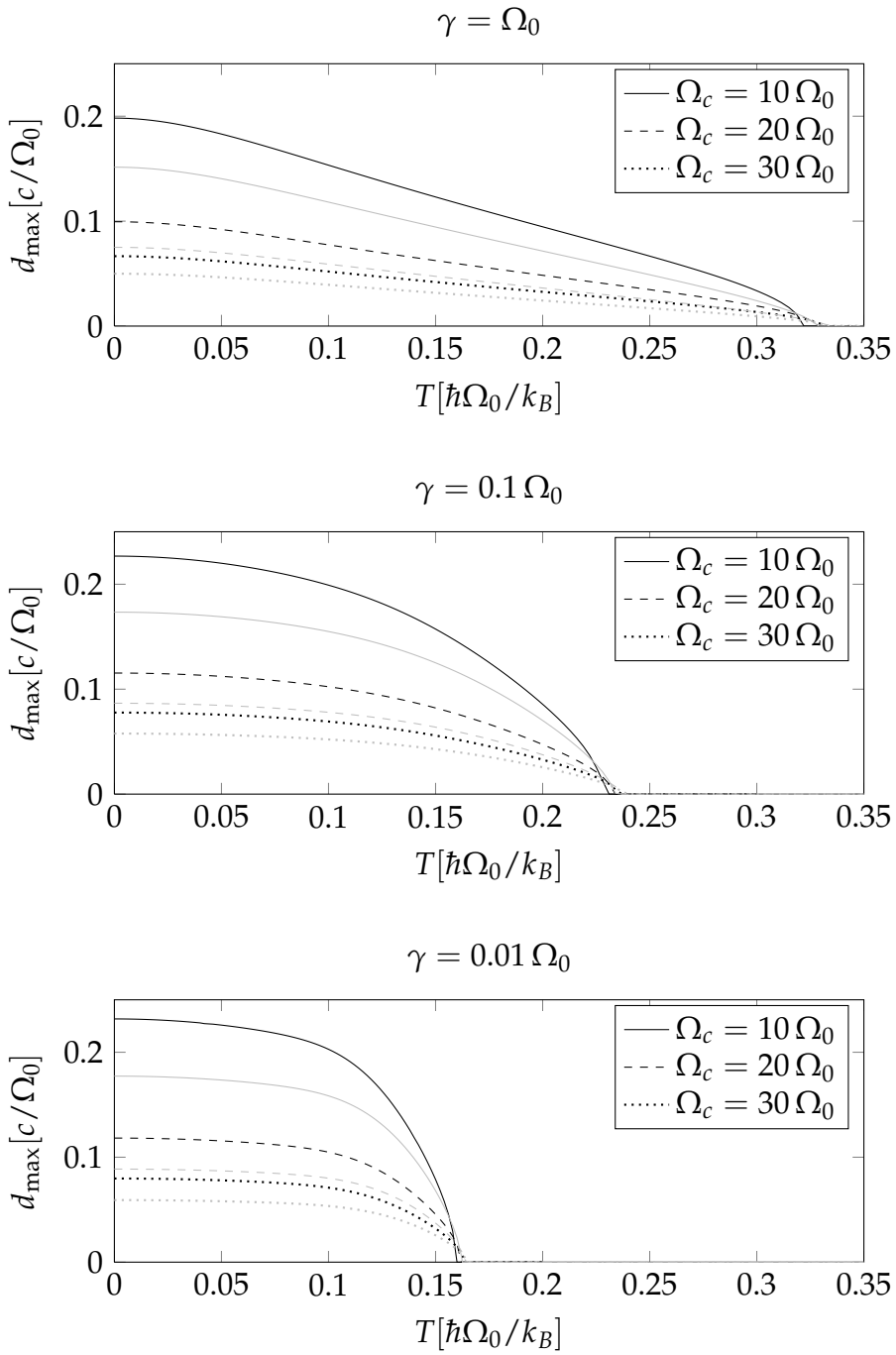

Figure 4.3.: Maximal distance $d_{\max}$ as a function of temperature T. The Drude cut-off is shown in gray and the exponential cut-off with $s = 1$ in black.

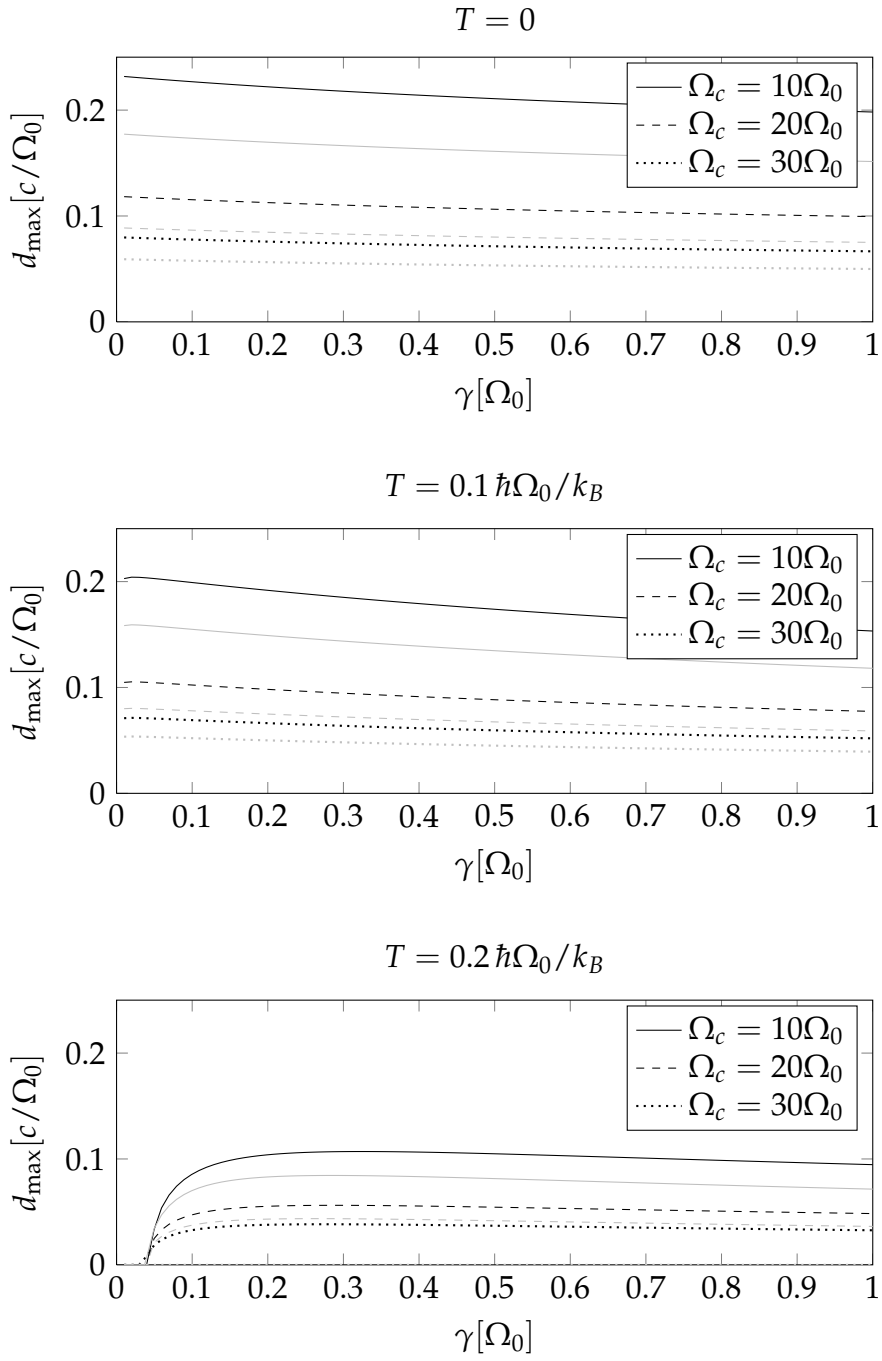

Figure 4.4.: Maximal distance $d_{\max}$ as a function of the coupling strength γ. The Drude cut-off is shown in gray and the exponential cut-off with $s = 1$ in black.

4.3.2. Three-Dimensional Bath

In figures 4.5, 4.6, 4.7, and 4.8 exactly the same parameter ranges are plotted (in black) for a three-dimensional bath as in the previous chapter for a one-dimensional bath. The qualitative behavior is the same as before, however, the entanglement $E_{\mathcal{N}}$ as well as the maximal distance $d_{\max}$ is reduced by approximately one order of magnitude.

The reason for this decrease is the previously discussed change of the spectral parameter s from 1 to 3. This can be seen by comparing the three-dimensional results with the one-dimensional ones, where s has also been increased to 3. These are plotted in gray and show a very similar behavior. This leads us to conclude that the slightly different form of the damping kernel (3.3) and the bath-correlator (3.6) in one and three dimensions do not have a major influence on the entanglement. Only the spectral parameter s is relevant.

4.4. Entanglement Dynamics

4.4.1. Full Numerical Solution

In this section we will present a numerical solution of the entanglement dynamics. In equation (3.5) we have already written down the formal solution, which still requires two more steps to obtain the final result. First, the Green's function $\mathcal{G}(t)$ has to be calculated. It is the solution of the homogeneous part of (3.4). This is difficult to obtain, because it amounts to solving an integro-differential equation. Second, the inhomogeneous part has to be integrated, which also requires some numerical effort, because it involves a two-dimensional integration.

The first step is tackled by using the algorithm by Wilkie and Wong [WW08], which will be explained in more detail in appendix B. It numerically calculates the time dependent matrix $\mathcal{G}(t)$, which is stored in memory as a set of interpolation functions using splines. The main idea is that the integro-differential equation is discretized into a large set of coupled ordinary differential equations (ODEs), which can be solved using a standard ODE solver.

In step two, equation (3.5) is evaluated by nesting two one-dimensional integrations based on standard algorithms. Since the bath correlator also is not available in a closed analytic form, in fact, three numerical integrations have to be nested. This makes the calculation computationally very expensive. Typically, a single run over the maximum time range used in the following

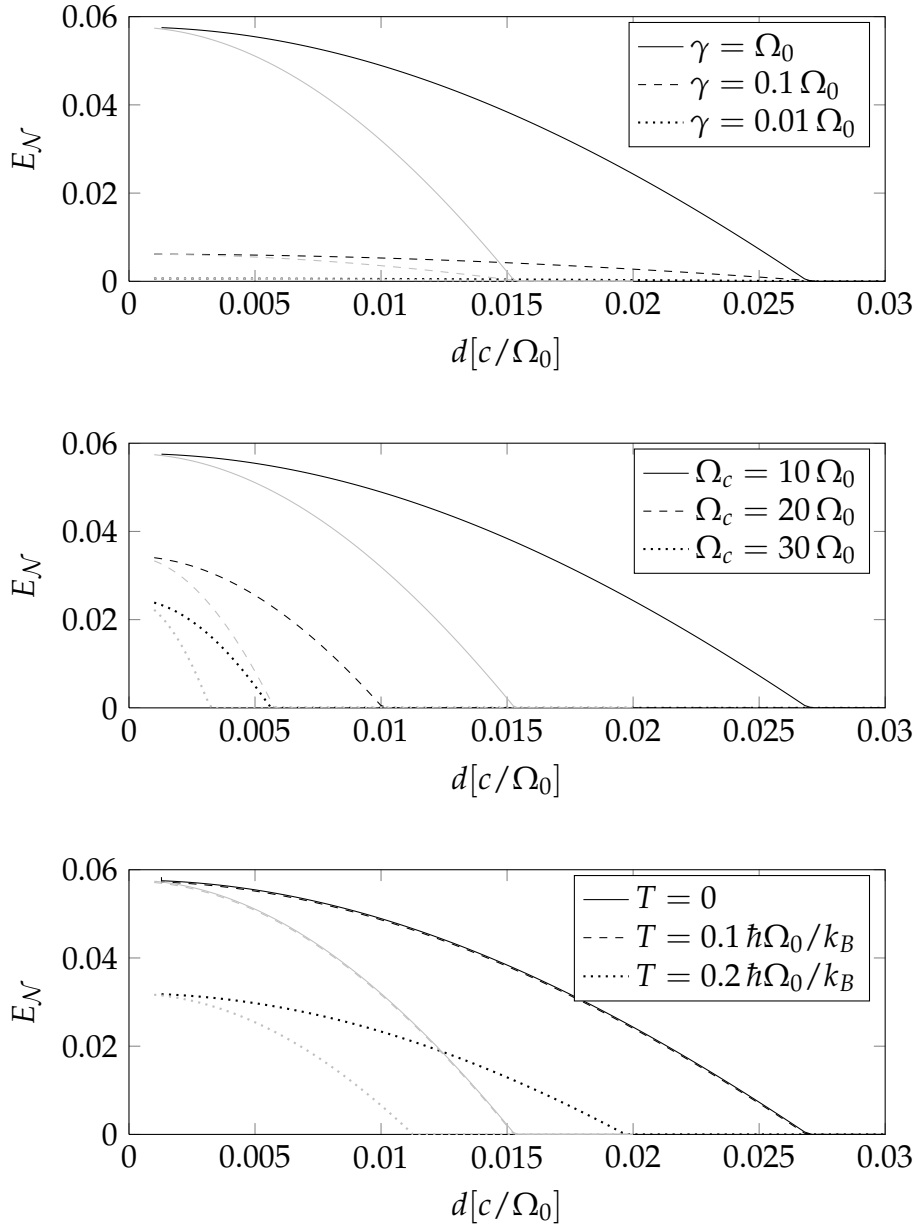

Figure 4.5.: Asymptotic entanglement as a function of distance d for a three-dimensional bath. The first plot shows the dependence on the coupling strength γ, the second plot the dependence on the cut-off frequency Ω_c, and the third on the temperature T. The entanglement drops to zero at a maximal distance $d_{\max}$. The three-dimensional bath with $s = 3$ is shown in black and the one-dimensional bath with exponential cut-off and $s = 3$ is shown in gray.

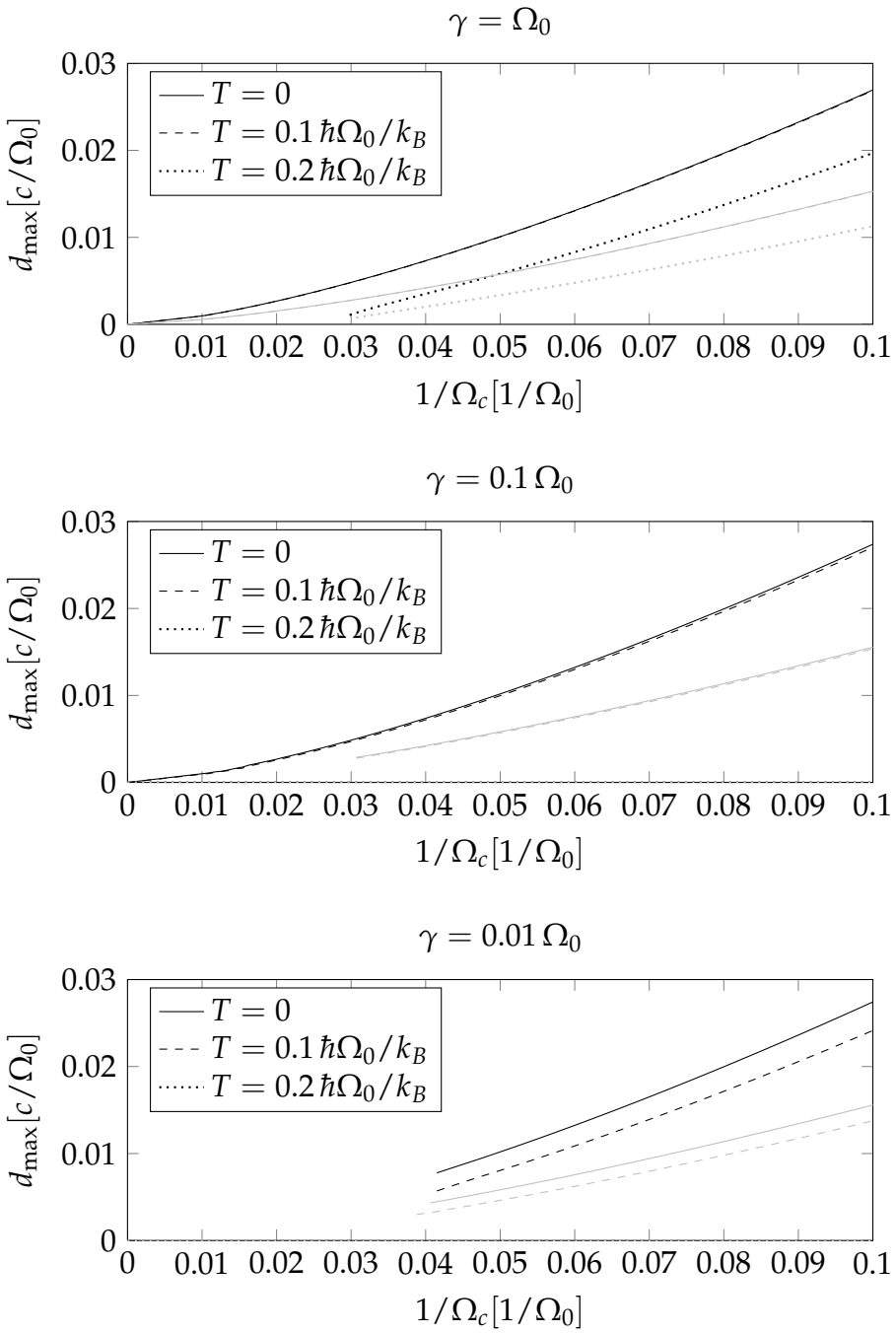

Figure 4.6.: Maximal distance $d_{\max}$ as a function of the inverse cut-off frequency $1/\Omega_c$. The three-dimensional bath with $s = 3$ is shown in black and the one-dimensional bath with exponential cut-off and $s = 3$ is shown in gray. The gaps in the plots are due to non-converging numerics. In all cases $d_{\max}$ smoothly goes to zero for $\Omega_c \to \infty$.

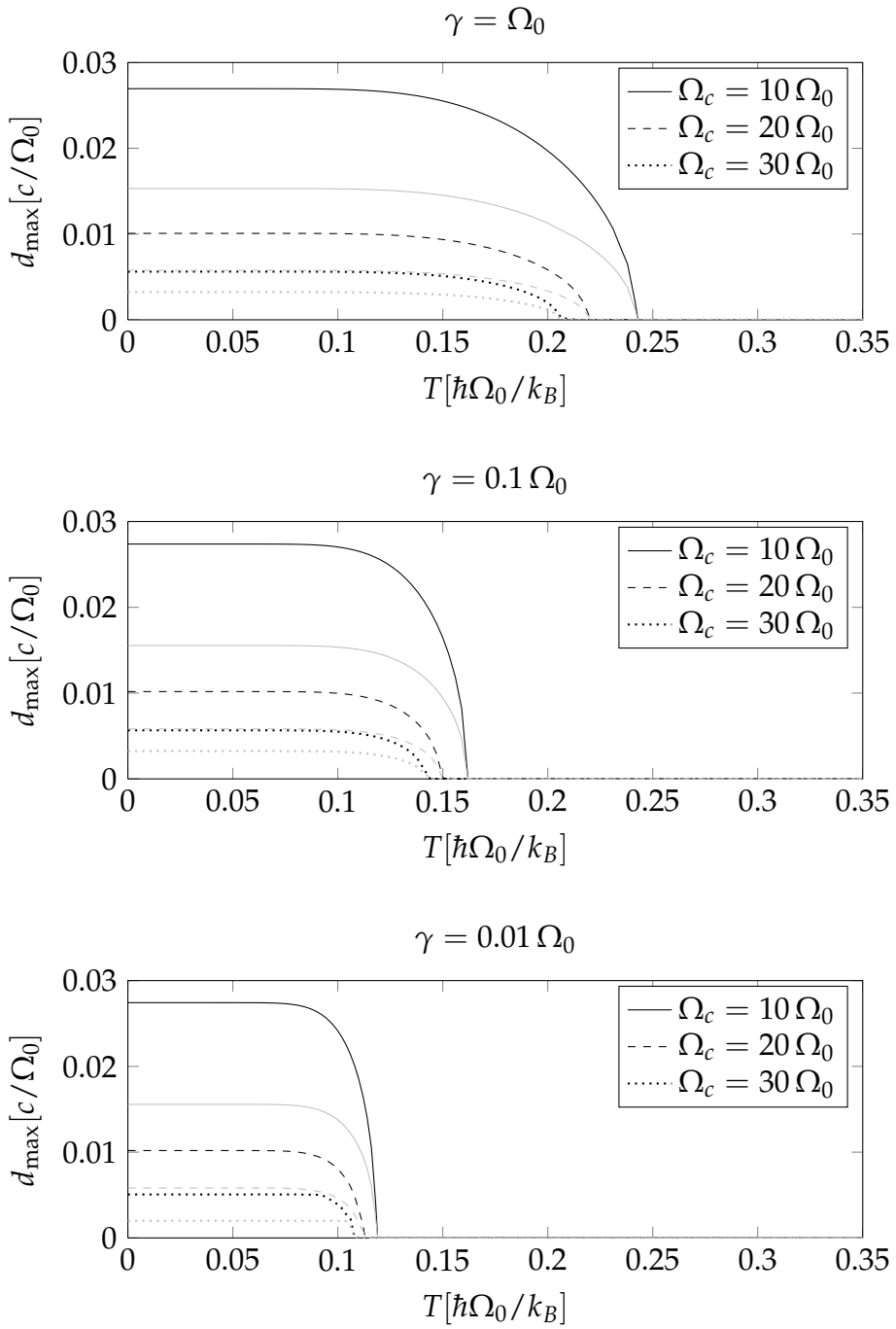

Figure 4.7.: Maximal distance $d_{\max}$ as a function of temperature T. The three-dimensional bath with $s = 3$ is shown in black and the one-dimensional bath with exponential cut-off and $s = 3$ is shown in gray.

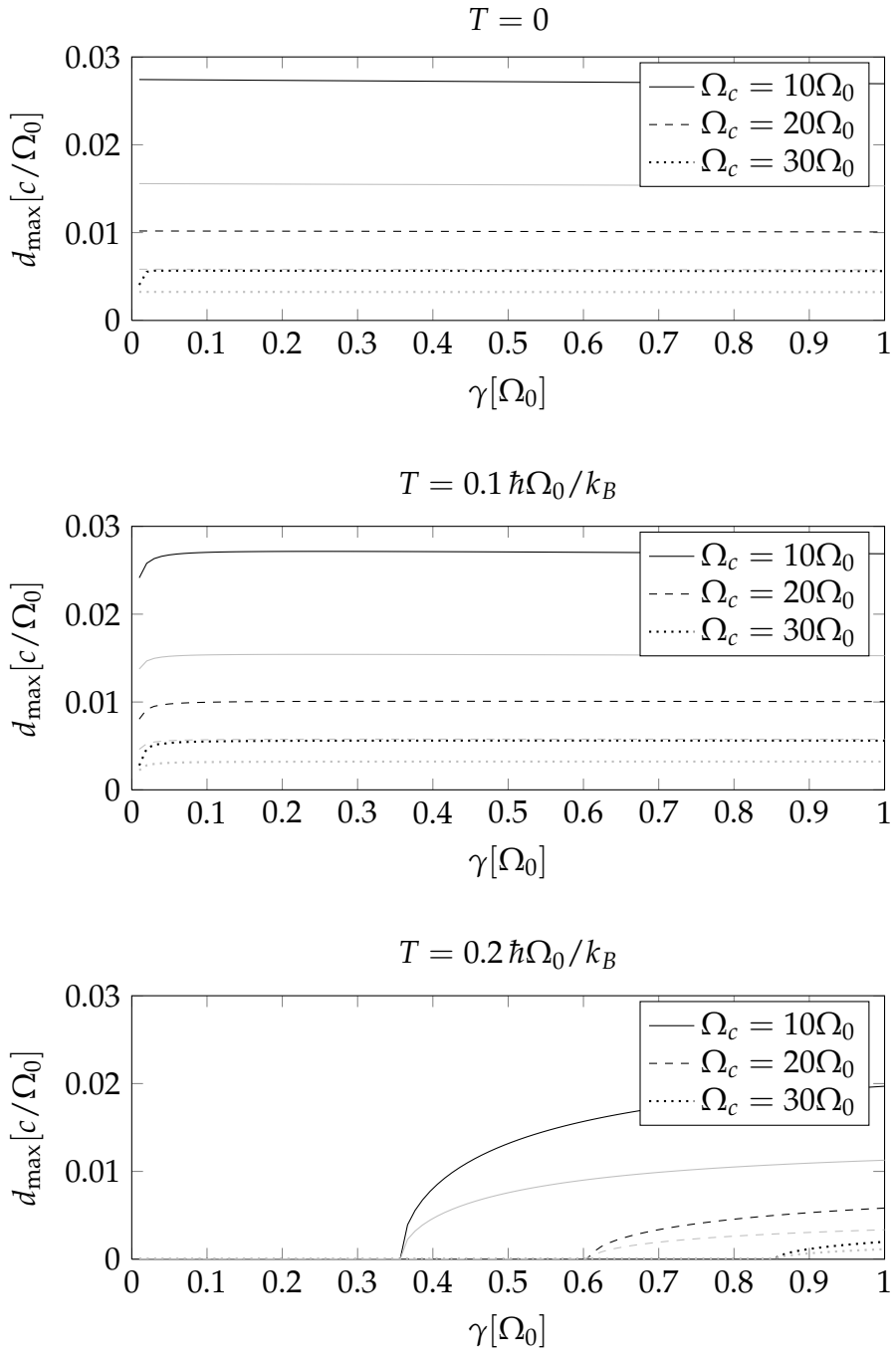

Figure 4.8.: Maximal distance $d_{\max}$ as a function of the coupling strength γ. The three-dimensional bath with $s = 3$ is shown in black and the one-dimensional bath with exponential cut-off and $s = 3$ is shown in gray.

figures ($t_{\max} = 205/\Omega_0$) with a given set of parameters takes a couple of days to complete (on an Intel E8500 CPU). Whereas we now have the full covariance matrix available, which for Gaussian states allows the calculation of the time evolution of any observable, we will only talk about the entanglement in the following. The entanglement is measured by the logarithmic negativity as discussed in section 2.2.6.

As the initial state of the two system oscillators we will choose their ground state, which has the covariance matrix ($\hbar$, m, $\Omega_0 = 1$)

$$C(0) = \mathrm{diag}(1, 1, 1, 1)\,.$$

Slightly more general initial states are discussed in section 4.4.4.

Again, we consider one- and three-dimensional baths. In figure 4.9 we compare the Drude cut-off in gray with the exponential cut-off ($s = 1$) in black for the one-dimensional bath. Figure 4.10 shows the one-dimensional bath with exponential cut-off ($s = 3$) in gray and the three-dimensional bath ($s = 3$) in black.

In both figures the top plot shows a larger time range and the bottom plot shows the same curves zoomed into the first peak visible at the left side of the top plot. As for the asymptotic entanglement, the value of the entanglement at a given time strictly decreases with increasing distance. The large change of the entanglement on a short time scale at the beginning of the time evolution is the result of the sudden switch-on of the coupling between the system oscillators and the bath. This *initial kick* is considered again in section 4.4.3.

At intermediate times the dynamics consist of oscillations, which can include so-called *sudden-death* and *revival* of the entanglement [YE04, FT06, MS06, SKR06, YE06, BFC07]. The oscillations are damped and converge to the equilibrium value discussed in the previous sections, which are indicated by the dotted horizontal lines.

Exactly as for the asymptotic entanglement, we see that the exact form of the cut-off is not very important. The most notable difference between the examined cases is caused by the value of the spectral parameter s.

It remains to be examined how the dynamics depend on the parameters coupling strength γ, cut-off Ω_c, and temperature T. Figures 4.11 to 4.18 contain corresponding plots. The first four figures show the one-dimensional bath and the remaining four figures show the three-dimensional bath. Since the effect of changes in the parameters qualitatively is the same for the one- and the three-dimensional case, we will discuss both at the same time.

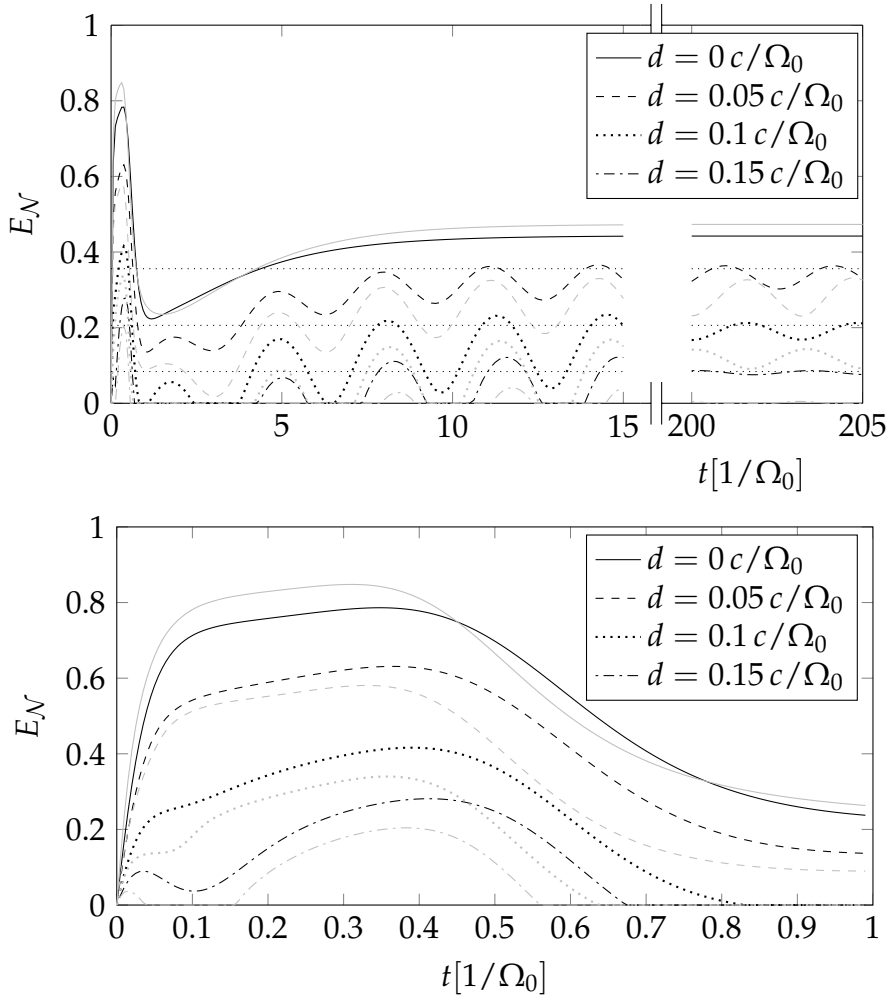

Figure 4.9.: Time evolution of the entanglement $E_{\mathcal{N}}$ for different distances d. The first plot shows the long-term evolution as it approaches the equilibrium value which is indicated by the horizontal dotted lines. The second plot zooms into to the first maximum seen on the left side of the first plot. The one-dimensional bath with exponential cut-off ($s = 1$) is drawn in black and the Drude cut-off in gray. The parameters are temperature $T = 0$, coupling $\gamma = 1\,\Omega_0$, and cut-off $\Omega_c = 10\,\Omega_0$.

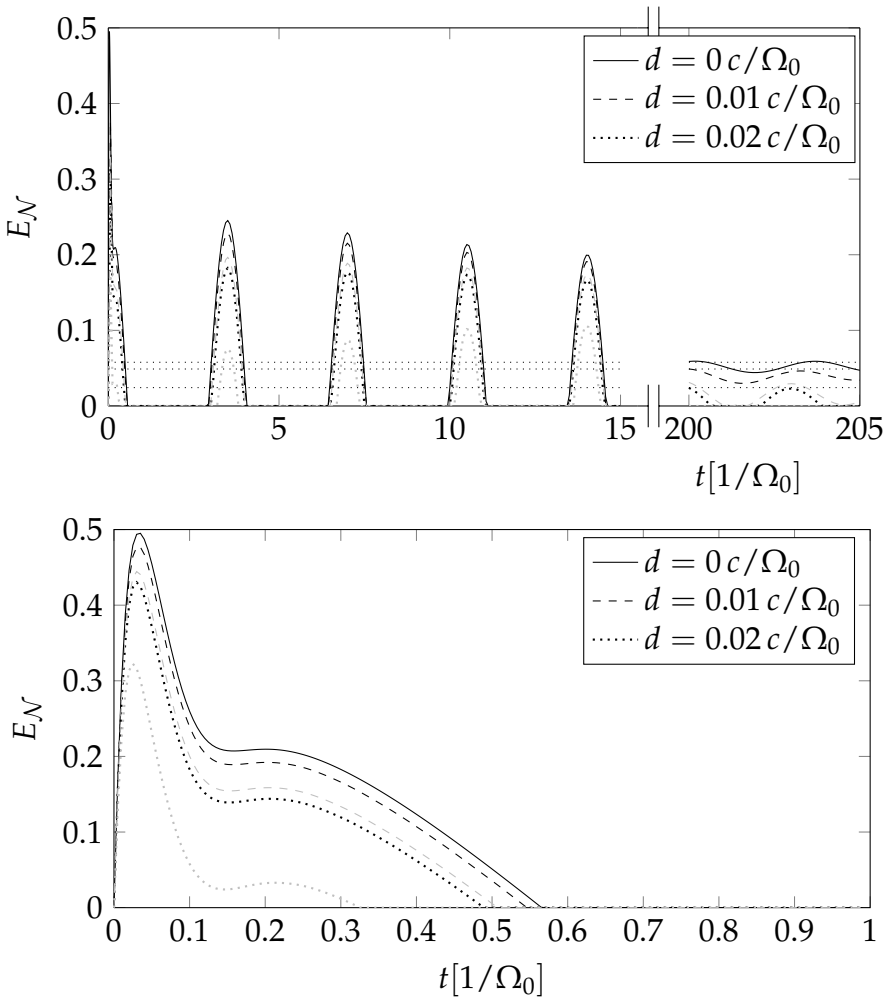

Figure 4.10.: Same plots as in figure 4.9, but showing the three-dimensional bath with $s = 3$ in black and the one-dimensional bath with exponential cut-off and $s = 3$ in gray. Only one solid line is shown here, because for $d = 0$ the three- and the one-dimensional bath are identical.

Figure 4.11 and 4.15 show that reducing the coupling strength γ by one or two orders of magnitude reduces the amount of entanglement approximately proportionally. However, it is important to note that the distance dependence of the entanglement is not influenced significantly.

The distance dependence is influenced considerably by the cut-off frequency Ω_c as can be seen in figures 4.12 and 4.16. A similar behavior as for the asymptotic value, which has been discussed in the previous section, can be seen for the whole dynamical evolution. The larger the cut-off, the sharper is the drop of the entanglement with distance.

Finally, the effect of non-zero temperature is displayed in figures 4.13, 4.14, 4.17, and 4.18. Unlike in the other figures, here, only one cut-off is drawn in each plot and the $T = 0$ case is drawn in gray for comparison. Clearly, the short-term dynamics are not influenced by the temperature. In the long term a rising temperature reduces the amount of entanglement in the system.

4.4.2. Short-Term Approximation

For a one-dimensional bath with Drude cut-off it is possible to write down the Laplace transformation of the homogeneous solution in analytical from (see appendix A). This enables us to make an analytical short-term approximation with the help of the Tauber and Abel theorem [Gol62]: Writing a Laplace transformed function $F(s)$ as a series with the coefficients a_n

$$F(s) = \sum_{n=1}^{\infty} a_n s^{-n}$$

it will look like

$$f(t) = \sum_{n=1}^{\infty} \frac{a_n t^{n-1}}{(n-1)!}$$

in the time domain. We can thus arrive at a second order expansion in time t by calculating a_1, a_2, and a_3 from the Laplace transformation. This can be achieved by taking the limits

$$\begin{aligned} \lim_{s\to\infty} sF(s) &= a_1\,, \\ \lim_{s\to\infty} \left(s^2F(s) - sa_1\right) &= a_2\,, \\ \text{and} \qquad \lim_{s\to\infty} \left(s^3F(s) - s^2a_1 - sa_2\right) &= a_3\,. \end{aligned}$$

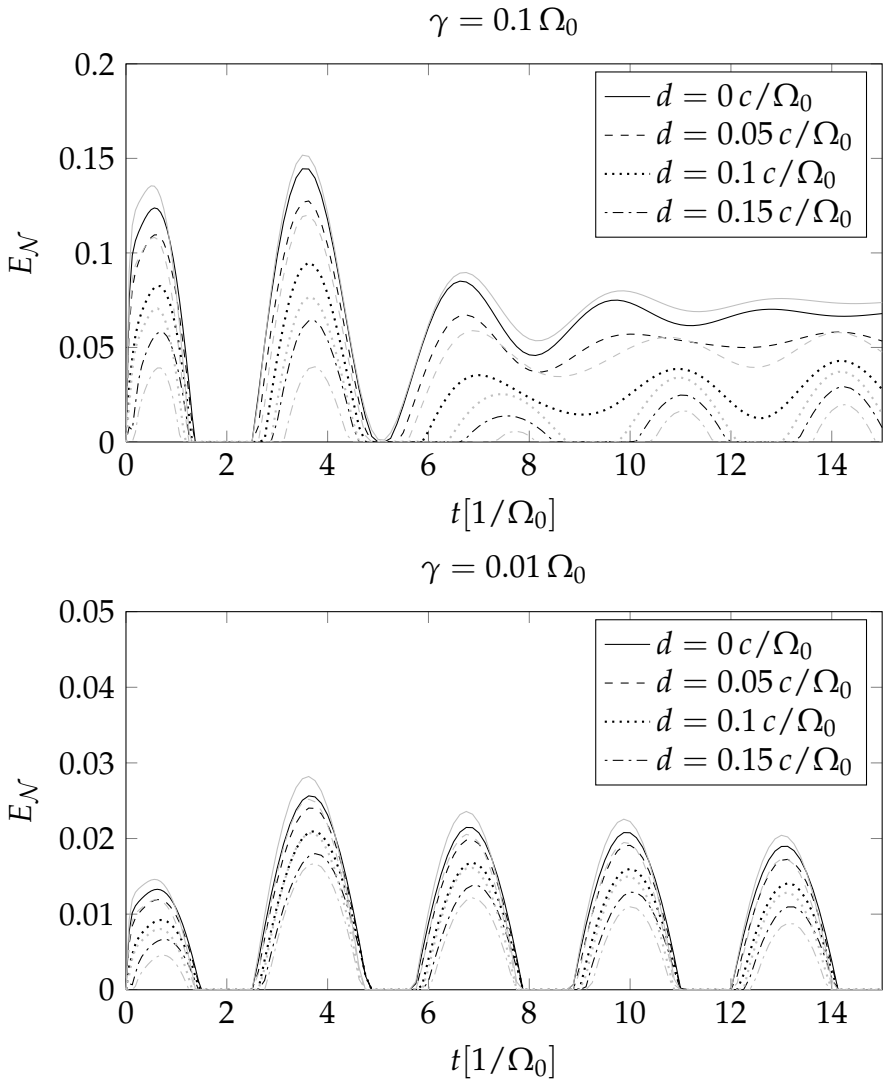

Figure 4.11.: Time evolution of the entanglement $E_{\mathcal{N}}$ for different distances d and coupling constants γ. Otherwise the same parameters as in figure 4.9 are used. The exponential cut-off with $s = 1$ is shown in black and the Drude cut-off is shown in gray.

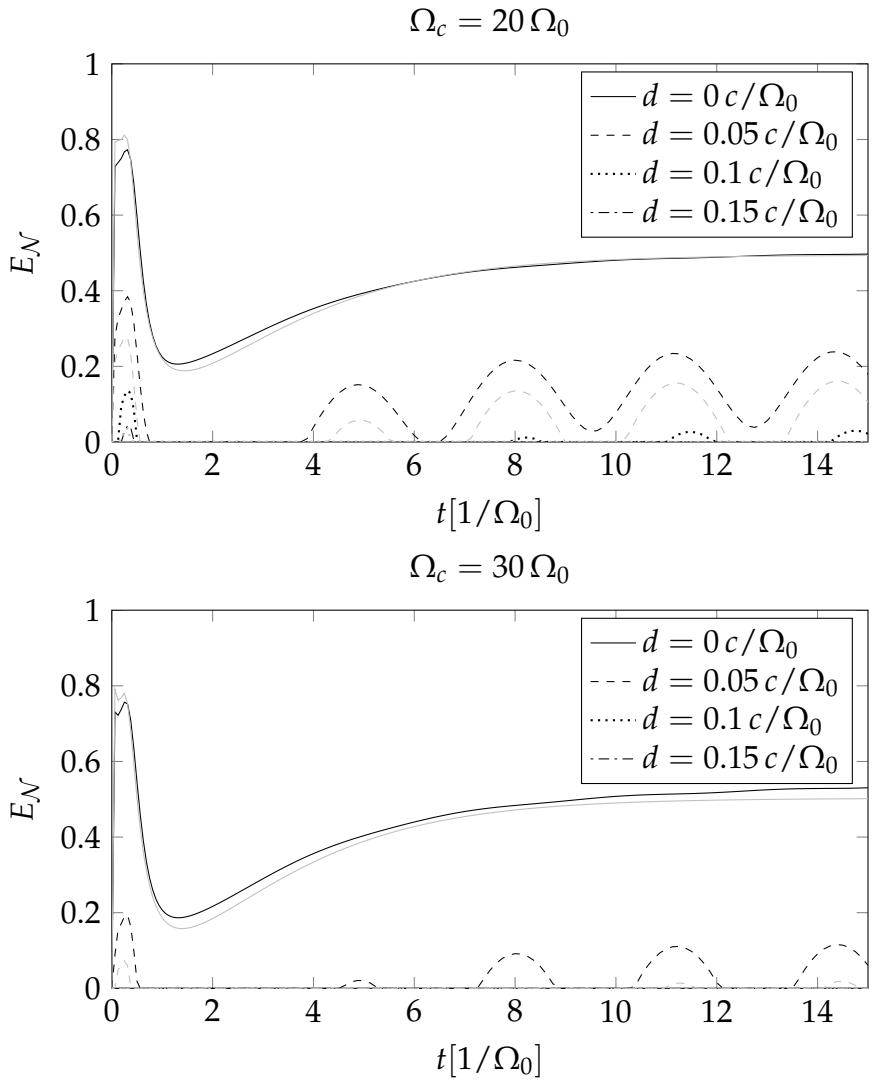

Figure 4.12.: Time evolution of the entanglement $E_{\mathcal{N}}$ for different distances d and cut-off frequencies Ω_c. Otherwise the same parameters as in figure 4.9 are used. The exponential cut-off with $s = 1$ is shown in black and the Drude cut-off is shown in gray.

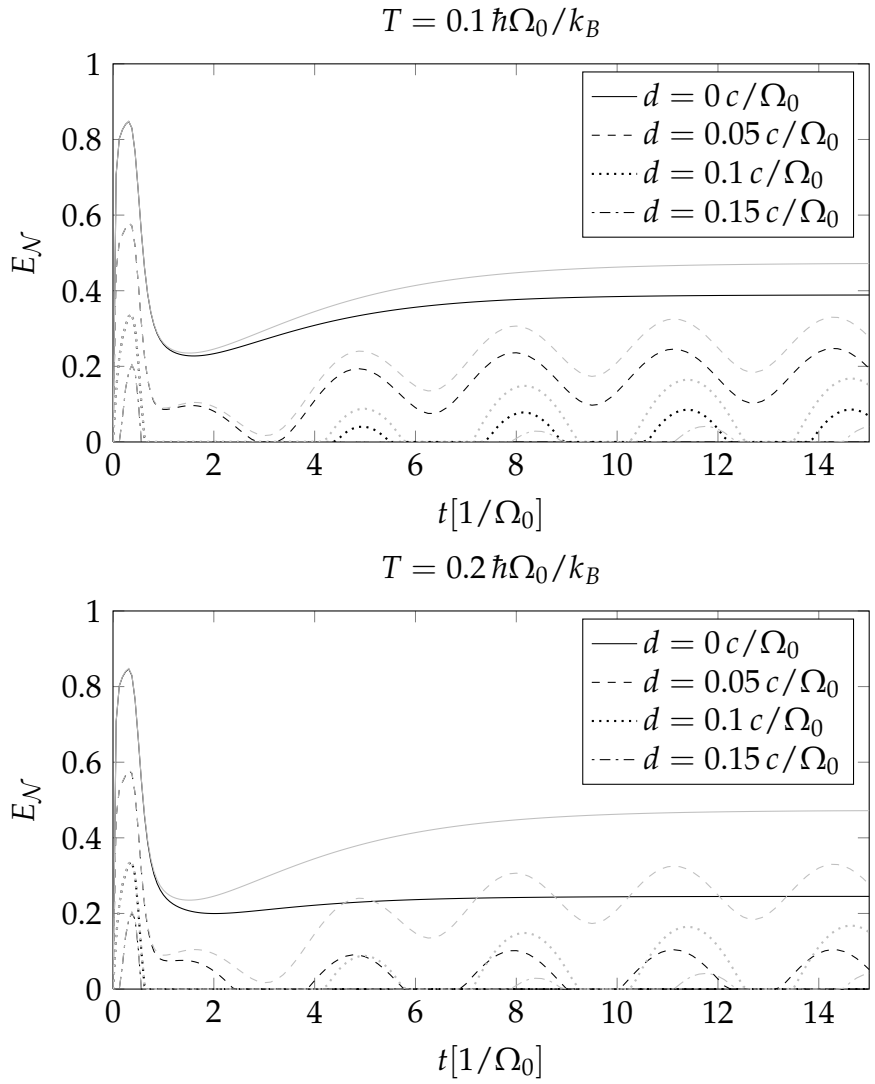

Figure 4.13.: Time evolution of the entanglement $E_{\mathcal{N}}$ for different distances d and temperatures T. Otherwise the same parameters as in figure 4.9 are used. The Drude cut-off is shown in black. The gray curves show the behavior at $T = 0$ for comparison.

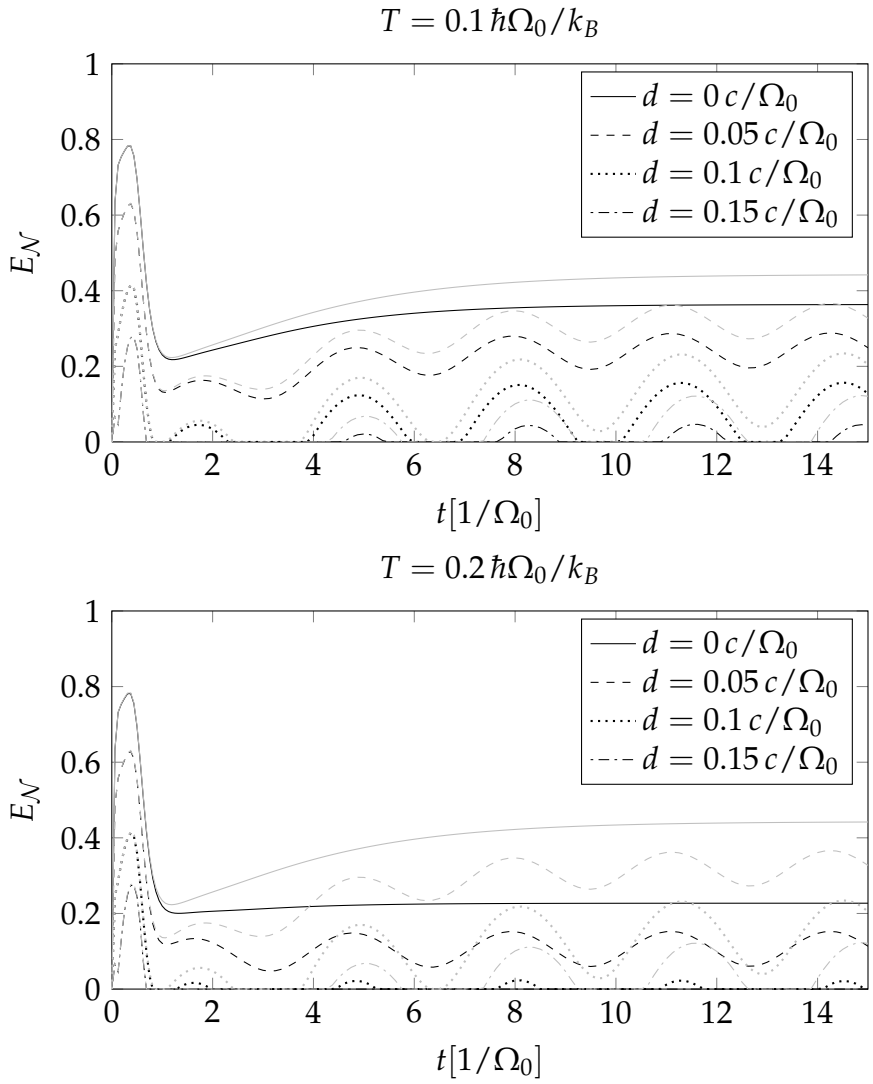

Figure 4.14.: Time evolution of the entanglement $E_\mathcal{N}$ for different distances d and temperatures T. Otherwise the same parameters as in figure 4.9 are used. The exponential cut-off is shown in black. The gray curves show the behavior at $T = 0$ for comparison.

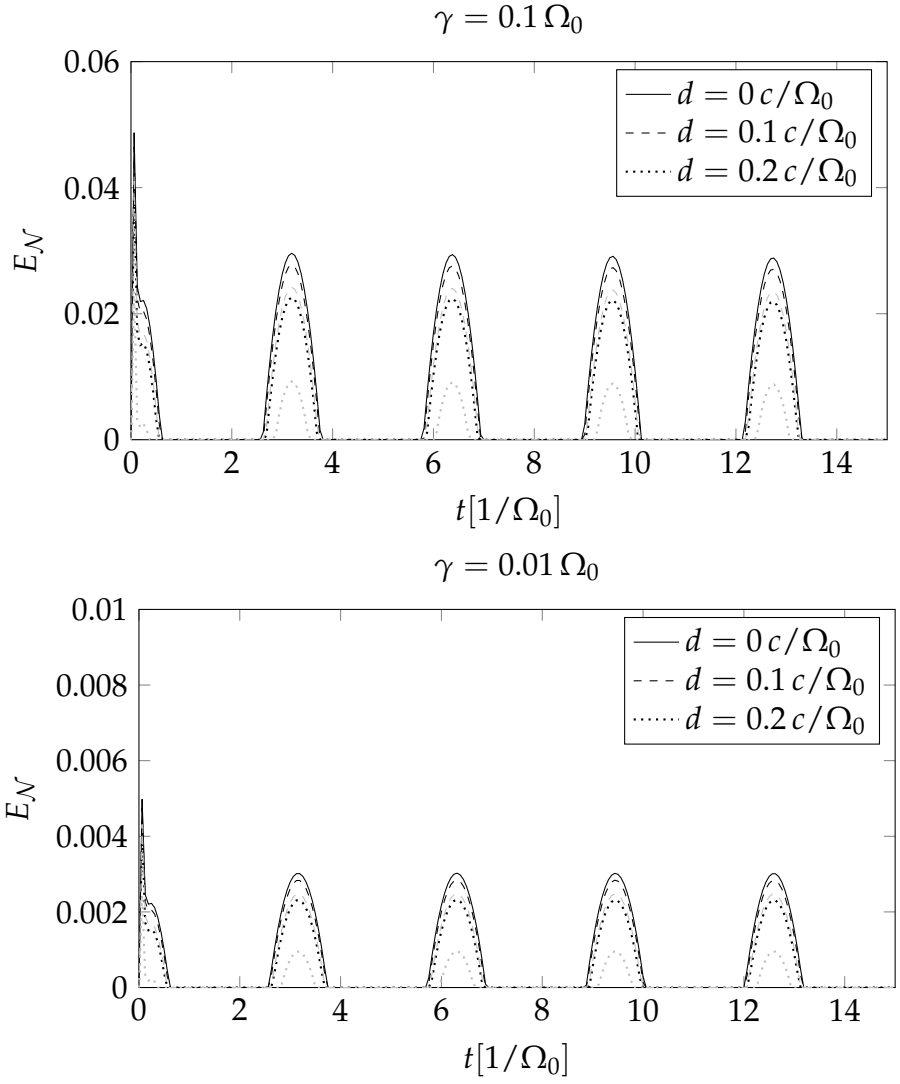

Figure 4.15.: Time evolution of the entanglement $E_\mathcal{N}$ for different distances d and coupling constants γ. Otherwise the same parameters as in figure 4.9 are used. The three-dimensional bath with exponential cut-off and $s = 3$ is shown in black and the one-dimensional bath with exponential cut-off and $s = 3$ is shown in gray.

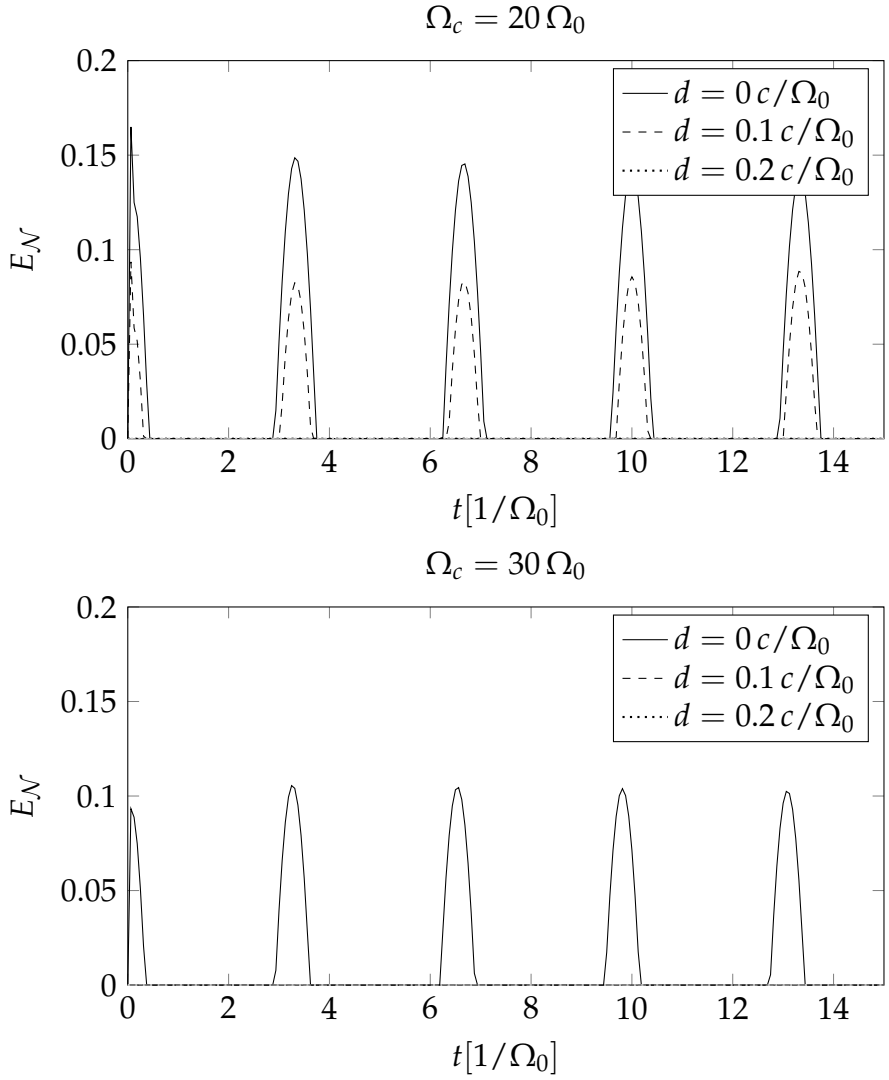

Figure 4.16.: Time evolution of the entanglement $E_{\mathcal{N}}$ for different distances d and cut-off frequencies Ω_c. Otherwise the same parameters as in figure 4.9 are used. The three-dimensional bath with exponential cut-off and $s = 3$ is shown in black and the one-dimensional bath with exponential cut-off and $s = 3$ is shown in gray.

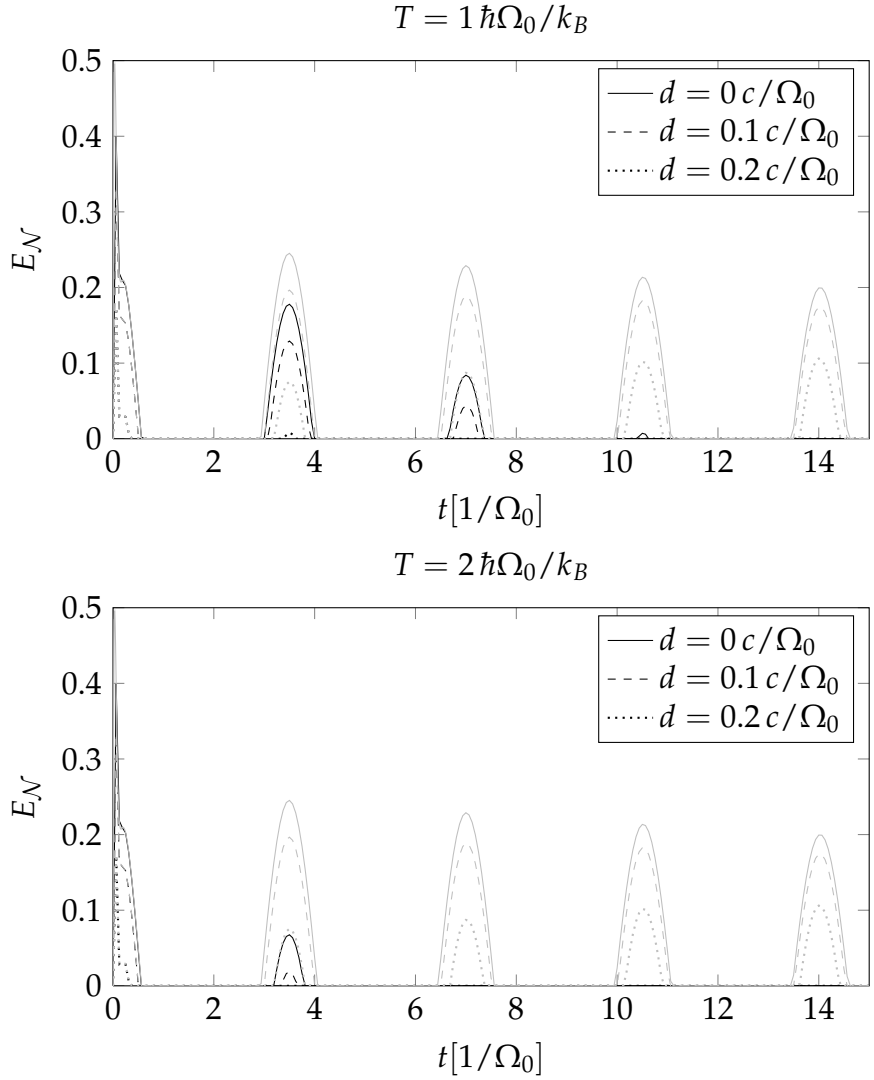

Figure 4.17.: Time evolution of the entanglement $E_\mathcal{N}$ for different distances d and temperatures T. Otherwise the same parameters as in figure 4.9 are used. The one-dimensional bath with exponential cut-off and $s = 3$ is shown in black. The gray curves show the behavior at $T = 0$ for comparison.

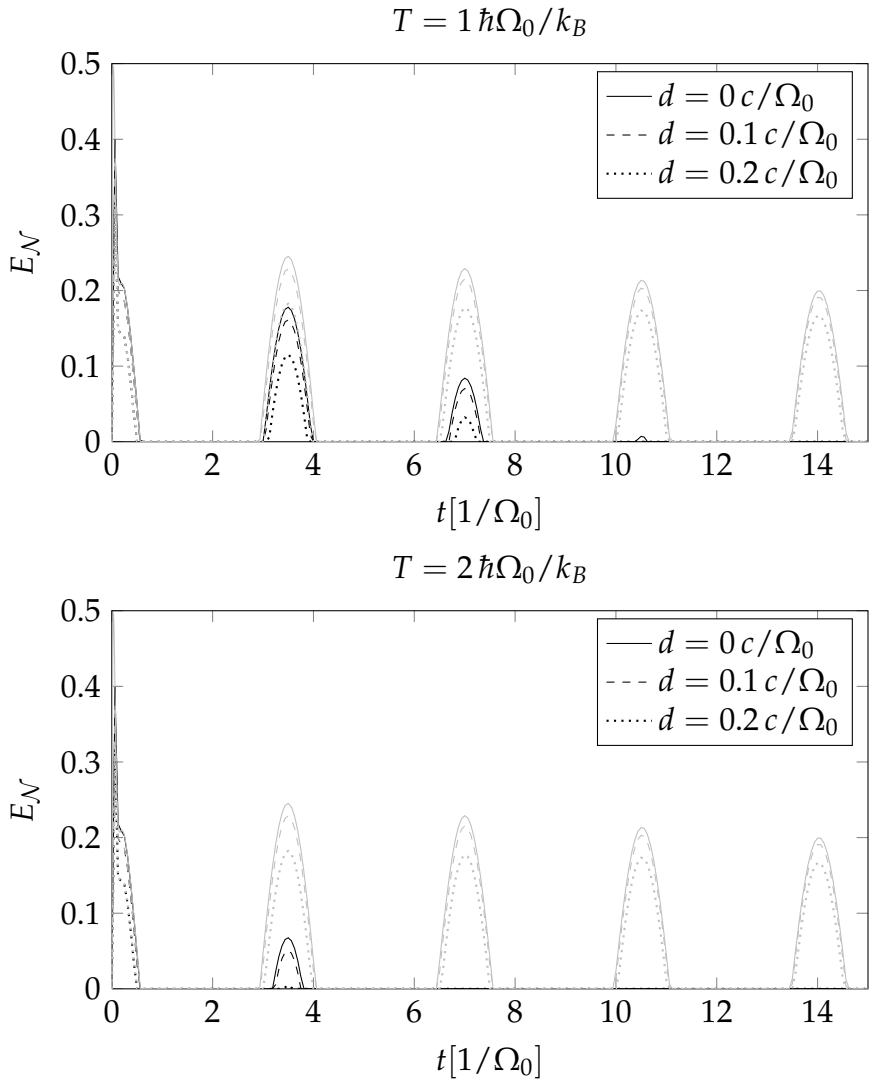

Figure 4.18.: Time evolution of the entanglement $E_{\mathcal{N}}$ for different distances d and temperatures T. Otherwise the same parameters as in figure 4.9 are used. The three-dimensional bath with exponential cut-off and $s = 3$ is shown in black. The gray curves show the behavior at $T = 0$ for comparison.

The resulting second order expression can be plugged into equation (3.5), which finally leads to the logarithmic negativity

$$E_{\mathcal{N}}(t) = \frac{2\gamma\Omega_c e^{-\Omega_c r}}{\log(2)} t + \frac{\gamma\Omega_c^2(2\log(\Omega_c) + 2\log(t) + 2\gamma_{\text{Euler}} - 3)}{\pi\log(2)} t^2 + \mathcal{O}(t^3)\,, \tag{4.3}$$

where $\gamma_{\text{Euler}} = 0.577\ldots$ is Euler's constant. A comparison between the analytical expression and the numerical results is shown in figure 4.19 for very short times.

4.4.3. The Initial Kick

We have observed very fast dynamics at the beginning of the time evolution in the previous section. This phenomenon is usually termed "initial kick", "initial slip", or "initial jolt" [HPZ92]. It is caused by the fact that we start with a factorizing initial state and then suddenly turn on the interaction between the system oscillators and the thermal bath.

In order to answer the question whether the initial kick can be observed in a real physical system, the different timescales involved have to be considered. All systems suitable for quantum information processing must be externally controllable, i.e. the interaction can be turned on and off. This means that the assumption of an initially uncorrelated state is viable, however, we can not expect that the interaction can be turned on infinitely fast, which gives us the first time scale, the switch-on time τ. The second time-scale is the inverse frequency of the fastest modes in the bath, which is fixed by the inverse cut-off $1/\Omega_c$.

In the case $\tau \ll 1/\Omega_c$ the kick exists and appears as calculated here. On the other hand, if $\tau \gg 1/\Omega_c$, the initial kick will be weakened, generally decreasing the amount of entanglement. Nevertheless, the results for $t \gg \tau$ can be considered correct.

If one is interested in the regime $\tau \gg 1/\Omega_c$ it also possible to remove the initial kick completely. The Langevin equation approach can still be pursued by separating the initial kick from the other terms resulting only in few additional complications [Hä97, HI05]. The main step is rewriting the integral in the

QLE (3.4)

$$\frac{d}{dt}\int_0^t dt'\,\Gamma(t-t')\mathbf{y}(t') = \int_0^t dt'\,\left[\dot{\Gamma}(t-t')\mathbf{y}(t')\right] + \Gamma(0)\mathbf{y}(t)$$
$$= \int_0^t dt'\,\left[\Gamma(t-t')\dot{\mathbf{y}}(t')\right] + \underbrace{\Gamma(t)\mathbf{y}(0)}_{\text{initial kick}}\,.$$

This produces a term which depends on the initial positions of the system oscillators and decays exponentially with time. It can be moved to the right hand side

$$\dot{\mathbf{y}}(t) + \mathcal{Z}\mathbf{y}(t) + \int_0^t dt'\,\Gamma(t-t')\dot{\mathbf{y}}(t') = \mathbf{B}(t) - \Gamma(t)\mathbf{y}(0) = \tilde{\mathbf{B}}(t)\,,$$

and then be absorbed in a new shifted bath operator $\tilde{\mathbf{B}}(t)$. This new bath operator is not stationary if averaged with respect to the usual thermal state ρ_T, but we can correct for this by using a shifted Gaussian state $\tilde{\rho}_T$ instead. However, the new bath operator $\tilde{\mathbf{B}}(t)$ by definition is not independent of the system operators any longer

$$\langle\{\mathbf{y}_i(t), \tilde{\mathbf{B}}_j(t)\}\rangle \neq 0\,.$$

This leads to new terms in equation (3.5). The problem still remains solvable with only a little more effort, but we have not followed that path, because we believe that including the initial kick is correct in our case. The current state of affairs concerning the initial kick and its removal is summarized by Fleming *et al.* [FRH10].

4.4.4. Maximal Entanglement

If we want to conclusively rule out the possibility of efficient entanglement generation in free thermal baths, we have to show that the maximal value of the entanglement during the entire time evolution is too small to be of practical use. While we will not be able to strictly prove this, we strongly believe that it is indeed the case and will provide some arguments here.

First let us start with the Drude cut-off in one dimension. When increasing the distance, only the first two maxima at the beginning survive (cf. figure 4.9). The second maximum is the global maximum for intermediate distances and

vanishes at a certain maximal distance $d_{\max}$. The behavior of $d_{\max}$ is depicted in figure 4.20. As in the asymptotic case, it is approximately proportional to $1/\Omega_c$ and does not significantly depend on γ. The step in the curves is caused by a shift in the position of the second maximum from $t \sim 2 \times d/c$ to $t \sim d/c$.

The analysis of the behavior of the first maximum is greatly simplified by the availability of the analytical short time approximation (section 4.4.2). It can be seen from the formula (4.3) that it decays exponentially in the distance d and cut-off Ω_c.

In the other cases the second maximum behaves similarly to the one-dimensional bath and $s = 1$ (figure 4.20 and 4.21). The first maximum, however, is difficult to treat numerically and no analytical solution is available. While we have not succeeded to numerically determine the type of decay, we still claim that it will be exponential with distance. The reason being that on a fundamental level entanglement can only be created by interaction. All the entanglement we see before the time r/c has passed must already have been present in the bath. Because the entanglement in the bath is known to decay exponentially with distance [SW85], we conclude that all cases behave similarly to the analytic result we have obtained for the Drude cut-off.

Finally, we discuss the effect of squeezing the initial state of the system oscillators. It is parameterized by the single mode squeezing parameter a, which is simply the ratio of the variances of the initial state

$$C(0) = \mathrm{diag}(1/a, 1/a, a, a)\,.$$

The uncertainty relations are unchanged, since the product $\langle x^2 \rangle \langle p^2 \rangle$ remains the same, however, the energy increases.

Based on numerical investigations, we see that squeezing can also increase the amount of entanglement, but does not significantly influence the distance at which the second maximum (one-dimensional Drude cut-off and exponential cut-off with $s = 1$) vanishes. The value of the first maximum increases proportionally with $1/a$.

4.5. Conclusion

We have discussed the entanglement of the long-term asymptotic state and the dynamical time evolution of a system of two harmonic oscillators coupled to a free bosonic bath. The asymptotic state exhibits a critical distance $d_{\max}$, at

which the entanglement vanishes and which is proportional to $1/\Omega_c$ with a proportionality constant of $\mathcal{O}(1)$. For the time evolution we also find a critical distance, at which the entanglement vanishes except for a peak exponentially decaying in r at the beginning of the time evolution due to the initial kick. It is also approximately proportional to $1/\Omega_c$ with a proportionality constant of $\mathcal{O}(1)$.

As we have argued in section 4.2, Ω_c is given by the system size. Therefore, we can conclude that *the environment does not entangle two quantum mechanical systems if they are further apart than a distance comparable to their own size.* Due to this, the effect of environmentally generated entanglement in a free bath is not useful in practice.

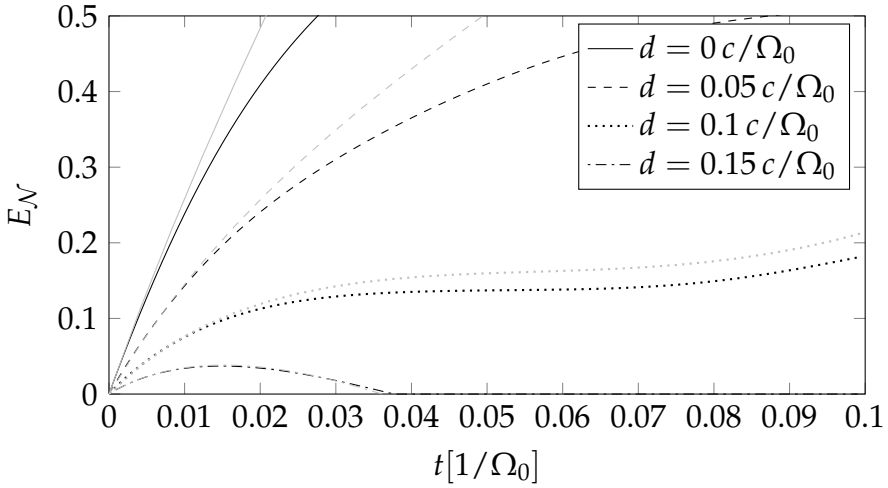

Figure 4.19.: Short-term evolution of the entanglement of the one-dimensional bath with Drude cut-off. The numerical data is shown in black and the analytical approximation in gray. The same parameters as in figure 4.9 are used.

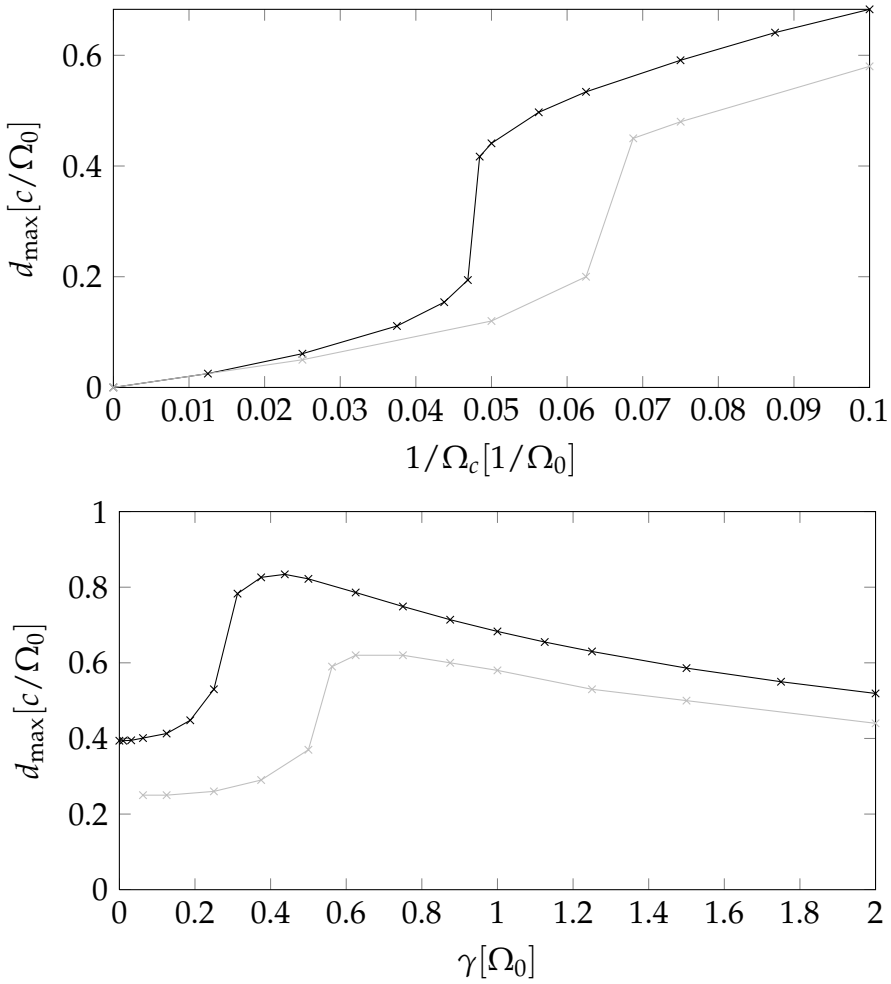

Figure 4.20.: Dependence of the maximal entanglement on the cut-off Ω_c and the coupling γ for the one-dimensional bath with exponential cut-off and $s = 1$ in black. The Drude cut-off is shown in gray. The steep ascent in the middle coincides with the time of occurrence of the maximal entanglement moving from $t \sim 2 \times d/c$ ($1/\Omega_c \lesssim 0.5/\Omega_0$) to $t \sim d/c$ ($1/\Omega \gtrsim 0.5/\Omega_0$).

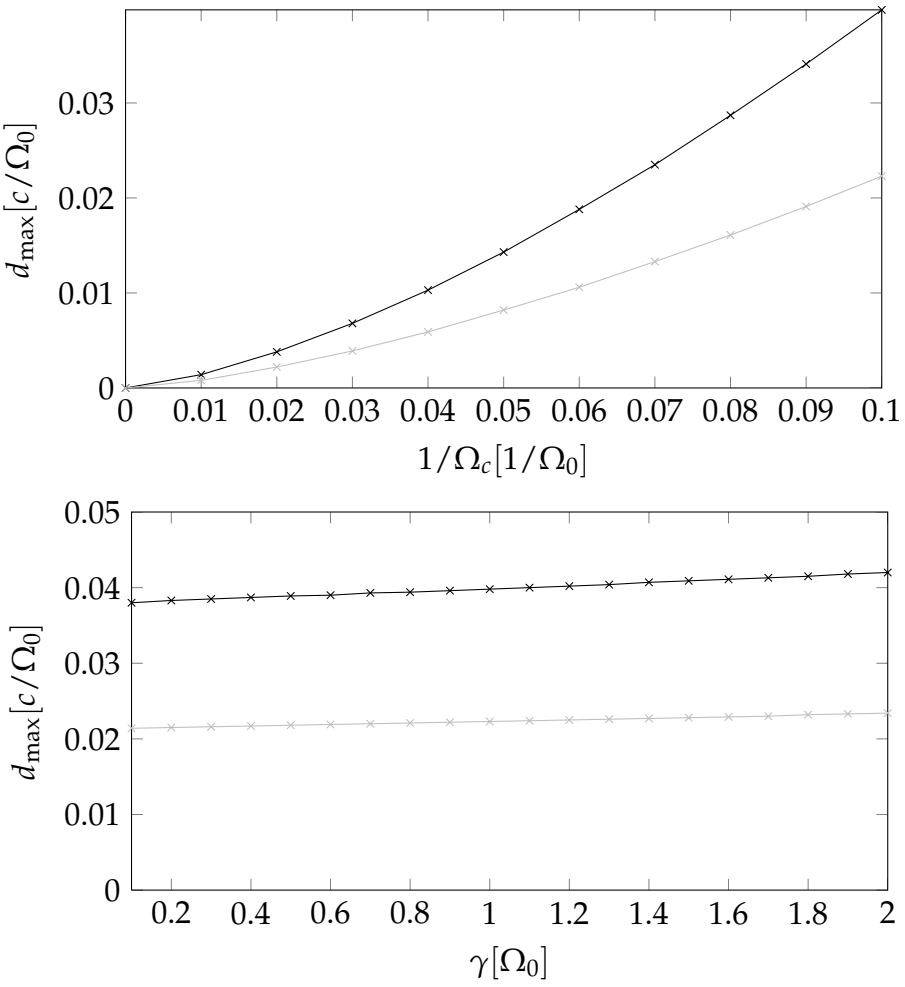

Figure 4.21.: Dependence of the maximal entanglement on the cut-off Ω_c and the coupling γ for the three-dimensional bath with exponential cut-off and $s = 3$ in black. The one-dimensional bath with exponential cut-off and $s = 3$ is shown in gray.

5. Cavity Environment

5.1. Introduction

So far we have treated free baths in different dimensions. Now, we are going to look at a geometrical constraint that drastically changes the coupling spectral density. We place the oscillators inside of a tube of infinite length with super-conducting walls and a quadratic cross section of side length a (see figure 5.1).

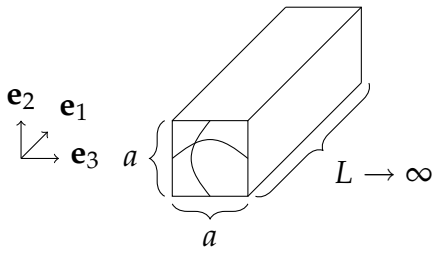

Figure 5.1.: Infinitely long tube of width a with super-conducting walls. The direction $\mathbf{e}_1$ points along the tube, whereas directions $\mathbf{e}_2$ and $\mathbf{e}_3$ span the cross section surface.

The walls impose a boundary condition on the possible environmental modes inside of the tube, which quantizes the transverse directions with the largest possible wavelength being $a/2$. This imposes a lower cut-off $\omega_0 = 2\sqrt{2}\pi c/a$ on the environmental frequencies. At the frequency of every allowed transverse excitation the coupling spectral density exhibits an integrable square root divergency, which is shown below.

As an approximation for low temperatures we are only going to consider the lowest transverse excitation in the tube. This leads to a coupling spectral density with only one divergency at the frequency ω_0.

In this situation most of the spectral weight is distributed close to the lower cut-off ω_0. This is very different from a free bath, where most of the spectral

weight is close to the upper cut-off. We have seen that increasing the upper cut-off reduces the amount of entanglement. Therefore, we have reason to expect more entanglement in an environment with a peak at low frequencies.

5.2. Coupling Spectral Density

Now, we are going to derive the exact form of the coupling spectral density of a quasi one-dimensional system in a tube. First, let us review how to rewrite the summation over wave vectors as a scalar integral over frequencies for a cubic box with side length L

$$\sum_{\mathbf{k}}(\dots) = 2\left(\frac{L}{2\pi}\right)^3 \int_0^\infty d\omega \frac{4\pi\omega^2}{c^3}(\dots)\,. \tag{5.1}$$

Going through the factors on the right hand side from left to right, the 2 is due to the two different polarizations of photons, the $La^2/(2\pi)^3$ is the quantization volume, $4\pi\omega^2$ is the result of integrating out the angles and c^3 is due to the relation $\omega = c\,|k|$.

By (5.1) we can write for the coupling spectral density

$$\begin{aligned}\sum_{\mathbf{k}} \frac{|g_{\mathbf{k}}|^2}{2m_{\mathbf{k}}\omega_{\mathbf{k}}}\delta(\omega-\omega_{\mathbf{k}}) &= 2\left(\frac{L}{2\pi}\right)^3 \int_0^\infty d\omega' \frac{4\pi\omega'^2}{2m\omega' c^3}\,|g_{\omega'}|^2\,\delta(\omega'-\omega) \\ &= \left(\frac{L}{2\pi}\right)^3 \frac{4\pi\omega}{mc^3}\,|g_\omega|^2 \stackrel{!}{=} \frac{2}{\pi} m\gamma\omega \left(\frac{\omega}{\Omega_c}\right)^{s-1} e^{-\omega/\Omega_c}\,.\end{aligned}$$

Comparing both sides, the coupling constants are read off as

$$\Rightarrow |g_\omega|^2 = \frac{4\pi m^2\gamma c^3}{L^3}\left(\frac{\omega}{\Omega_c}\right)^{s-1} e^{-\omega/\Omega_c}\,. \tag{5.2}$$

For a tube as described in section 5.1, we need to split the wave vector $\mathbf{k}$ into its components k_1, k_2, and $k_3 \in \mathbb{Z}\setminus\{0\}$

$$\mathbf{k} = \frac{2\pi k_1}{L}\mathbf{e}_1 + \frac{2\pi}{a}(k_2\mathbf{e}_2 + k_3\mathbf{e}_3)\,.$$

Only the k_1 component can approximated by an integral due to the large length of the tube in this direction. For this, we need to make a change of variables

$k_1 \to |\mathbf{k}| = k$ which induces a new line element

$$\Rightarrow \qquad k_1 = \frac{L}{2\pi}\sqrt{|\mathbf{k}|^2 - \frac{4\pi^2}{a^2}(k_2^2+k_3^2)}$$
$$\Rightarrow \qquad dk_1 = \frac{L}{2\pi}\frac{k\,dk}{\sqrt{k^2 - \frac{4\pi^2}{a^2}(k_2^2+k_3^2)}}\,.$$

Again, we rewrite the sum over the wave vectors into an integral, but this time only for the k_1 component. At the same time we will examine what happens to an additional term $e^{i\mathbf{kr}}$ as it occurs in the damping kernel (3.3) and in the bath correlator (3.6). We assume that $\mathbf{r} \parallel \mathbf{e}_1$

$$\begin{aligned}
&\sum_{\mathbf{k}} \frac{|g_{\mathbf{k}}|^2}{2m_{\mathbf{k}}\omega_{\mathbf{k}}}\delta(\omega-\omega_{\mathbf{k}})\,e^{i\mathbf{kr}} \\
&= 2\cdot 8\sum_{k_1,k_2,k_3=1}^{\infty}\frac{|g_{\mathbf{k}}|^2}{2m_{\mathbf{k}}\omega_{\mathbf{k}}}\delta(\omega-\omega_{\mathbf{k}})\cos(\mathbf{kr}) \\
&= 16\sum_{k_2,k_3=1}^{\infty}\int_0^{\infty} dk_1 \frac{|g_{\mathbf{k}}|^2}{2m_{\mathbf{k}}\omega_{\mathbf{k}}}\delta(\omega-\omega_{\mathbf{k}})\cos(k_1 r_1) \\
&= 16\sum_{k_2,k_3=1}^{\frac{4\pi c}{a}(k_2^2+k_3^2)<\omega^2} \frac{L}{2\pi}\int_0^{\infty} dk \frac{k\,|g_{\mathbf{k}}|^2\cos\left(r_1\sqrt{k^2-\frac{4\pi^2}{a^2}(k_2^2+k_3^2)}\right)}{2m_{\mathbf{k}}\omega_{\mathbf{k}}\sqrt{k^2-\frac{4\pi^2}{a^2}(k_2^2+k_3^2)}}\delta(\omega-\omega_{\mathbf{k}})\,.
\end{aligned}$$

Switching the integration from wave vectors to frequencies $\omega = ck$ and employing (5.2), we have

$$\begin{aligned}
&= 8\sum_{k_2,k_3=1}^{\frac{\omega_0^2}{2}(k_2^2+k_3^2)<\omega^2} \frac{L}{2\pi c}\int_0^{\infty} d\omega' \frac{|g_{\omega'}|^2\cos\left(r_1\sqrt{\omega'^2-\frac{4\pi^2}{a^2}(k_2^2+k_3^2)}\right)}{m\sqrt{\omega'^2-\frac{4\pi^2c^2}{a^2}(k_2^2+k_3^2)}}\delta(\omega-\omega') \\
&= \sum_{k_2,k_3=1}^{\frac{\omega_0^2}{2}(k_2^2+k_3^2)<\omega^2} \frac{4L}{\pi c}\frac{|g_{\omega}|^2\cos\left(r_1\sqrt{\omega^2-\frac{4\pi^2}{a^2}(k_2^2+k_3^2)}\right)}{m\sqrt{\omega^2-\frac{4\pi^2c^2}{a^2}(k_2^2+k_3^2)}} \\
&= \sum_{k_2,k_3=1}^{\frac{\omega_0^2}{2}(k_2^2+k_3^2)<\omega^2} \frac{16m\gamma c^2}{a^2}\frac{\cos\left(r_1\sqrt{\omega^2-\frac{4\pi^2}{a^2}(k_2^2+k_3^2)}\right)}{\sqrt{\omega^2-\frac{4\pi^2c^2}{a^2}(k_2^2+k_3^2)}}\left(\frac{\omega}{\Omega_c}\right)^{s-1} e^{-\omega/\Omega_c}\,.
\end{aligned}$$

At low temperatures the first excitation is the most important one. For this reason we approximate the sum over k_2 and k_3 by its first term $k_2, k_3 = 1$ only. We also replace all occurrences of a by $\omega_0 = 2\sqrt{2}\pi c/a$. Then the coupling spectral density ($r = 0$) is

$$J(\omega > \omega_0) = \frac{2m\gamma\omega_0^2}{\pi^2\sqrt{\omega^2 - \omega_0^2}} \left(\frac{\omega}{\Omega_c}\right)^{s-1} e^{-\omega/\Omega_c} . \tag{5.3}$$

In the damping kernel

$$\Gamma_r(t) = \sum_{\mathbf{k}} \frac{g_k^2}{M m_k \omega_k^2} \cos(w_k t) e^{-i\mathbf{kr}} = 4\int_0^\infty d\omega \, \frac{J(\omega)}{\omega} \cos(\omega t) \cos(r\sqrt{\omega^2 - \omega_0^2})$$

and the bath correlator

$$K_r(t) = 4\int_0^\infty d\omega \, J(\omega) \coth\left(\frac{\omega}{2T}\right) \cos(\omega t) \cos(r\sqrt{\omega^2 - \omega_0^2}) ,$$

the term $e^{i\mathbf{kr}}$ turns into a factor $\cos(r\sqrt{\omega^2 - \omega_0^2})$.

As a final step, we check that we can recover the free case by considering all excitations, taking the limit $a \to \infty$, and making k_2, k_3 continuous. We obtain

$$\begin{aligned}
&\sum_{k_2,k_3=1}^{\frac{\omega_0^2}{2}(k_2^2+k_3^2)<\omega^2} \frac{2m\gamma\omega_0^2}{\pi^2\sqrt{\omega^2 - \frac{\omega_0^2}{2}(k_2^2+k_3^2)}} \left(\frac{\omega}{\Omega_c}\right)^{s-1} e^{-\omega/\Omega_c} \\
&\to \frac{2m\gamma\omega_0^2}{\pi^2} \iint_0^{\frac{\omega_0^2}{2}(k_2^2+k_3^2)<\omega^2} \frac{1}{\sqrt{\omega^2 - \frac{\omega_0^2}{2}(k_2^2+k_3^2)}} \left(\frac{\omega}{\Omega_c}\right)^{s-1} e^{-\omega/\Omega_c} \, dk_2 \, dk_3 \\
&= \frac{2m\gamma\omega_0^2}{\pi^2} \int_0^{\sqrt{2}\frac{\omega}{\omega_0}} dr \int_0^{\frac{\pi}{2}} d\varphi \frac{r}{\sqrt{\omega^2 - \frac{\omega_0^2}{2}r^2}} \left(\frac{\omega}{\Omega_c}\right)^{s-1} e^{-\omega/\Omega_c} \\
&= \frac{2m\gamma\omega_0^2}{\pi^2} \frac{\pi}{2} 2\frac{\omega}{\omega_0^2} \left(\frac{\omega}{\Omega_c}\right)^{s-1} e^{-\omega/\Omega_c} = \frac{2}{\pi} m\omega\gamma \left(\frac{\omega}{\Omega_c}\right)^{s-1} e^{-\omega/\Omega_c} ,
\end{aligned}$$

which is the free coupling spectral density.

5.3. Results

Apart from the fact that some special care has to be taken of the singularity in the coupling spectral density, exactly the same numerical code as for the free bath can be used to determine the time evolution of the entanglement of the two system oscillators inside of a cavity. Some details of how the singularity is handled are covered in appendix B. In this chapter we will only treat the time evolution.

All the results are shown in figures 5.2 to 5.9 on the following pages. They are displayed as two-dimensional density plots, in which the x-axis denotes the time t and the y-axis denotes the distance d. The value of the entanglement is encoded in levels of gray as depicted by the scale on the right hand side of the plots. To aid the eye, the area, in which the entanglement is exactly zero, is separated from the area, in which the entanglement is non-zero, by a continuous black line. In some areas the numerical algorithm did not produce valid results due to convergence problems and running time constraints. These are filled with a crosshatch pattern. The plots are organized in the following way: Figures 5.2 to 5.4 contain the results for a coupling constant of the value $\gamma = 0.1\,\Omega_0$, figures 5.5 to 5.7 for $\gamma = 0.01\,\Omega_0$, and figures 5.8 to 5.9 for $\gamma = \Omega_0$. In each of the sets the frequency of the divergency is increased stepwise from slightly below the system oscillator frequency Ω_0 to slightly above Ω_0.

As the initial state we use a (separable) squeezed state with $a = 10$ as defined in section 4.4.4, because the additional energy contained in it enhances the amount of entanglement that can occur during the evolution.

The effect of entanglement creation is most pronounced if the divergency of the coupling spectral density ω_0 is close to the oscillator frequency Ω_0. If ω_0 is smaller than Ω_0, the range over which entanglement is generated increases, but the total amount is smaller. On the other hand, if ω_0 is slightly larger than Ω_0, the range decreases, but the amount of entanglement generated for small distances increases.

Varying the coupling strength γ reveals that smaller coupling strengths lead to smoother dynamics with less oscillations. Also it takes longer for entanglement to build up. Increasing the coupling strength, on the other hand, increases the amplitude of the oscillations and leads to a quicker appearance of entanglement.

As expected, increasing the temperature of the bath decreases the produced entanglement as shown in figure 5.9.

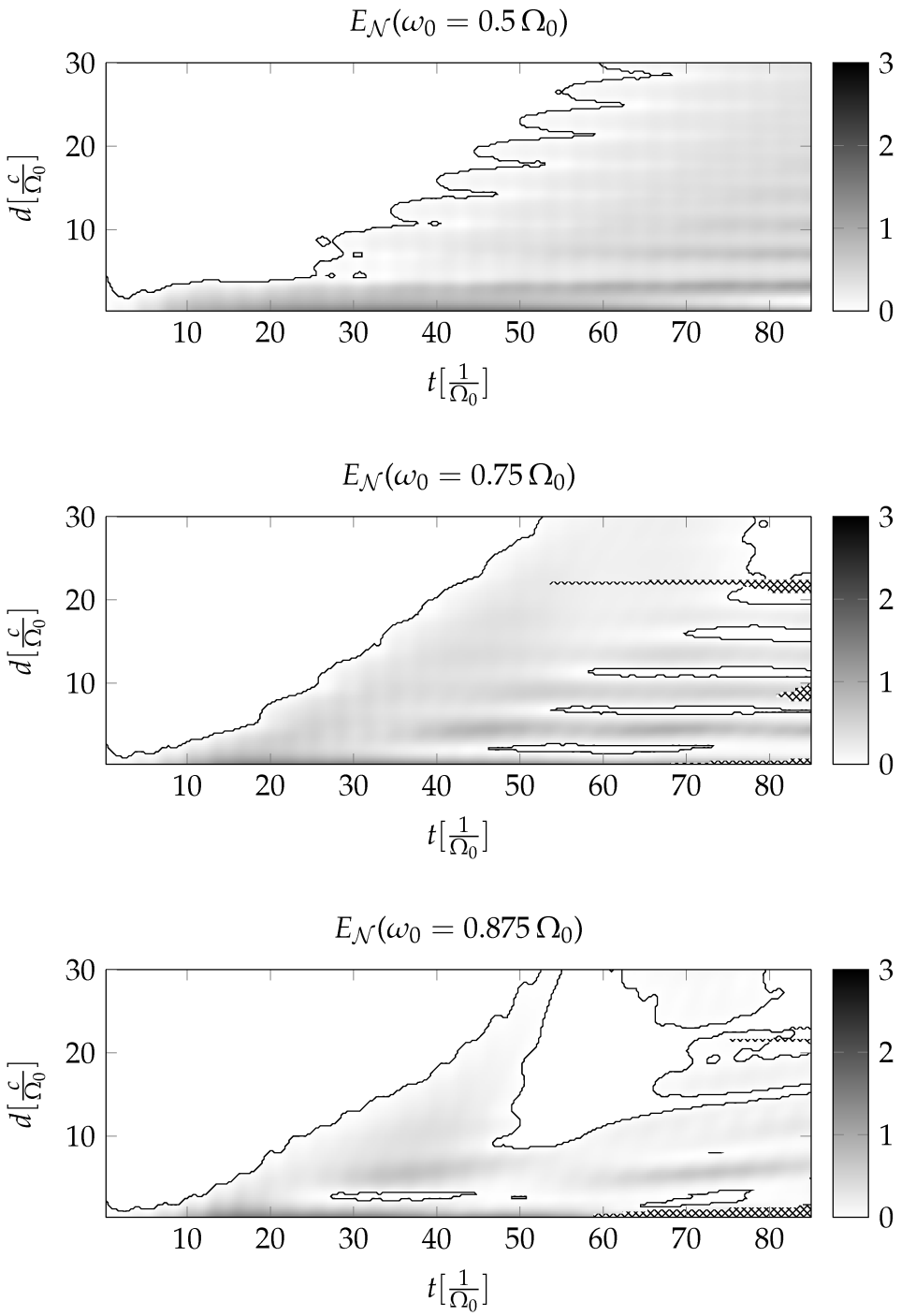

Figure 5.2.: Dynamics of the entanglement for $\gamma = 0.1\,\Omega_0$. The crosshatch pattern covers areas with no results.

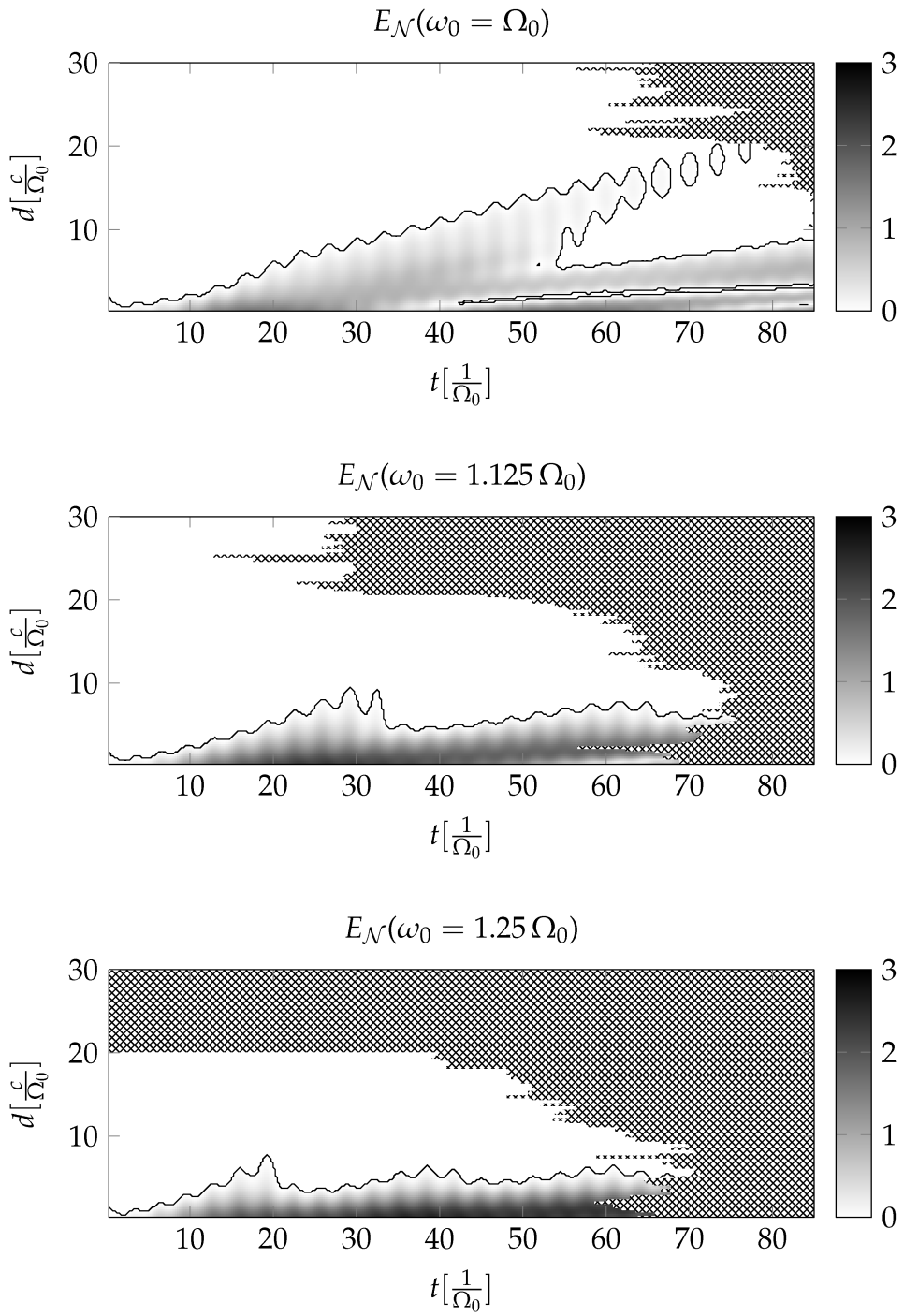

Figure 5.3.: Dynamics of the entanglement for $\gamma = 0.1\,\Omega_0$. The crosshatch pattern covers areas with no results.

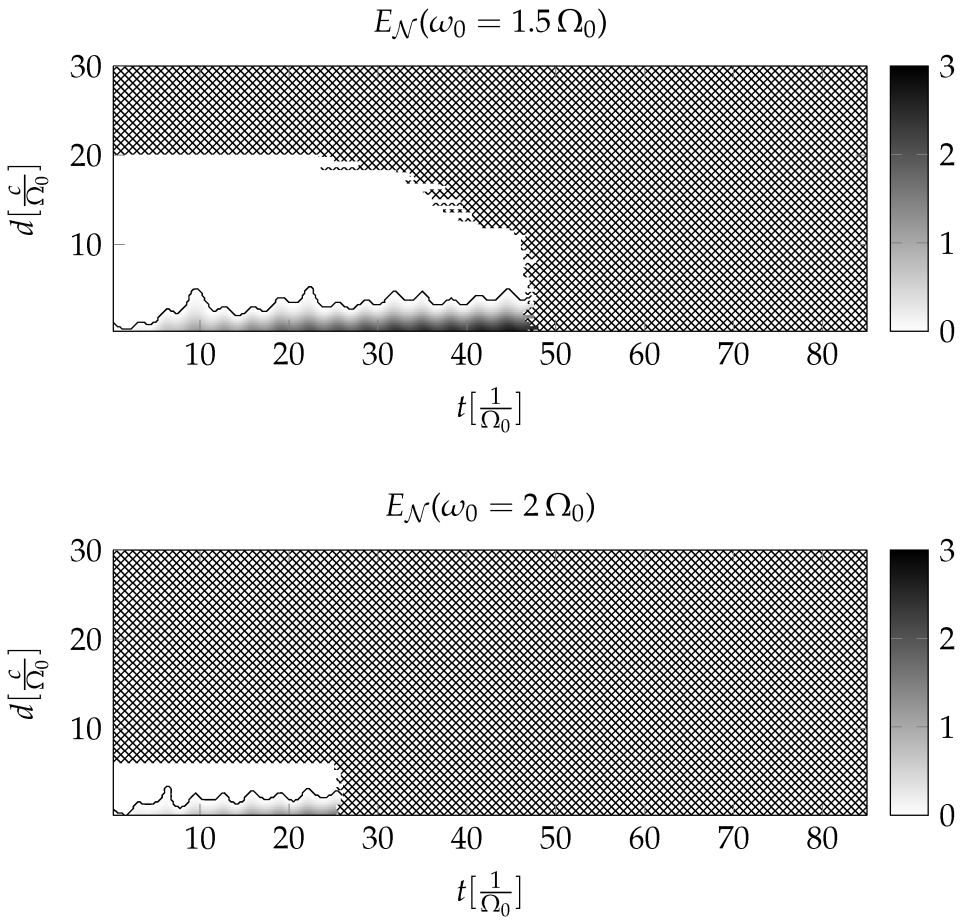

Figure 5.4.: Dynamics of the entanglement for $\gamma = 0.1\,\Omega_0$. The crosshatch pattern covers areas with no results.

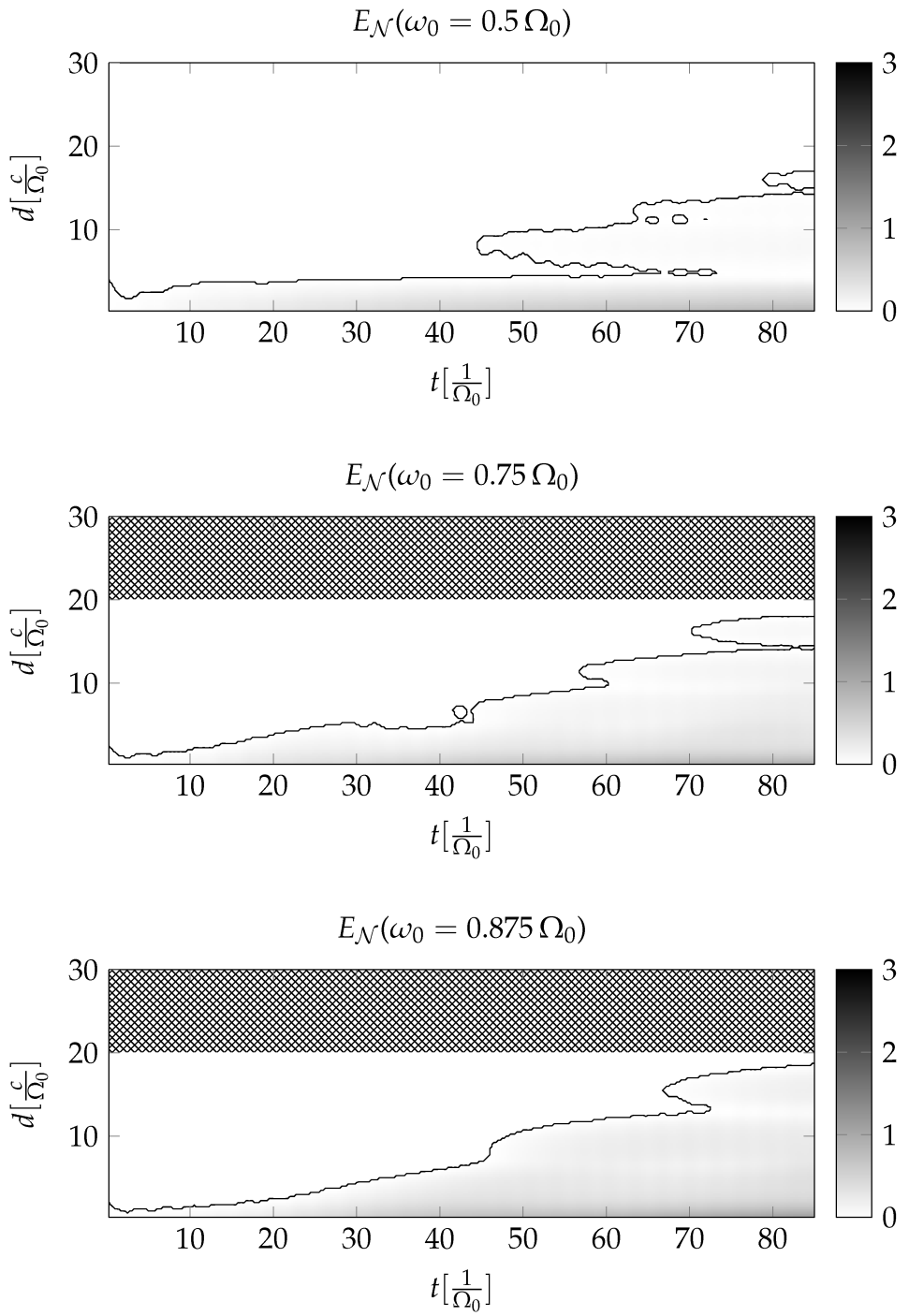

Figure 5.5.: Dynamics of the entanglement for $\gamma = 0.01\,\Omega_0$. The crosshatch pattern covers areas with no results.

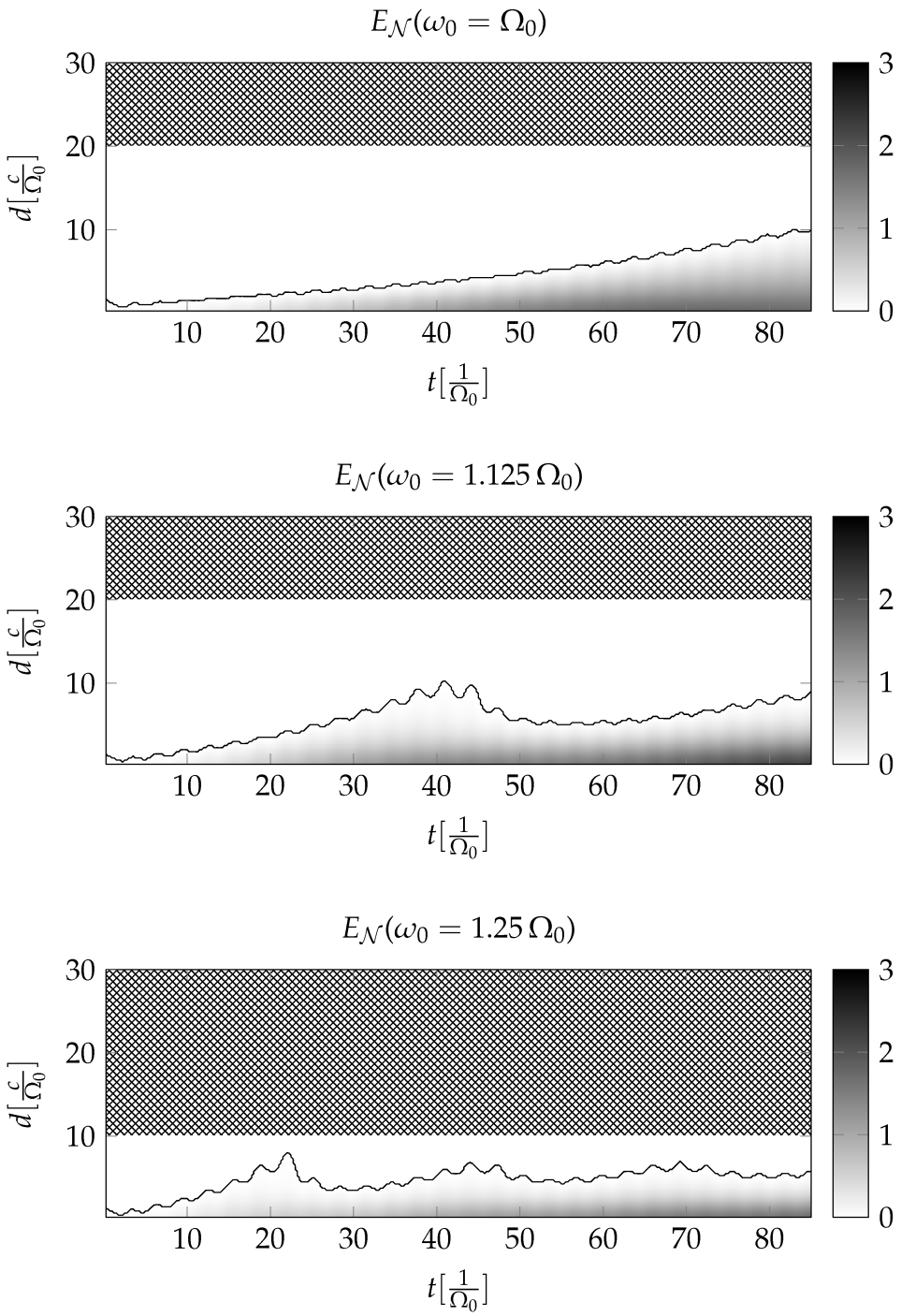

Figure 5.6.: Dynamics of the entanglement for $\gamma = 0.01\,\Omega_0$. The crosshatch pattern covers areas with no results.

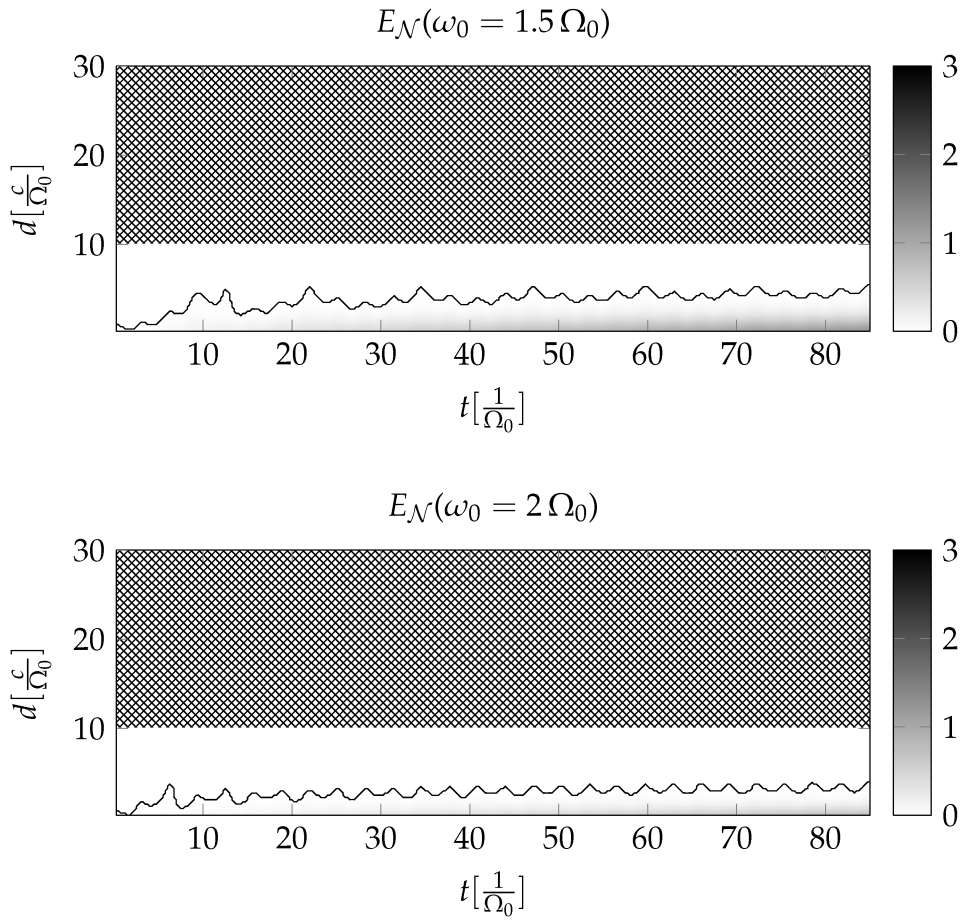

Figure 5.7.: Dynamics of the entanglement for $\gamma = 0.01\,\Omega_0$. The crosshatch pattern covers areas with no results.

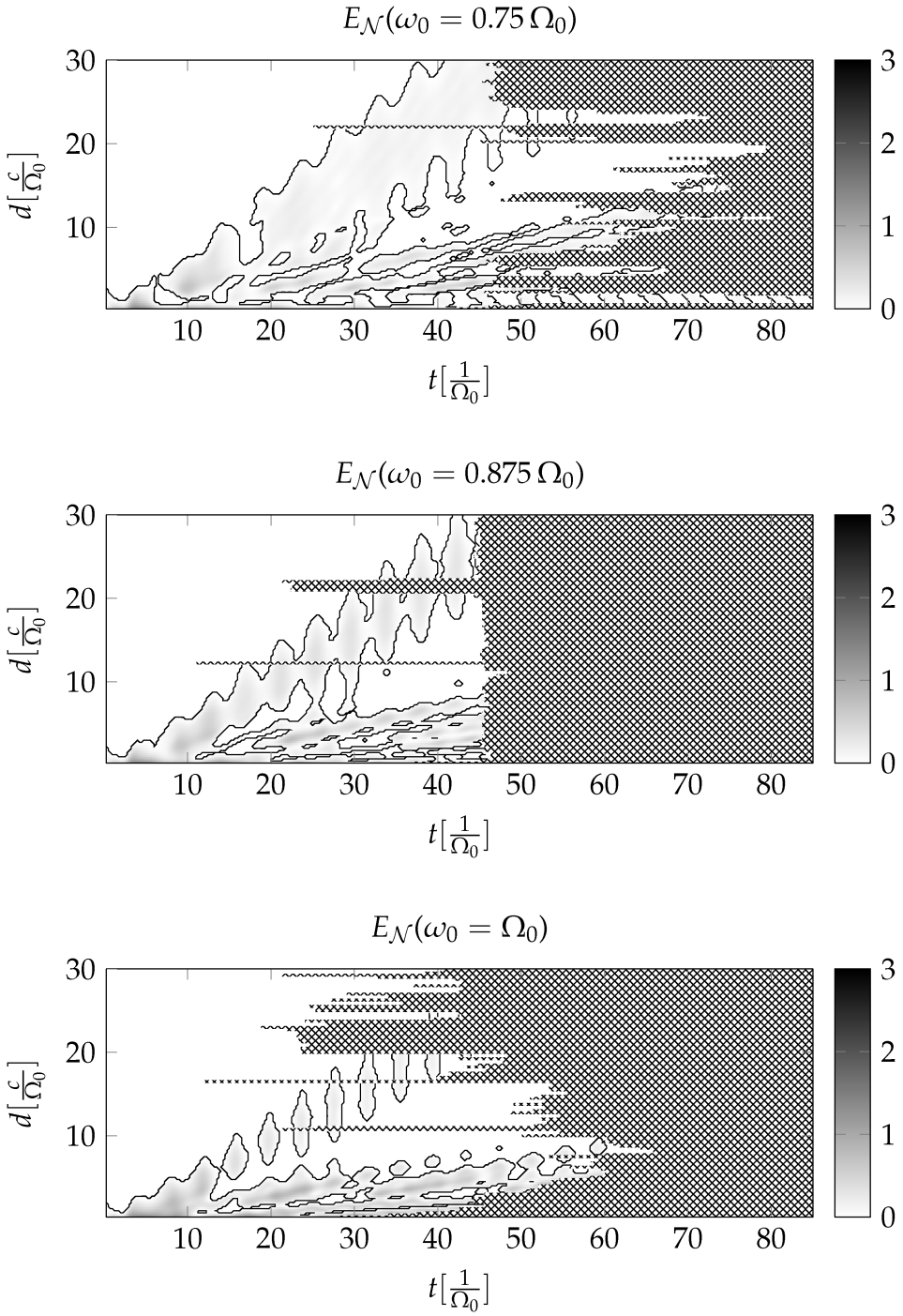

Figure 5.8.: Dynamics of the entanglement for $\gamma = \Omega_0$. The crosshatch pattern covers areas with no results.

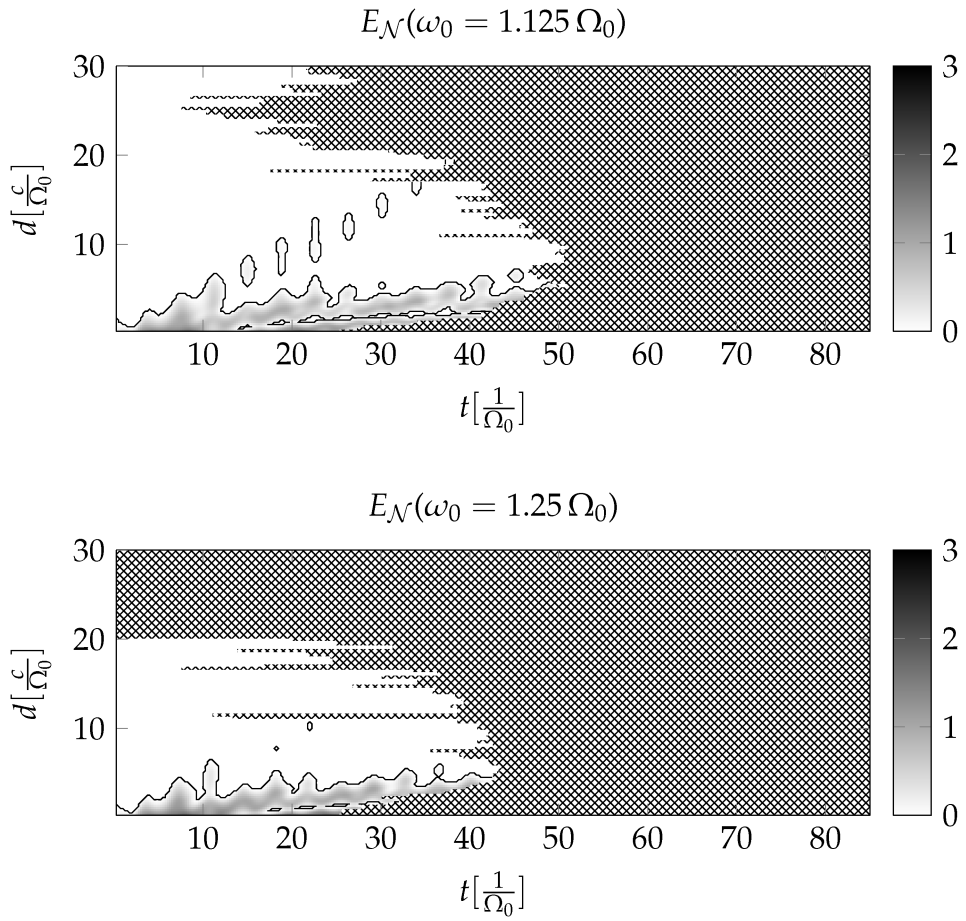

Figure 5.9.: Dynamics of the entanglement for $\gamma = \Omega_0$. The crosshatch pattern covers areas with no results.

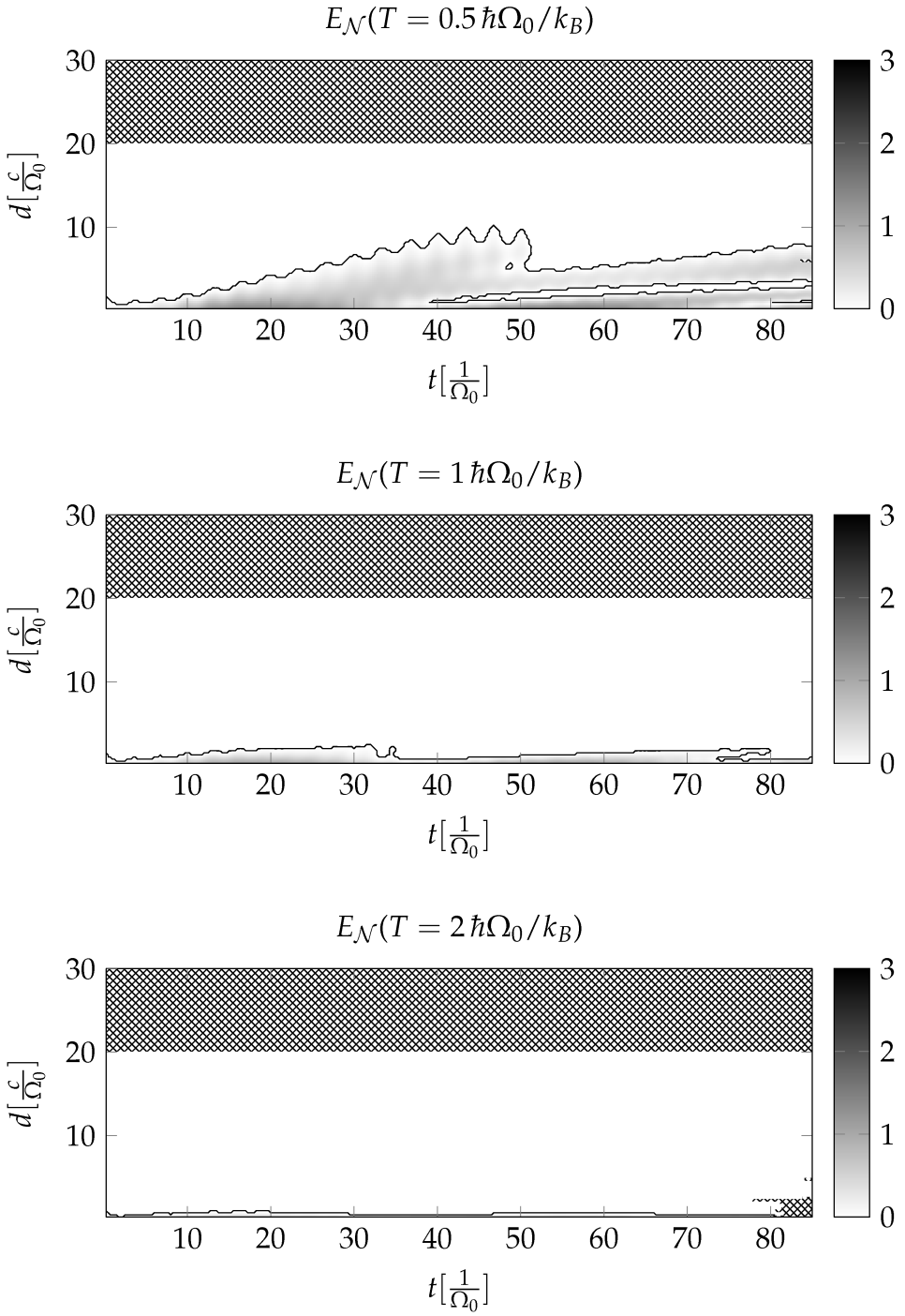

Figure 5.10.: Dynamics of the entanglement at finite temperature ($\gamma = 0.1\,\Omega_0$, $\omega_0 = \Omega_0$). The crosshatch pattern covers areas with no results.

5.4. Comparison with an Approximation

In his PhD thesis [Que11] Friedemann Queisser has examined an approximation to the model presented here. It is based on the idea that the large peak in the coupling spectral density can be replaced by two harmonic coupling oscillators, one representing the symmetric modes and one representing the anti-symmetric modes. Their coupling strength is denoted by g_{ω_0}. The effect of the modes in the coupling spectral density which are further away from the peak is combined into a free bath interacting with the system oscillators in Born-Markov-approximation with a coupling strength of γ. He is able to derive a distance dependent relation between the two coupling constants g_{ω_0} and γ. This enables us to directly compare the results, because the same set of parameters is used as in this work.

As shown in figures 5.11 and 5.12 the qualitative agreement is very good. The largest amount of entanglement creation can be seen for ω_0 being close to Ω_0 and increasing the coupling strength γ increases the amount of oscillation of the entanglement as well decreasing the distance over which entanglement is created.

5.5. Conclusion

We claim that, contrary to the free bath (cf. figure 5.13), in the cavity practicable amounts of entanglement are created by coupling the two system oscillators to the bath even over large distances. The situation is different than in the free bath, due to the divergency in the coupling spectral density. A single frequency dominates the spectrum, which then mediates an indirect interaction between the system oscillators stronger than the decoherence effect caused by the other bath modes.

Clearly, entanglement is only created after the time $t > d/c$ has passed, which preserves causality. Only at very short distances this can be violated due to bath intrinsic entanglement. The robustness of the qualitative behavior under the approximation of Friedemann Queisser supports this statement. The possibility of an experimental implementation of this effect remains subject to further work.

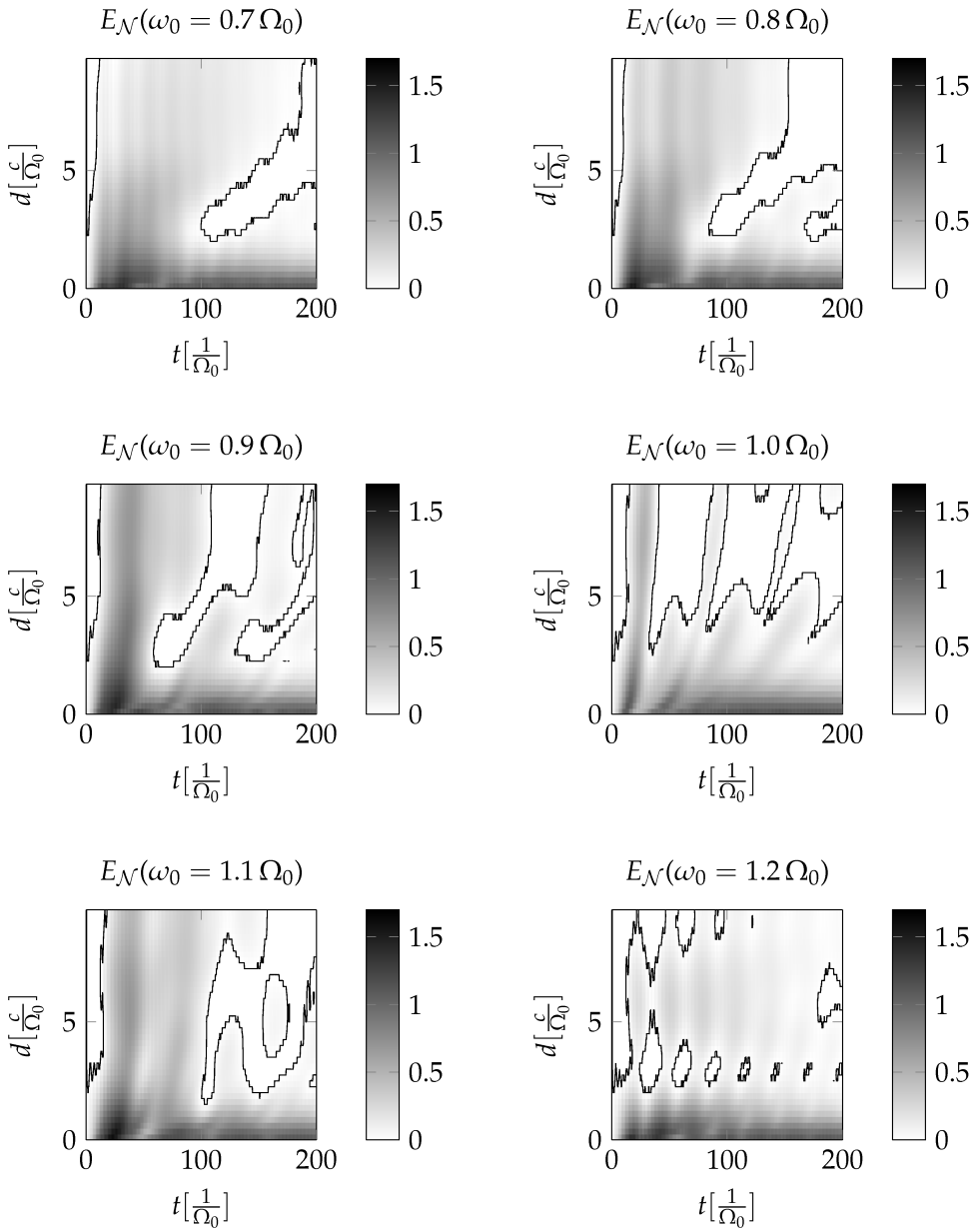

Figure 5.11.: Time evolution of the entanglement in the approximation of the cavity environment by Friedemann Queisser [Que11]. Parameters: $\gamma = 0.02\,\Omega_0$, $\Omega_c = 5\,\Omega_0$, $T = 0.01\,\Omega_0$, $a = 5\,\Omega_0$, $s = 1$. Figures included with permission of the author.

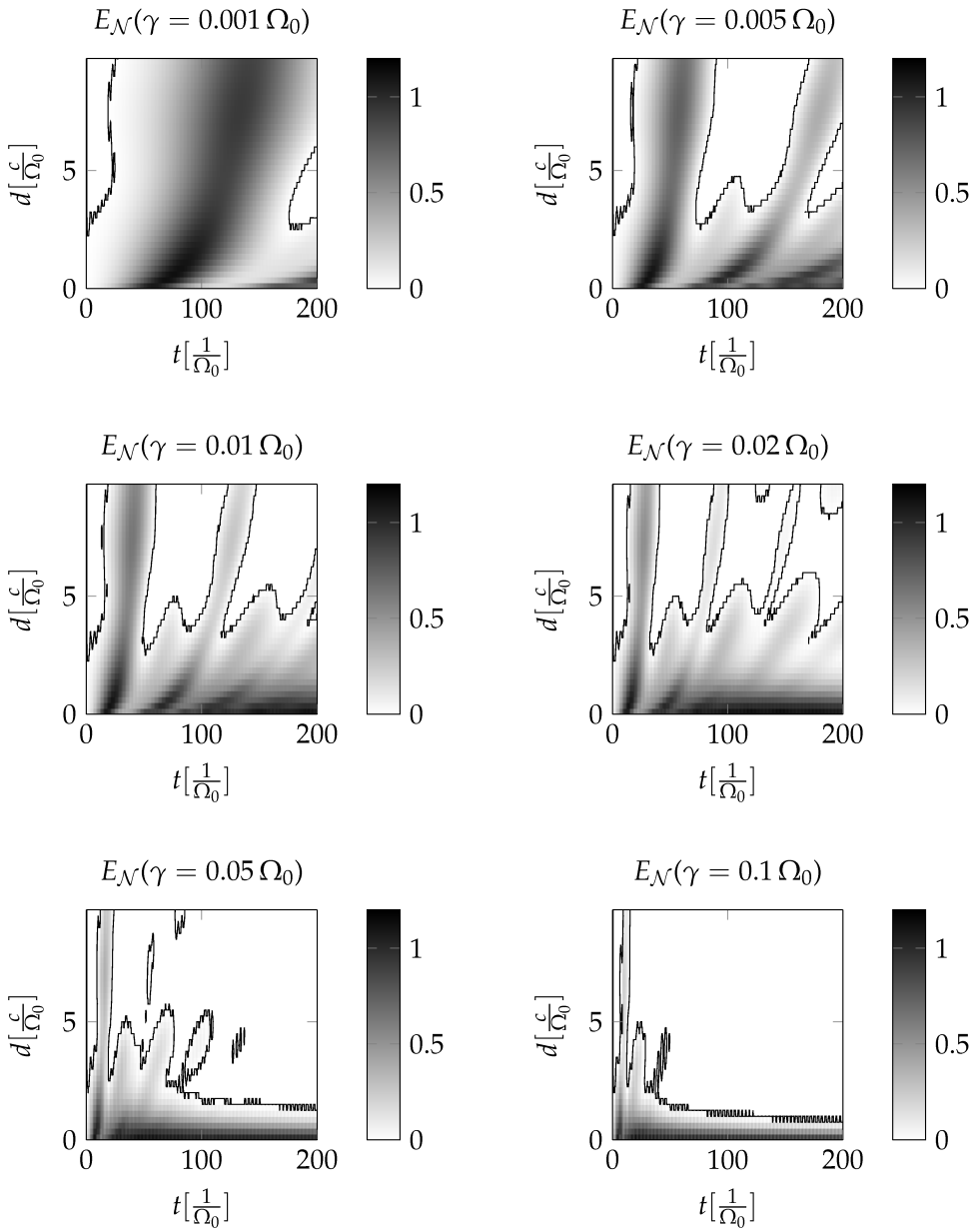

Figure 5.12.: Time evolution of the entanglement in the approximation of the cavity environment by Friedemann Queisser [Que11]. Parameters: $\Omega_0 = \omega_0$, $\Omega_c = 5\,\Omega_0$, $T = 0.01\,\Omega_0$, $a = 5\,\Omega_0$, $s = 1$. Figures included with permission of the author.

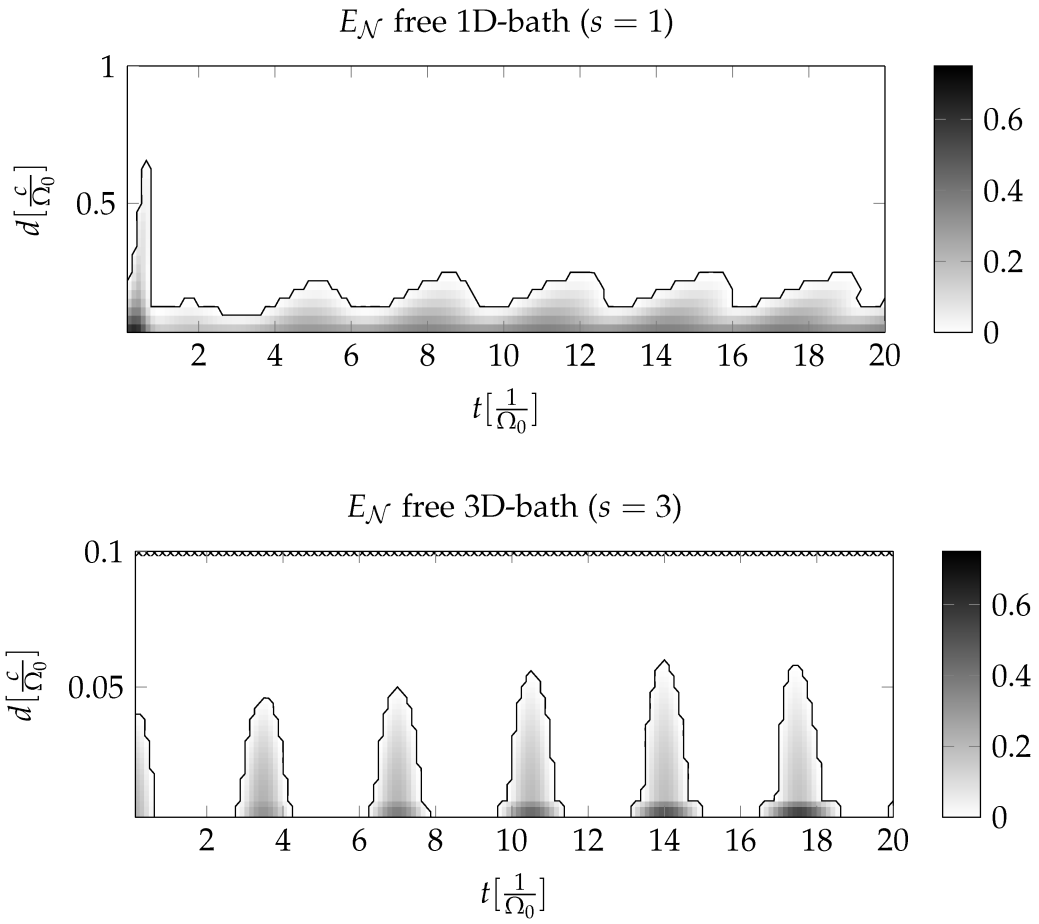

Figure 5.13.: Time evolution of the entanglement in a free bath as presented in the previous chapter. Here, the entanglement evolution is shown in the form of a density plot for better comparison with the results presented in this chapter. The parameters are the same as in figure 4.9. Due to the comparably large scale and the coarse-grained resolution, the first large peak for the three-dimensional bath (bottom plot) is not visible.

6. Summary and Conclusion

We calculate the entanglement dynamics of two harmonic oscillators coupled to a common bosonic environment. The calculation is exact, fully taking into account all non-Markovian and retardation effects. Also, no rotating wave approximation is performed. Two different cases are considered. The first one is the general case of a free bath of one and three dimensions as well as ohmic and super-ohmic coupling spectral densities. The second one is the special case of a restricted geometry with the bath modes contained in an infinitely long tube with a square-shaped cross-section.

We numerically determine a relation between the size of the individual oscillators and the maximal separation $d_{\max}$ at which entanglement seizes to be generated by the free bath. It is shown that they are proportional with a proportionality constant of $\mathcal{O}(1)$, i.e. that the two oscillators effectively have to be touching each other. Due to this, we claim that environmentally induced interaction does not have any advantages over direct coupling. Apparently, entanglement cannot be obtained "for free".

The situation can be different, however, if the coupling spectral density is modified, for example by a geometrical restriction imposed on the bosonic modes by a super-conducting cavity. Here, a peak at a single frequency dominates the spectral density, mediating a long-range coherent interaction. We find that significant amounts of entanglement are created over distances larger than the size of the individual systems even for finite temperatures. Whether the effect can be observed experimentally for the type of bath we have implemented in this work remains to be investigated. A different experimental approach to modify the coupling spectral density is presented in [KMJ$^+$10].

Sparked by the initial idea of entanglement generation by Braun in 2002 [Bra02] quite a number of authors have published positive results for two-level systems [BFP03, BF06a, STP06, CL07, FNGM09, RBK11] and harmonic oscillators [BF06b, HB08, PR08, Isa08, XSS08, LSF10] with no spatial separation. These works qualitatively agree with our results in the limit separation distance $d \to 0$, but we find that the results for this limit do not extend to significant finite

distances.

Less publications have tried to include spatial separation in their calculations [BF05, STP07, MNBF09, CP09, ASH09], but all employ various kinds of approximations and disagree with our result. One of the first was also by Daniel Braun [Bra05], who predicts entanglement generation over arbitrarily large distances with only a polynomial decay. However, the model is dissipation-less, therefore possessing a non-local conserved observable, which we believe is the reason for the contradictory result. Another model with a non-local conserved observable has been checked by Friedemann Queisser [Que11] to also contradict our fully dissipative model. The only work we are aware of, which tries to correct the flaws found in the above mentioned publications, is by Fleming *et al.* [FCAH10]. There, the even stronger statement is made that for two-state systems embedded in a common bath no asymptotic entanglement can be found, regardless of the distance d.

In conclusion, this work dispels a common misunderstanding about the possibility of entanglement generation in bosonic baths. We also propose a new approach to create entanglement over finite distances, which can be useful for various quantum informational tasks.

A. Laplace Transformation of the Green's Function

The Laplace transformation of the Green's function $\tilde{\mathcal{G}}(s)$ is a rather complicated expression which is also not very instructive. It is printed here for reference

$$\tilde{\mathcal{G}}(s) = \frac{1}{D}\begin{pmatrix} G_1 & G_2 & G_3 & G_4 \\ G_2 & G_1 & G_4 & G_3 \\ G_5 & G_6 & G_7 & G_8 \\ G_6 & G_5 & G_8 & G_7 \end{pmatrix}.$$

All matrix elements

$$G_1 = s^3 + \frac{2\gamma\Omega_c s^2}{\Omega_c + s} + \Omega_0^2 s$$

$$G_2 = \frac{2e^{-ds}\gamma\Omega_c^2 s^2}{s^2 - \Omega_c^2} - \frac{2e^{-\Omega_c d}\gamma\Omega_c s^3}{s^2 - \Omega_c^2}$$

$$G_3 = \Omega_0^2 + s^2 + \frac{2\gamma\Omega_c s}{\Omega_c + s}$$

$$G_4 = \frac{2e^{-ds}\gamma\Omega_c^2 s}{s^2 - \Omega_c^2} - \frac{2e^{-\Omega_c d}\gamma\Omega_c s^2}{s^2 - \Omega_c^2}$$

$$G_5 = \frac{4\gamma^2\Omega_c^2 s^2\left(e^{-\Omega_c d}s - e^{-ds}\Omega_c\right)^2}{\left(s^2 - \Omega_c^2\right)^2} - \left(\Omega_0^2 + \frac{2\gamma\Omega_c s}{\Omega_c + s}\right)^2 + s\left(-s\Omega_0^2 - \frac{2\gamma\Omega_c s^2}{\Omega_c + s}\right)$$

$$G_6 = \frac{2e^{-ds}\gamma\Omega_c^2 s^3}{s^2 - \Omega_c^2} - \frac{2e^{-\Omega_c d}\gamma\Omega_c s^4}{s^2 - \Omega_c^2}$$

$$G_7 = s^3 + \frac{2\gamma\Omega_c s^2}{\Omega_c + s} + \Omega_0^2 s$$

$$G_8 = \frac{2e^{-ds}\gamma\Omega_c^2 s^2}{s^2 - \Omega_c^2} - \frac{2e^{-\Omega_c d}\gamma\Omega_c s^3}{s^2 - \Omega_c^2}$$

have the same denominator

$$D = -\frac{4\gamma^2\Omega_c^2 s^4 e^{-2\Omega_c d}}{\left(s^2-\Omega_c^2\right)^2} + \frac{4\gamma^2\Omega_c^2 s^2}{(\Omega_c+s)^2} - \frac{4\gamma^2\Omega_c^4 s^2 e^{-2ds}}{\left(s^2-\Omega_c^2\right)^2} + \frac{8\gamma^2\Omega_c^3 s^3 e^{-\Omega_c d - ds}}{\left(s^2-\Omega_c^2\right)^2} + \frac{4\gamma\Omega_0^2\Omega_c s}{\Omega_c+s} + \frac{4\gamma\Omega_c s^3}{\Omega_c+s} + \Omega_0^4 + 2\Omega_0^2 s^2 + s^4 .$$

B. Numerical Algorithms

First attempts to solve equation (3.4) were made with the Durbin formula [Dur74]. The Laplace transformation of the solution has to be known analytically for this approach to be feasible, which limits it to a Drude cut-off. Massive improvements of the run-time could be achieved by implementing the epsilon acceleration described in [PH84]. Still, the limitation to the Drude cut-off remained.

Subsequently, switching to the algorithm of Wilkie and Wong [WW08], which we will restate in this appendix, removed this restriction and enabled the use of any cut-off function. The algorithm can be employed to solve generalized Langevin equations (GLEs) of the type

$$\dot{X}_j(t) = a_j(\mathbf{X}, t) - \int_0^t dt' \, \gamma_j(t - t') b_j(\mathbf{X}(t'), t') + f_j(t) \,,$$

where $j = 1, \ldots, N$, $\mathbf{X} = (X_1, \ldots, X_N)$, $a_j(\mathbf{X}, t)$ and $b_j(\mathbf{X}, t)$ are some arbitrary functions, $\gamma_j(t - t')$ is the memory kernel and f_j is the noise term. Of course, it is also possible to trivially include multiple memory kernels per equation due to the linearity of the integral.

Now, a helper function is defined

$$\lambda_j(t, u) = \int_0^t dt' \, \gamma_j(t - t' + u) b_j(\mathbf{X}(t'), t') \,, \tag{B.1}$$

which can be used to rewrite the GLE as

$$\boxed{\dot{X}_j(t) = a_j(\mathbf{X}, t) - \lambda_j(t, 0) + f_j(t)} \,.$$

Equation (B.1) is the solution of the ordinary differential equation

$$\dot{\lambda}_j(t, u) = \gamma_j(u) b_j(\mathbf{X}(t), t) + \frac{\partial \lambda_j(t, u)}{\partial u} \,,$$

which can be turned into an equation algebraic in u via the Fourier transformation $\Lambda_j(t,s) = \frac{1}{\sqrt{2\pi}} \int_{-\infty}^{\infty} du\, e^{-ius} \lambda_j(t,u)$

$$\boxed{\dot{\Lambda}_j(t,s) = \Lambda_j(s) b_j(\mathbf{X}(t),t) + is\Lambda_j(t,s)}\,.$$

Finally, discretizing the inverse Fourier transformation on a grid $s_j(k) = (-n_j^{\text{grid}} + k - 1)s_j^{\max}/n_j^{\text{grid}}$ for $k = 1, \ldots, 2n_j^{\text{grid}} + 1$ with $\Delta s_j = s_j^{\max}/n_j^{\text{grid}}$ leads to

$$\boxed{\lambda_j(t,0) = \frac{1}{\sqrt{2\pi}} \int_{-\infty}^{\infty} ds\, \Lambda_j(t,s) \approx \frac{\Delta s_j}{\sqrt{2\pi}} \sum_{k=1}^{2n_j^{\text{grid}}+1} \Lambda_j(t, s_j(k))}\,.$$

The boxed equations form a coupled system of $2n_j^{\text{grid}} + 1$ ordinary differential equations (ODEs), which can be reduced to $n_j^{\text{grid}} + 1$ equations if $\gamma_j(t)$ is real and symmetric. Now, we have transformed the problem of solving the GLE into one that can be tackled by standard algorithms.

More specifically, in our case we have $N = 4$ and the equations

$$\begin{aligned}
\dot{X}_1(t) &= X_3(t) \\
\dot{X}_2(t) &= X_4(t) \\
\dot{X}_3(t) &= -\Omega_0^2 X_1 - \dot{\lambda}_1(t,0) \\
\dot{X}_4(t) &= -\Omega_0^2 X_2 - \dot{\lambda}_2(t,0)\,,
\end{aligned}$$

as well as the equations

$$\begin{aligned}
\dot{\Lambda}_1(t,s) &= \Gamma(s) X_1 + \Gamma_d(s) X_2 + is\Lambda_1(t,s) \\
\dot{\Lambda}_2(t,s) &= \Gamma(s) X_2 + \Gamma_d(s) X_1 + is\Lambda_2(t,s)\,.
\end{aligned}$$

The free bath is calculated on a grid of size $n^{\text{grid}} = 10000$ and $s^{\max} = 10\,\Omega_c$. These values are the same for all equations. Thus, we drop the index j on $s^{\max}$ and n^{grid}. Integrating the coupled ODEs can be achieved easily by the algorithms included in the GNU Scientific Library (GSL) [Gou09], which are very fast and feature automatic error estimation and choice of step size.

For the tube a regular grid is not optimal due to the singularity in the spectral coupling density. We use a grid with points distributed according to the formula

$$s(k) = \frac{s^{\max} - \omega_0}{(n^{\text{grid}})^2} \cdot k^2 + \omega_0\,,$$

where $k = 1, \ldots, n^{\text{grid}}$. The now k-dependent grid spacing is then given by

$$\Delta s(k) = \frac{2k}{(n^{\text{grid}})^2}(s^{\max} - \omega_0)\,.$$

This allows for sufficient convergence properties with similar grid sizes as for the case of the free bath.

Bibliography

[AGR82] Aspect, Alain ; Grangier, Philippe ; Roger, Gérard: Experimental realization of Einstein-Podolsky-Rosen-Bohm gedankenexperiment: A new violation of Bell's inequalities. *Physical Review Letters*, **49**(2):91, July 1982. 3

[ASH09] Anastopoulos, C. ; Shresta, S. ; Hu, B.: Non-Markovian entanglement dynamics of two qubits interacting with a common electromagnetic field. *Quantum Information Processing*, **8**(6):549–563, December 2009. 1, 82

[BBC+93] Bennett, Charles H. ; Brassard, Gilles ; Crépeau, Claude ; Jozsa, Richard ; Peres, Asher ; Wootters, William K.: Teleporting an unknown quantum state via dual classical and Einstein-Podolsky-Rosen channels. *Physical Review Letters*, **70**(13):1895, March 1993. 6

[BBPS96] Bennett, Charles H. ; Bernstein, Herbert J. ; Popescu, Sandu ; Schumacher, Benjamin: Concentrating partial entanglement by local operations. *Physical Review A*, **53**(4):2046, April 1996. 9

[BDF+99] Bennett, Charles H. ; DiVincenzo, David P. ; Fuchs, Christopher A. ; Mor, Tal ; Rains, Eric ; Shor, Peter W. ; Smolin, John A. ; Wootters, William K.: Quantum nonlocality without entanglement. *Physical Review A*, **59**(2):1070, February 1999. 6

[BDSW96] Bennett, Charles H. ; DiVincenzo, David P. ; Smolin, John A. ; Wootters, William K.: Mixed-state entanglement and quantum error correction. *Physical Review A*, **54**(5):3824, November 1996. 9

[Bel64] Bell, John: On the Einstein-Podolsky-Rosen paradox. *Physics*, **1**(3):195, 1964. 3

[BF05] Benatti, F ; Floreanini, R: Controlling entanglement generation in external quantum fields. *Journal of Optics B: Quantum and Semiclassical Optics*, **7**(10):S429–S434, October 2005. 82

[BF06a] Benatti, F. ; Floreanini, R.: Asymptotic entanglement of two independent systems in a common bath. *International Journal of Quantum Information*, **4**(3):395–404, June 2006. 81

[BF06b] Benatti, F ; Floreanini, R: Entangling oscillators through environment noise. *Journal of Physics A: Mathematical and General*, **39**(11):2689–2699, March 2006. 81

[BFC07] Bellomo, B. ; Franco, R. Lo ; Compagno, G.: Non-Markovian effects on the dynamics of entanglement. *Physical Review Letters*, **99**(16):160502, October 2007. 43

[BFP03] Benatti, Fabio ; Floreanini, Roberto ; Piani, Marco: Environment induced entanglement in markovian dissipative dynamics. *Physical Review Letters*, **91**(7):070402, August 2003. 1, 81

[BP02] Breuer, Heinz-Peter ; Petruccione, Francesco: *The theory of open quantum systems*. Oxford University Press, 2002. ISBN 9780198520634. 18, 24, 29

[BR01] Briegel, Hans J. ; Raussendorf, Robert: Persistent entanglement in arrays of interacting particles. *Physical Review Letters*, **86**(5):910, January 2001. 7

[Bra02] Braun, Daniel: Creation of entanglement by interaction with a common heat bath. *Physical Review Letters*, **89**(27):277901, December 2002. 1, 81

[Bra05] Braun, Daniel: Entanglement from thermal blackbody radiation. *Physical Review A*, **72**(6):062324, December 2005. 1, 82

[BW92] Bennett, Charles H. ; Wiesner, Stephen J.: Communication via one- and two-particle operators on Einstein-Podolsky-Rosen states. *Physical Review Letters*, **69**(20):2881, November 1992. 6

[CB97] Cleve, Richard ; Buhrman, Harry: Substituting quantum entanglement for communication. *Physical Review A*, **56**(2):1201, August 1997. 7

[CL83a] Caldeira, A. O. ; Leggett, A. J.: Path integral approach to quantum Brownian motion. *Physica A: Statistical and Theoretical Physics*, **121**(3):587–616, September 1983. 18

[CL83b] Caldeira, A. O. ; Leggett, A. J.: Quantum tunnelling in a dissipative system. *Annals of Physics*, **149**(2):374–456, September 1983. 24

[CL07] Choi, Taeseung ; Lee, Hyuk-jae: Quantum entanglement induced by dissipation. *Physical Review A*, **76**(1):012308, July 2007. 1, 81

[CP09] Cirone, Markus A ; Palma, G. Massimo: Entanglement induced by tailored environments. *Advanced Science Letters*, **2**(4):503–505, December 2009. 1, 82

[DC06] Duarte, O. S. ; Caldeira, A. O.: Effective coupling between two Brownian particles. *Physical Review Letters*, **97**(25):250601–4, December 2006. 21

[Dek85] Dekker, H.: Exactly solvable model of a particle interacting with a field: The origin of a quantum-mechanical divergence. *Physical Review A*, **31**(2):1067, February 1985. 19

[Dur74] Durbin, F.: Numerical inversion of Laplace transforms: An efficient improvement to Dubner and Abate's method. *The Computer Journal*, **17**(4):371 –376, November 1974. 85

[DV07] Datta, Animesh ; Vidal, Guifré: Role of entanglement and correlations in mixed-state quantum computation. *Physical Review A*, **75**(4):042310, April 2007. 6, 7

[Eke91] Ekert, Artur K.: Quantum cryptography based on Bell's theorem. *Physical Review Letters*, **67**(6):661, August 1991. 6

[EPR35] Einstein, A. ; Podolsky, B. ; Rosen, N.: Can quantum-mechanical description of physical reality be considered complete? *Physical Review*, **47**(10):777, May 1935. 3

[FC72] Freedman, Stuart J. ; Clauser, John F.: Experimental test of local hidden-variable theories. *Physical Review Letters*, **28**(14):938, April 1972. 3

[FCAH10] Fleming, C. H ; Cummings, N. I ; Anastopoulos, Charis ; Hu, B. L: Non-Markovian dynamics and entanglement of two-level atoms in a common field, arXiv:1012.5067, December 2010. 82

[FK87] Ford, G. W. ; Kac, M.: On the quantum Langevin equation. *Journal of Statistical Physics*, **46**(5):803–810, March 1987. 22

[FKM65] Ford, G. W. ; Kac, M. ; Mazur, P.: Statistical mechanics of assemblies of coupled oscillators. *Journal of Mathematical Physics*, **6**(4):504, April 1965. 17

[FNGM09] Ferraro, E ; Napoli, A ; Guccione, M ; Messina, A: Entanglement sudden death and sudden birth in two uncoupled spins. *Physica Scripta*, **T135**:014032, July 2009. 1, 81

[FRH10] Fleming, C. H ; Roura, Albert ; Hu, B. L: Exact analytical solutions to the master equation of quantum brownian motion for a general environment, arXiv:1004.1603, April 2010. 56

[FT06] Ficek, Z. ; Tanaś, R.: Dark periods and revivals of entanglement in a two-qubit system. *Physical Review A*, **74**(2):024304, 2006. 43

[FV63] Feynman, R. P. ; Vernon, F. L.: The theory of a general quantum system interacting with a linear dissipative system. *Annals of Physics*, **24**:118–173, October 1963. 18

[GKS76] Gorini, Vittorio ; Kossakowski, Andrzej ; Sudarshan, E. C. G.: Completely positive dynamical semigroups of n-level systems. *Journal of Mathematical Physics*, **17**(5):821, May 1976. 18

[Gol62] Goldenberg, H.: The evaluation of inverse Laplace transforms without the aid of contour integration. *SIAM Review*, **4**(2):94–104, April 1962. 46

[Gou09] Gough, Brian: *GNU Scientific Library Reference Manual*. Network Theory Ltd., 3rd revised edition, January 2009. ISBN 0954612078. 86

[Gur03] Gurvits, Leonid: Classical deterministic complexity of edmonds' problem and quantum entanglement. In *Proceedings of the thirty-fifth annual ACM symposium on Theory of computing*, pages 10–19. ACM, San Diego, CA, USA, June 2003. ISBN 1-58113-674-9. 5

[GZ04] Gardiner, Crispin W. ; Zoller, Peter: *Quantum noise*. Springer, October 2004. ISBN 3540223010, 9783540223016. 31

[HB08] Hörhammer, Christian ; Büttner, Helmut: Environment-induced two-mode entanglement in quantum Brownian motion. *Physical Review A*, **77**(4):042305–9, April 2008. 1, 27, 81

[HHH96] Horodecki, Michał ; Horodecki, Paweł ; Horodecki, Ryszard: Separability of mixed states: necessary and sufficient conditions. *Physics Letters A*, **223**(1-2):1–8, November 1996. 8

[HHH98] Horodecki, Michał ; Horodecki, Paweł ; Horodecki, Ryszard: Mixed-state entanglement and distillation: Is there a "bound" entanglement in nature? *Physical Review Letters*, **80**(24):5239, June 1998. 9

[HHH+05] Horodecki, Michał ; Horodecki, Paweł ; Horodecki, Ryszard ; Oppenheim, Jonathan ; Sen(De), Aditi ; Sen, Ujjwal ; Synak-Radtke, Barbara: Local versus nonlocal information in quantum-information theory: Formalism and phenomena. *Physical Review A*, **71**(6):062307, June 2005. 6

[HHHH09] Horodecki, Ryszard ; Horodecki, Paweł ; Horodecki, Michał ; Horodecki, Karol: Quantum entanglement. *Reviews of Modern Physics*, **81**(2):865–78, June 2009. 3, 9

[HI05] Hänggi, Peter ; Ingold, Gert-Ludwig: Fundamental aspects of quantum brownian motion. *Chaos: An Interdisciplinary Journal of Nonlinear Science*, **15**(2):026105, June 2005. 55

[HPZ92] Hu, B. L. ; Paz, Juan Pablo ; Zhang, Yuhong: Quantum brownian motion in a general environment: Exact master equation with nonlocal dissipation and colored noise. *Physical Review D*, **45**(8):2843, April 1992. 55

[Hä97] Hänggi, Peter: Generalized langevin equations: A useful tool for the perplexed modeller of nonequilibrium fluctuations? In *Stochastic Dynamics*, volume 484 of *Lecture Notes in Physics*, pages 15–22. Springer, 1997. 55

[Isa08] Isar, Aurelian: Asymptotic entanglement in open quantum systems. *International Journal of Quantum Information*, **06**(Supp):689, July 2008. 1, 81

[JL03] Jozsa, Richard ; Linden, Noah: On the role of entanglement in quantum-computational speed-up. *Proceedings of the Royal Society of London. Series A: Mathematical, Physical and Engineering Sciences*, **459**(2036):2011–2032, August 2003. 7

[JZK+03] Joos, Erich ; Zeh, H. Dieter ; Kiefer, Claus ; Giulini, Domenico ; Kupsch, I.O. Stamatescu Joachim: *Decoherence and the Appearance of a Classical World in Quantum Theory*. Springer, Berlin, 2nd edition, May 2003. ISBN 9783540003908. 1

[KMJ+10] Krauter, Hanna ; Muschik, Christine A ; Jensen, Kasper ; Wasilewski, Wojciech ; Petersen, Jonas M ; Cirac, J. Ignacio ; Polzik, Eugene S: Entanglement generated by dissipation, arXiv:1006.4344, June 2010. 81

[KW04] Koashi, Masato ; Winter, Andreas: Monogamy of quantum entanglement and other correlations. *Physical Review A*, **69**(2):022309, February 2004. 4

[Lin76] Lindblad, G.: On the generators of quantum dynamical semigroups. *Communications in Mathematical Physics*, **48**(2):119–130, June 1976. 18

[LSF10] Li, Gao-xiang ; Sun, Li-hui ; Ficek, Zbigniew: Multi-mode entanglement of n harmonic oscillators coupled to a non-Markovian reservoir. *Journal of Physics B: Atomic, Molecular and Optical Physics*, **43**(13):135501, July 2010. 1, 81

[MNBF09] McCutcheon, D. P. S. ; Nazir, A. ; Bose, S. ; Fisher, A. J.: Long-lived spin entanglement induced by a spatially correlated thermal bath. *Physical Review A (Atomic, Molecular, and Optical Physics)*, **80**(2):022337–6, August 2009. 1, 82

[Mor65] Mori, Hazime: Transport, collective motion, and Brownian motion. *Progress of Theoretical Physics*, **33**(3):423–455, March 1965. 17, 24

[MS06] Malinovsky, Vladimir S. ; Sola, Ignacio R.: Phase-Controlled collapse and revival of entanglement of two interacting qubits. *Physical Review Letters*, **96**(5):050502, February 2006. 43

[MS07] Methot, A. A. ; Scarani, V.: An anomaly of non-locality. *Quantum Information and Computation*, **7**(1–2):157–170, January 2007. 5

[Nak58] Nakajima, Sadao: On quantum theory of transport phenomena: Steady diffusion. *Progress of Theoretical Physics*, **20**(6):948–959, December 1958. 18

[NC00] Nielsen, Michael A. ; Chuang, Isaac L.: *Quantum Computation and Quantum Information*. Cambridge University Press, October 2000. ISBN 9780521635035. 1

[OZ01] Ollivier, Harold ; Zurek, Wojciech H.: Quantum discord: A measure of the quantumness of correlations. *Physical Review Letters*, **88**(1):017901, December 2001. 6

[Per96] Peres, Asher: Separability criterion for density matrices. *Physical Review Letters*, **77**(8):1413, August 1996. 8

[PH84] Piessens, Robert ; Huysmans, Rudi: Algorithm 619: Automatic numerical inversion of the Laplace transform [D5]. *ACM Trans. Math. Softw.*, **10**(3):348–353, September 1984. 85

[Pop95] Popescu, Sandu: Bell's inequalities and density matrices: Revealing "hidden" nonlocality. *Physical Review Letters*, **74**(14):2619, April 1995. 5

[PR94] Popescu, Sandu ; Rohrlich, Daniel: Quantum nonlocality as an axiom. *Foundations of Physics*, **24**(3):379–385, March 1994. 4

[PR97] Popescu, Sandu ; Rohrlich, Daniel: Thermodynamics and the measure of entanglement. *Physical Review A*, **56**(5):R3319, November 1997. 9

[PR08] Paz, Juan Pablo ; Roncaglia, Augusto J.: Dynamics of the entanglement between two oscillators in the same environment. *Physical Review Letters*, **100**(22):220401–4, June 2008. 1, 81

[Que11] Queisser, Friedemann: *The Impact of Decoherence and Dissipation on Cosmological Systems and on the Generation of Entanglement*. Ph.D. thesis, University of Cologne, February 2011. 20, 77, 78, 79, 82

[RB01] Raussendorf, Robert ; Briegel, Hans J.: A one-way quantum computer. *Physical Review Letters*, **86**(22):5188, May 2001. 7

[RBK11] Rao, D. D. Bhaktavatsala ; Bar-Gill, Nir ; Kurizki, Gershon: Generation of macroscopic superpositions of quantum states by linear coupling to a bath. *Physical Review Letters*, **106**(1):010404, January 2011. 1, 81

[Sch35] Schrödinger, E.: Discussion of probability relations between separated systems. *Mathematical Proceedings of the Cambridge Philosophical Society*, **31**(04):555–563, October 1935. 3

[Sen60] Senitzky, I. R.: Dissipation in quantum mechanics. The harmonic oscillator. *Physical Review*, **119**(2):670, July 1960. 17

[SH04] Shiokawa, K. ; Hu, B. L.: Qubit decoherence and non-Markovian dynamics at low temperatures via an effective spin-boson model. *Physical Review A*, **70**(6):062106, December 2004. 11

[Sim00] Simon, R.: Peres-Horodecki separability criterion for continuous variable systems. *Physical Review Letters*, **84**(12):2726, March 2000. 13, 14

[SKR06] Sainz, I. ; Klimov, A. B. ; Roa, Luis: Entanglement dynamics modified by an effective atomic environment. *Physical Review A*, **73**(3):032303, March 2006. 43

[SMD94] Simon, R. ; Mukunda, N. ; Dutta, Biswadeb: Quantum-noise matrix for multimode systems: U(n) invariance, squeezing, and normal forms. *Physical Review A*, **49**(3):1567, March 1994. 12, 14

[SSM88] Simon, R. ; Sudarshan, E. C. G. ; Mukunda, N.: Gaussian pure states in quantum mechanics and the symplectic group. *Physical Review A*, **37**(8):3028, April 1988. 26

[STH77] Shibata, Fumiaki ; Takahashi, Yoshinori ; Hashitsume, Natsuki: A generalized stochastic liouville equation. Non-Markovian versus memoryless master equations. *Journal of Statistical Physics*, **17**(4):171–187, October 1977. 18

[STP06] Solenov, Dmitry ; Tolkunov, Denis ; Privman, Vladimir: Coherent interaction of spins induced by thermal bosonic environment. *Physics Letters A*, **359**(2):81–85, November 2006. 1, 81

[STP07] Solenov, Dmitry ; Tolkunov, Denis ; Privman, Vladimir: Exchange interaction, entanglement, and quantum noise due to a thermal bosonic field. *Physical Review B*, **75**(3):035134, January 2007. 82

[SW85] Summers, Stephen J. ; Werner, Reinhard: The vacuum violates bell's inequalities. *Physics Letters A*, **110**(5):257–259, July 1985. 57

[Uhl98] Uhlmann, Armin: Entropy and optimal decompositions of states relative to a maximal commutative subalgebra. *Open Systems & Information Dynamics*, **5**(3):209–228, September 1998. 10

[Ull66] Ullersma, P.: An exactly solvable model for Brownian motion : I. derivation of the Langevin equation. *Physica*, **32**(1):27–55, January 1966. 18

[UZ89] Unruh, W. G. ; Zurek, W. H.: Reduction of a wave packet in quantum Brownian motion. *Physical Review D*, **40**(4):1071, August 1989. 19

[Vid03] Vidal, Guifré: Efficient classical simulation of slightly entangled quantum computations. *Physical Review Letters*, **91**(14):147902, October 2003. 7

[VW02] Vidal, G. ; Werner, R. F.: Computable measure of entanglement. *Physical Review A*, **65**(3):032314, February 2002. 10, 14, 15

[Wei08] Weiss, Ulrich: *Quantum dissipative systems*. World Scientific, June 2008. ISBN 9789812791627. 17, 18

[Wer89] Werner, Reinhard F.: Quantum states with Einstein-Podolsky-Rosen correlations admitting a hidden-variable model. *Physical Review A*, **40**(8):4277, October 1989. 5

[Wey27] Weyl, H.: Quantenmechanik und Gruppentheorie. *Zeitschrift für Physik*, **46**(1):1–46, November 1927. 11

[Wig32] Wigner, E.: On the quantum correction for thermodynamic equilibrium. *Physical Review*, **40**(5):749, June 1932. 11

[Wil36] Williamson, John: On the algebraic problem concerning the normal forms of linear dynamical systems. *American Journal of Mathematics*, **58**(1):141–163, January 1936. 14

[WW08] Wilkie, Joshua ; Wong, Yin Mei: A linearly scaling grid method for generalized Langevin and other integrodifferential equations. *Journal of Physics A: Mathematical and Theoretical*, **41**(33):335005, July 2008. 38, 85

[XSS08] Xiang, Shao-Hua ; Shao, Bin ; Song, Ke-Hui: Environment-assisted creation and enhancement of two-mode entanglement in a joint decoherent model. *Physical Review A*, **78**(5):052313, November 2008. 1, 81

[YE04] Yu, T. ; Eberly, J. H.: Finite-Time disentanglement via spontaneous emission. *Physical Review Letters*, **93**(14):140404, September 2004. 43

[YE06] Yu, T. ; Eberly, J.H.: Sudden death of entanglement: Classical noise effects. *Optics Communications*, **264**(2):393–397, August 2006. 43

[YS92] Yurke, Bernard ; Stoler, David: Einstein-Podolsky-Rosen effects from independent particle sources. *Physical Review Letters*, **68**(9):1251, March 1992. 6

[Yur86] Yurke, Bernard: Quantizing the damped harmonic oscillator. *American Journal of Physics*, **54**(12):1133–1139, December 1986. 19

[Zeh70] Zeh, H.: On the interpretation of measurement in quantum theory. *Foundations of Physics*, **1**(1):69–76, March 1970. 4

[Zel06] Zell, Thomas: *Verschränkung zweier Oszillatoren im Caldeira-Leggett-Modell*. Diploma thesis, University of Cologne, December 2006. 29

[ZHSL98] Życzkowski, Karol ; Horodecki, Paweł ; Sanpera, Anna ; Lewenstein, Maciej: Volume of the set of separable states. *Physical Review A*, **58**(2):883, August 1998. 10

[Zur81] Zurek, W. H.: Pointer basis of quantum apparatus: Into what mixture does the wave packet collapse? *Physical Review D*, **24**(6):1516, September 1981. 4

[Zwa60] Zwanzig, Robert: Ensemble method in the theory of irreversibility. *The Journal of Chemical Physics*, **33**(5):1338, November 1960. 18

[Zwa73] Zwanzig, Robert: Nonlinear generalized Langevin equations. *Journal of Statistical Physics*, **9**(3):215–220, November 1973. 18

Erklärung

Ich versichere, dass ich die von mir vorgelegte Dissertation selbständig angefertigt, die benutzten Quellen und Hilfsmittel vollständig angegeben und die Stellen der Arbeit – einschließlich Tabellen, Karten und Abbildungen –, die anderen Werken im Wortlaut oder dem Sinn nach entnommen sind, in jedem Einzelfall als Entlehnung kenntlich gemacht habe; dass diese Dissertation noch keiner anderen Fakultät oder Universität zur Prüfung vorgelegen hat; dass sie – abgesehen von unten angegebenen Teilpublikationen – noch nicht veröffentlicht worden ist sowie, dass ich eine solche Veröffentlichung vor Abschluss des Promotionsverfahrens nicht vornehmen werde.
Die Bestimmungen der Promotionsordnung sind mir bekannt. Die von mir vorgelegte Dissertation ist von Herrn PD Dr. Rochus Klesse betreut worden.

Köln, den 16. Juni 2011

Thomas Zell

Teilpublikationen

[ZQK09] Zell, Thomas ; Queisser, Friedemann ; Klesse, Rochus: Distance dependence of entanglement generation via a bosonic heat bath. *Physical Review Letters*, **102**(16):160501–4, April 2009.

Acknowledgements

First and foremost, I would like to thank my advisor Rochus Klesse for his friendly support and his willingness to answer questions and discuss problems at any time. I am also very grateful for the rich collaboration with Friedemann Queisser. Prof. Meschede was a great mentor to me in the Bonn-Cologne Graduate School. Furthermore, I thank Prof. Kiefer for being a referee in my thesis committee.

My fellow PhD candidates Stefan Borghoff, Jakob Müller-Hill, Sebastian Schmittner, and Andrea Wolff have always been encouraging and have contributed to this thesis by discussions, proof reading and creating a friendly atmosphere in our office. Finally, I would like to thank for the infinite moral support by my wife Magdalena.

This work was financially supported by the Bonn-Cologne Graduate School (BCGS) and the Deutsche Forschungsgemeinschaft (DFG).